Exploration of the Mechanisms of Unconsciousness Induced by Propofol with Positron Emission Tomography (PET) Functional Brain Imaging

Guoming Xie M.D., M.Sc.

Dept. Neurology and Neurosurgery

McGill University

Montreal, Quebec, Canada

June 2006

A thesis submitted to the Faculty of Graduate Studies and Research in partial fulfilment of the requirements for the degree of Doctor of Philosophy

Your file Votre référence
ISBN: 978-0-494-27858-1
Our file Notre référence
ISBN: 978-0-494-27858-1

ACKNOWLEDGMENTS

I sincerely thank Dr. Pierre Fiset my supervisor for his valuable help and guidance over my graduate study. I would like to thank my co-supervisor Dr. Alain Dagher for his time, support, and guidance. This thesis would not have been completed without their constructive criticisms and scientific expertise.

I extend my special gratitude to my advisory committee member, Dr. Gilles Plourde for devoting his time and research project and making him available whenever I needed. I sincerely appreciate his contribution to this work.

I would like to thank Dr. Roger Gunn for teaching me how to do the compartmental analysis for tracer kinetic modeling and his overall contribution to first project. I also wish to thank Drs. Tomas Paus and Ernst Meyer for their helpful criticisms and comments that helped me to improve the quality of my research of second project. I am grateful to Dr. Alan Evans for his overall support as well as his effort in creating such a nice environment at the PET unit. I would also like to thank Dr. Joseph Rochford for his valuable advice when I was taking his statistical class.

I owe a tremendous debt to all members of Department of Anaesthesia, Royal Victoria Hospital, especially all anesthesiologists (Dr.

Steve Backman, Dr. Daniel Chartrand, Dr. Alain Deschamps, Dr. Thierry Daloze) who participated in the PET studies and also provided a nice office space and an enjoyable learning environment that contributed to my education over the last four and half years.

I also extend my appreciation to Mr. Sylvain Milot for providing expert image analysis, our cyclotron staff for providing the radioisotopes, and our PET technicians and Ms. Louise Ullyatt for their assistance with PET experiments.

Finally, I would like to thank my wonderful wife, Zhen Shen, and daughter, Qin Xie, for their love and encouragement in helping me pursue my goals.

This work was supported by International Anesthesia Research Society grant of Dr. Pierre Fiset and Canadian Institutes of Health Research grant of Dr. Gilles Plourde.

TABLE OF CONTENTS

LIST OF TABLES

LIST OF FIGURES

ABSTRACT

In anesthesia practice, consciousness is often equated with the waking state and with the ability to respond to stimuli in the integrated manner. The reversible loss of consciousness is induced by the general anesthetic, which have a wide range of molecular structure and physicochemical characteristics. The mechanisms of unconsciousness induced by anesthetic agents are not well understood. The studies I have conducted for my Ph.D. have focused on how anesthetic drugs produce unconsciousness in human subjects. In two separate PET studies, receptor imaging and regional CBF analysis were used to examine the unconsciousness induced by propofol, a popular general anesthetic. The first study evaluated kinetic analysis methods for estimation of the receptor availability of the muscarinic receptor using dynamic positron emission tomography (PET) studies with [N-11C-methyl]-benztropine. The study also investigated the effect of propofol on central muscarinic receptor availability during general anesthesia. The results of this study suggested the propofol-related reductions in muscarinic receptor availability. The second study identified the brain function changes specifically linked to the difference in levels of consciousness. We used physostigmine (an anticholinestherase) to restore consciousness in the

subjects anesthetized with a constant concentration of propofol. The results revealed that the thalamus and precuneus/cuneus jointly play a critical role in controlling the changes in the level of consciousness during general anesthesia.

Together, these two studies support a hypothesis that the joint deactivations of a Common Midline Core, which includes the medial thalamus, midline precuneus/cuneus, prefrontal cortex and other related cortical areas, contribute to the unconsciousness induced by general anesthetics. These deactivations are mediated, at least partially, by a reduction in the central cholinergic transmission.

ABRÉGÉ

En anesthésie, la conscience est souvent définie comme l'état d'éveil, et comme la capacité de répondre aux stimuli simples de façon cohérente. La perte de conscience est induite de façon réversible par les anesthésiques généraux qui varient considérablement dans leurs structures moléculaires et leurs caractéristiques physico-chimiques. Les mécanismes qui sous-tendent la perte de conscience induite par les anesthésiques ne sont pas bien compris. Les études que j'ai menées pour l'obtention de mon doctorat ont pour sujet les mécanismes de production de l'inconscience par les anesthésiques généraux chez l'humain. Dans deux études distinctes avec le Tomographe à Émission de Positrons (TEP), l'une sur les récepteurs muscariniques et l'autre sur le débit sanguin régional cérebral, nous avons examiné l'inconscience produite par le propofol, un anesthésique général largement utilisé en clinique. Dans la première étude, nous avons évalué différentes méthodes d'analyse cinétique pour l'estimation de la disponibilité des récepteurs muscariniques suite à des études dynamiques au TEP avec la N 11C-methyl benztropine. Nous avons aussi étudié les effets du propofol sur la disponibilité des récepteurs muscariniques pendant l'anesthésie générale. Nos résultats suggèrent une diminution de la disponibilité des récepteurs

muscariniques par la propofol. La deuxième étude porte sur les changements des fonctions cérébrales spécifiquement liés aux changements dans l'état de conscience. Nous avons utilié la physostimine (un agent anticholinestérasique) pour provoquer le retour de la conscience chez 4 sujets anesthésiés avec une concentration stable de propofol. Les résultats montrent que le thalamus et le cuneus/précuneus jouent conjointement un rôle central dans le contrôle des changements de niveau de conscience pendant l'anesthésie générale.

Ces deux études supportent l'hypothèse que la désactivation du 'Common Midline Core', qui comprend le thalamus médian, le cunéus/précunéus, le cortex préfrontal et dautres régions corticales, contribuent à l'inconscience induite par les anesthésiques généraux. Ces désactivations sont tributaires, au moins en partie, de la réduction de la transmission dans le système cholinergique central.

CONTRIBUTIONS OF AUTHORS

Chapter 2 is based on the published manuscript entitled "PET Quantification of Muscarinic Cholinergic Receptors with [N-11C-methyl-benztropine and application to studies of Propofol-induced Unconsciousness in Healthy Human Volunteers", by Xie G, Gunn RN, Dagher A, Daloze T, Plourde G, Backman SB, Diksic M, Fiset P. I analyzed the data and wrote the manuscript. Dr. Fiset, Dr. Plourde, Dr. Daloze and Dr. Backman performed the human subject experiments. Dr. Diksic provided [N-11C-methyl-benztropine. Dr. Gunn, Dr. Dagher, Dr. Fiset, and Dr. Plourde contributed to the data analysis and the writing of the manuscript.

Chapter 3 may contain one or two manuscripts. I participated in the study, analyzed the data and wrote the chapter. Dr. Plourde, Dr. Backman, Dr. Chartrand and Dr. Fiset and Dr. Deschamps performed the human subject experiments. Dr. Plourde, Dr. Dagher, and Dr. Fiset, contributed to the data analysis and the revision of the chapter.

Chapter 1 GENERAL INTRODUCTION

1.1 Consciousness

1.1.1 Concept of consciousness

The concept of consciousness contains a number of different concepts and denotes a number of different phenomena. Consciousness refers to many different entities and has been studied by many disciplines, ranging from philosophy and cognitive science to psychology and neurobiology. It is not possible to provide an all-encompassing definition of the term consciousness, but it would be beneficial to distinguish three principal meanings (Zeman et al., 1997; Zeman, 2001).

The first meaning of consciousness, defined by Zeman, is called the "waking state", which describes the abilities to perceive, interact and communicate with the environment in an integrated manner. So a person with consciousness is awake, aroused, alert or vigilant in contrast to drowsiness or coma. The second meaning of consciousness defined by Zeman is the content of subjective experience. When we are conscious, we are always conscious of something that is the content of experience from moment to moment. This concept of consciousness highlights the qualitative, subjective dimension of experience and is widely used in the field of philosophy. The third meaning of consciousness defined by Zeman

is synonymous with the mind, where person with consciousness is able to have expressions of belief, hope, fear, intent, desire, etc.

Most of the researches related to consciousness have focused on its first and second meaning, rather than this third meaning. The first meaning has been widely used in medical field. Medical doctors use the Glasgow Coma Scale to objectively define the different states of consciousness. In the operation room, anesthesiologists are able to suppress and restore the consciousness of a patient by regulating the concentration of anesthetic agents.

1.1.2 Consciousness and sleep

The physiological mechanisms that underlie consciousness and unconsciousness are the sleep-wake mechanisms, as sleep is a state of physiological reversible unconsciousness. The process about how the brain transfers from sleep to wakefulness was explored by Morruzzi and Magoun (1949). They demonstrated that a cut through the mid-brain of a cat at a high level resulted in a state of continuous slow wave sleep, while a slightly lower cut produced a state of continuous wakefulness. Moreover, stimulating the mid-brain near the central canal in the sleeping cat resulted in immediate wakefulness and activated EEG. Those observations gave

birth to the concept of the reticular activating mechanism that a column of cells surrounding the central canal, the mid-brain reticular substance, received input from all the ascending tracts of the brain stem (Figure 1-1). This activity could be relayed to the entire cortex through thalamus resulting in wakefulness with general cortical activation. Their work has been repeated and confirmed (Sinton and McCarley, 2000). Further animal experimental studies identified that a series of specialized nodes also play important roles in the maintenance and modulation of wakefulness, which includes basal forebrain, caudate, subthalamus, and hypothalamus (Figure 1-2) (Jones, 1998; Zeman, 2001).

The transition from wakefulness to sleep is less well known. Recent evidence suggests that there is an arousal inhibitory mechanism (AIM), which transfers the brain from wakefulness to sleep by a thalamo-cortial mechanism. McCarley (2004) and Steriade (2004) studied sleep onset in both cat and man. They demonstrated that at the onset of drowsiness, sleep spindles appear in the thalamus and later spread to involve the cortex. Using positron emission tomography (PET), Maquet (2000) studied wakefulness and sleep. He found that there was a much lower blood flow in the thalamus and upper brain stem than elsewhere

Figure 1-1: The reticular activating system

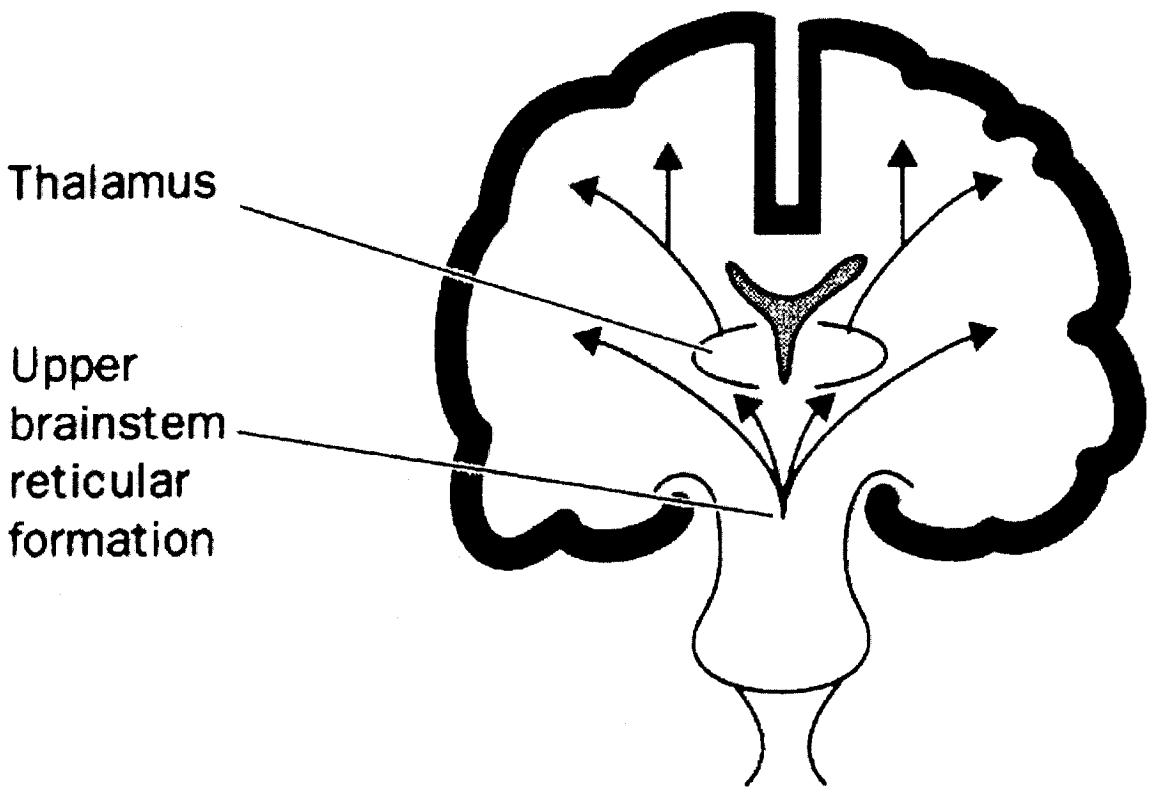

A schematic diagram of the reticular activating system, indicating pathways of activation which involve and those which bypass the thalamus (From Zeman 1997)

Figure 1-2: A sagittal drawing of a cat brain indicating the structure implicated in generating and maintaining the waking states

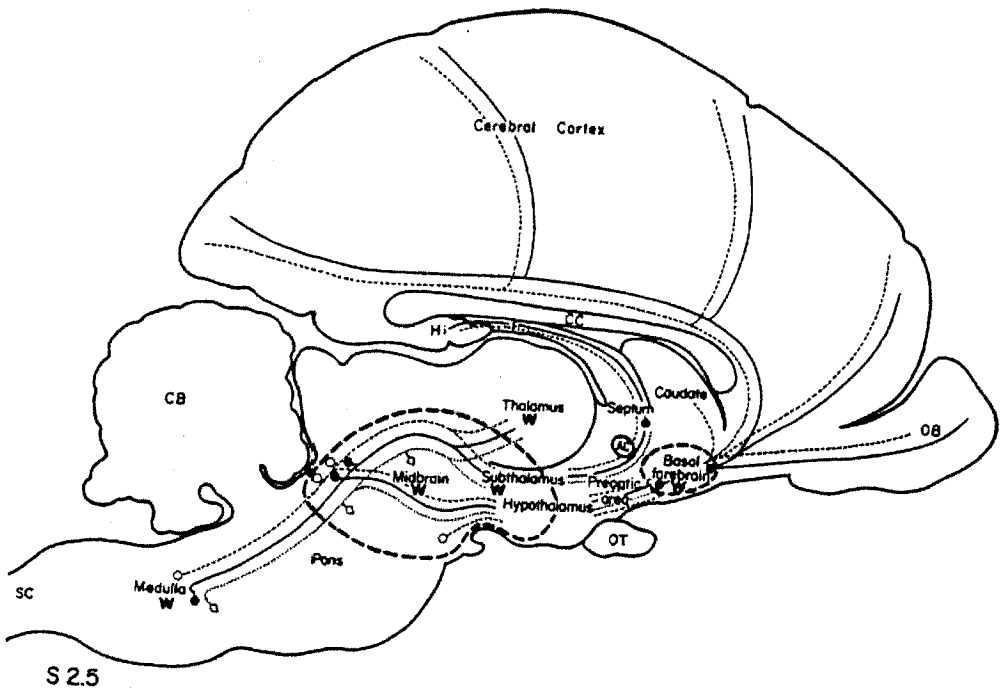

A capital drawing of a cat brain indicating the structure implicated in generating and maintaining the waking states. Areas marked with a W are those from where cells are maximally active during wakefulness. Area encircled by dashed lines in bold are those where selective lesions most commonly cause coma. AC= anterior commissure; CB = cerebellum; CC = corpus callosum; Hi = hippocampus, OB = olfactory bulb; OT = optic tracts; SC = spinal cord (From Jones, 1998).

during deep sleep. This finding strongly supports those of Steriade in the demonstration of a deactivating process at the thalamic level in slow wave sleep and the presence of an AIM.

1.1.3 Consciousness and anesthesia

In neurological and anesthesia practice, consciousness is often equated with the waking state, and with the ability to respond to stimuli in an integrated manner associated with this state. Arousal is necessary for the emergence of consciousness. Those aspects of consciousness are partially depressed or totally lost during anesthesia and regained after anesthesia. The reversible loss of consciousness is induced by the hypnotic or general anesthetic agents, which have a wide range of molecular structure and physicochemical characteristics. The mechanisms of unconsciousness induced by anesthetic agents are not well understood. Since Meyer and Overton (Meyer et al. 1899) discovered a correlation between anesthetic potency and partitioning into fat-like solvents (oil/gas partition coefficient), the traditional view had been that general anesthetics act by disrupting the structure or dynamic properties of the lipid portions of nerve membranes. However, by the early 1980s, accumulating evidence posed serious quantitative problems for this simple unifying idea. Taken

together with positive evidence for the direct involvement of proteins, this has led to the almost complete abandonment of theories that postulate changes in the properties of the bulk lipid bilayer (Franks et al, 1984, 1987). The available evidence strongly suggests that general anesthetics act by binding directly to proteins and probably exert their primary effects at a relatively small number of CNS targets (Franks et al. 1991,1994, 1998). These are most likely to be postsynaptic ligand-gated ion channels. Some agents act predominantly at excitatory receptors and some predominantly potentiate inhibitory synaptic receptors. In addition, some agents are clearly effective at both inhibitory and excitatory postsynaptic receptor, so the balance between the inhibition of excitatory synapses and the potentiation of inhibitory synapses that may cause general anesthesia still needs to be established. It is not known whether these cellular events exert their action in relation with specific structures of the brain.

1.1.4 The neural substrates of conscious states

The theories concerning the neural substrates of consciousness tend to fall into two classes: (1) neuronal-specificity and (2) process-coherence (Cariani 2000). Neuronal-specificity theories postulate specific neurons whose activation supports representation that determine the existence of

conscious awareness (Crick 1994). The neuronal-specificity embodies the notion of structurally localizable seats of consciousness. Process-coherence theories emphasize particular relational patterns of activity, such as adaptive resonances (Grossberg 1999), coherent oscillations (Llinas et al., 1998), interneural synchronies (Engel and Singer 2001) and temporal coherences (John et al., 1997, 2005). Recently Crick and Koch (2003) introduced a concept of " framework" for consciousness. This framework offers a coherent scheme for explaining the neural correlates of (visual) consciousness in terms of competing cellular assemblies.

Most theories of general anesthesia have focused on basic modes of how a neural signalling system might be disrupted. These theories tend to fall into three groups: (1) suppression of neural signal production, (2) blockade of neural signal transmission, and (3) disruption of the coherence of neural signals themselves or neural processes that interpret them. Although many studies are aimed to explore the effects of anesthetic agents on synaptic and axonal sites, higher level functional consequences are still conceptualized in terms of signal-suppressions or transmission blockades. Due to the centrality of the thalamus in its connections to the rest of the system, suppression of thalamic activity is believed to turn off the entire system.

1.1.5 Unconsciousness and signal supression

The suppression of thalamocortical loops and their modulation by mid-brain reticular input play a critical rule for the switching of conscious state, but we do not know how these circuits are functionally incapacitated. It is difficult to use a purely suppressive theory to explain the conditions, such as chloralose anesthesia and epileptic seizure, in which increased neural discharge rates are associated with loss of conscious awareness. With the theory of signal suppression and transmission block, Angel (1993) presents the excitatory and inhibitory effects that propofol and other general anesthetics can have on thalamic and cortical neurons. These findings are consistent with the general reductions in regional cortical glucose metabolism (Alkire et al., 1995) and the regional reduction of cerebral blood flow in thalamus (Fiset et al., 1999) in their PET study of the effects of propofol. Therefore, suppression of activity may be sufficient to induce unconsciousness, but the existence of cases in which elevated neural discharge is associated with loss of consciousness implies that a sufficient level of neural activity by itself may not be sufficient to support consciousness. In order to keep consciousness, the neural discharge activity must be appropriately organized.

1.1.6 Unconsciousness and process-coherence theories and regenerative process

Process-coherence theories emphasize the importance of the proper form of neural signals as well as the functional organization of the system that interprets these signals. The coherence message is traditionally encoded in the discharge rate profile. Almost all anesthetic agents affect neural discharge rates. Anesthetic agents are also known to alter the temporal response characteristics of synapses and axons (Kendig at al., 1979, Kendig 2002). Many general anesthetics, such as halothane, enflurance, and lidocaine, alter axonal membrane threshold recovery process, abolishing superexcitable phases (Butterworth et al., 1989). These findings suggested that general anesthetics produce unconsciousness because they disrupt activity-dependent process, which remove the temporal context essential for interpreting nerve impulse patterns. If temporal patterning of neural discharge is critical to system functioning, the changes in neuronal temporal response might disrupt the functional organization of the whole system. General anesthetics might not only block the neural signals but also disable the neural computational architectures that normally interpret those signals. Cariani (2000)

suggested that a self-sustaining and self-regenerating set of signaling processes might be the underlying mechanism of process-coherence. Neural signaling patterns would not be capable of regenerating themselves under a certain threshold of activity, therefore, streams of consciousness are not sustained. The switching between different sets of self-regenerative signals would cause the different states and contents of consciousness.

1.2 General anesthetic agents

1.2.1 Class of general anesthetic agents

General anesthetic agents are classified into two main categories: the nonopioid intravenous anesthetics and the inhalation anesthetics. At present, the commonly used inhalation anesthetics are nitrous oxide, halothane, enflurane, isoflurane, desflurane and sevoflurane. Sevoflurane is useful in adults and children for both induction and maintenance of anesthesia in inpatient and outpatient surgery. Of all currently used anesthetics, the physical, pharmacodynamic, and pharmacokinetic properties of sevoflurane come closest to those of the ideal anesthetic. These properties include: inherent stability, low flammability, non-pungent odor, lack of irritation to airway passages, low blood/gas solubility allowing

rapid induction of and emergence from anesthesia, minimal cardiovascular and respiratory side effects, minimal end-organ effects, minimal effect on cerebral blood flow, low reactivity with other drugs, and a vapor pressure and boiling point that enables delivery using standard vaporization techniques (Delgado-Herrera et al., 2001). The nonopioid intravenous anesthetics can be further broken down into barbiturates, benzodiazepines and other drugs such as etomidate, ketamine, and propofol.

Among all nonopioid intravenous anesthetics, propofol is a relatively new intravenous anesthetic. Propofol was first synthesized in the early 1970s and introduced into clinical practice in the late 1980s. Propofol is rapidly metabolized and highly lipophilic. Those properties are responsible for a pharmacokinetic profile that is more suitable for continuous intravenous administration and have led to the development of computer driven administration systems that allow targeting of a precise brain concentration, depending on the height, the weight, the age and the gender of the patient (Shafer et al., 1993).

1.2.2 Interactions of anesthetic agents with synaptic transmission

1.2.2.1 The γ-amino butyric acid receptor type A ($GABA_A$ receptor)

General anesthetics might act by potentiating inhibitory synaptic transmission, and the $GABA_A$ receptor channel has been considered as a potential target. GABA is the most important inhibitory neurotransmitter in mammalian brain. Most anesthetics, such as benzodiazepines, barbiturates, volatile anesthetics and propofol, are very effective at potentiating responses to GABA (Franks et al., 1994). The degree of anesthetic potentiation of GABA receptors depends on their subunit compositions and the distribution of subunits throughout the CNS varies greatly (Yamakura et al., 2001). GABA receptor a, b, r subunits are critical for potentiation of agonist-induced currents by volatile anesthetics (Mihic et al., 1997). Agonist potentiation by propofol is affected by a point mutation of $GABA_A$ receptor b subunit (Krasowski et al., 1998). Although uncertainties remain as to the extent to which intact GABAergic synapses are potentiated, there are accumulating evidences that point to the $GABA_A$ receptor channel as a target for most general anesthetics.

1.2.2.2 The N-methyl-D-aspartate (NMDA) receptor

Glutamate is the major excitatory neurotransmitter in the mammalian brain. Among its receptors, the N-methyl-D-aspartate (NMDA) is the most

complex. Its activation leads to a series of intracellular events involving several second messenger systems. Ketamine is a non-competitive NMDA antagonist, which exerts its anesthetic effects largely by inhibiting the NMDA receptors (Franks & Lieb 1994). The anesthesia provided by ketamine is characterized by a relatively selective loss of higher cognitive functions but it usually preserves arousal. All NMDA receptors are strongly inhibited by both nitrous oxide (Yamakura and Harris, 2000) and xenon (Franks et al. 1998), both of them do not potentiate GABAA receptors. It had been speculated by de Sousa et al (2000) that there are at least two different routes to anesthesia, volatile anesthetics potentiating GABAergic synapses and xenon inhibiting glutamatergic synapses.

1.2.2.3 The cholinergic system

The prominent role in memory and consciousness played by the CNS cholinergic system is evident from the effects of the muscarinic antagonist scopolamine. The techniques, such as *in vivo* microdialysis and chemical neuroanatomy, have expanded our understanding of CNS cholinergic pathways. Two cholinergic groups of nuclei are involved in CNS projection systems. The brain stem group (laterodosal tegmental and pedunculopontine tegmental nuclei) projects rostrally along a dorsal

pathway to the thalamus and the pontine reticular formation and ventrally along a pathway to the basal forebrain. The basal forebrain group (medial septum, diagonal band of Broca and nucleus basalis of Meynert) projects to the neocortex and the hippocampus as well as to the amygdaloid complex. Afferent input to the cholinergic nuclei comes from various parts of the CNS including cortical areas, hippocampus, stria terminalis, preoptic area, thalamus, hypothalamus, amygdala, and several brain stem nuclei. These input have been characterized as serotonergic, noradrenergic, dopaminergic and GABAergic. It is postulated that alteration of central cholinergic transmission may play an important role in the mechanism by which general anesthetic drugs produce unconsciousness (Durieux ME, 1996).

Acetylcholine is the physiologic agonist for both nicotinic and muscarinic receptors. These two receptors are completely different entities. The nicotinic receptor is a multi-subunit, ligand-gated ion channel or an ionotropic receptor and the muscarinic receptor is a single-subunit, G-protein-coupled receptor or metabotropic receptor. Despite the fact that neuronal nicotinic receptors are very sensitive to anesthetic agents, there is no evidence as the their role in the CNS mechanism of anesthesia. It has been suggested that neural nicotinic receptors do not have a primary

role in unconsciousness, but may be involved in the generation of CNS side effects of general anesthesia (Downie et al, 2000).

In the central nervous system cholinergic transmission is mainly mediated by muscarinic receptors. There are five subtypes that are all expressed in the brain of mammals (m1-m5). Muscarinic stimulation, by administration of the cholinesterase inhibitor, physostigmine, induces a diffuse increase in alertness, making the individual more receptive to external and internal inputs, while muscarinic inhibition, in contrast, leads to sedation or non-REM sleep, depending on the prior state of the subject (Durieux et al., 1996). Our research group has conducted a series of studies on volunteers in which propofol was used to induce unconsciousness (Meuret et al., 2000). These studies demonstrated that physostigmine reverses the propofol-induced unconsciousness and associated depression of the auditory steady-state response (ASSR) and the bispectral index (BIS) in human volunteer. The reversal of the unconsciousness and depression of the ASSR and BIS was blocked by pretreatment with scopolamine. These findings support the hypothesis that the loss of consciousness produced by propofol is mediated, at least in part, via interruption of central cholinergic muscarinic transmission.

1.2.3 Action of anesthetic agents in the central nervous system

1.2.3.1 Action of anesthetics to produce immobility

In the past 15 years, researchers have demonstrated that the spinal motor neurons are depressed by inhaled anesthetics (Zentner et al., 1992, Rampil et al., 1996). It was also demonstrated that movement responses to noxious stimulation could occur despite an electroencephalogram made essentially isopotential by isoflurance (Rampil and Laster, 1992), after removal of cortex and thalamus (Rampil et al., 1993), and after hypothermic transection of the spinal cord (Rampil, 1994). The supporting evidence was provided by the findings that neither freezing the cerebral hemispheres (Todd et al., 1993) nor causing forebrain ischemia (McFarlane et al., 1991) nor using brain-preferential anesthetic procedures (Borger and Antognini, 1994) blocked moverment. All above evidences support the conclusion that immobility may be achieved by action at the level of the spinal cord. Several neurotransmitters are plausible candidates for mediating immobility. After reviewing the extensive literature on the results of interfering with ion channels, Sonner et al. (2003) concluded that the actions on multiple receptor systems may provide an explanation of how inhaled anesthetics achieve immobility.

1.2.3.2 Action of anesthetics to produce amnesia

For many anesthetics the dose to suppress consciousness significantly exceeds that required to prevent memory storage (Chortkorff et al., 1995). Memory can be blocked at anesthetic concentrations that do not suppress consciousness. Therefore we can believe that the amnestic effects of anesthetics are mediated by some processes other than those that block consciousness. In a series of PET studies, Veselis et al. (1997A, 1997B, 2002) demonstrated that the effects of anesthetics on episodic memory are related to actions primarily on the dorsolateral prefrontal cortex. The anterior cingulate, thalamus, and parietal association areas may also be affected. Intracerebral electroencephalographic recording in epileptic patients reveal progressive suppression of γ activity in the hippocampus with increased concentrations of sevoflurane (Uchida et al., 2000). This result is supported by subsequent neurophysiologic studies in animals that demonstrated septal-hippocampal inactivation and suppression of γ activity by both volatile and non-volatile anesthetics (Ma et al., 2002).

1.2.3.3 Action of anesthetics to suppress consciousness

Immobilization is likely mediated by effects of the spinal cord while amnesia is probably mediated by effects on the dorsolateral prefrontal cortex and limbic system. The mechanism of action of anesthetic to suppress consciousness is the primary concern of this thesis. We have previously introduced the theories concerning the neural substrate of consciousness, the theories about how a neural signalling system might be disrupted, and the interactions of anesthetic agents with synaptic transmission. In the following paragraphs, we will discuss how PET functional brain imaging could help us to explore mechanisms of unconsciousness induced by general anesthetics.

1.3 Positron Emission Tomography

1.3.1 Basic principles

PET combines the technique of scintigraphy and computerized tomography. It utilizes the density of the signal emitted by the labelled compound (radiotracer) to reconstruct quantitative images of the tracer's concentration. The ability of PET to acquire non-invasive functional images makes it a unique tool for studying pharmacokinetic, physiological

and biochemical process in vivo in humans. PET provides two kinds of information: functional information, such as regional cerebral blood flow, metabolism or receptor occupancy during a particular task, and anatomical localization (Cherry and Phelps, 1996). So far its principal roles include the in vivo measurement of blood flow, metabolism and receptor concentrations. This technique is making use of an increasing variety of radiolabelled tracers.

The positron emitting isotopes commonly used for PET tracers are mostly ^{11}Carbon, ^{13}Nitrogen, ^{15}Oxygen, ^{18}Fluorine. The half-lives of ^{11}Carbon, ^{13}Nitrogen, ^{15}Oxygen, ^{18}Fluorine are 20.4, 9.96, 2.05, 109.7 minutes. They are produced by chemical reactions involving one of the several common isotopes in a cyclotron. The short half-lives of the isotopes reduces the dose of radiation to the subject and allow for repeat studies to be performed and also necessitates the presence of an on-site cyclotron. The radioisotope then undergoes chemical synthesis producing the requiring compound incorporating a positron emitting label. A wide variety of molecules such as receptor agonists, water, enzyme substance or precursor can be labelled. High initial yields of positron emitters and fast subsequent synthesis produce tracers with high specific activity. The specific activity of a compound is defined to be the ratio of radioactivity to

mass of the compound. It should be ensured that the concentrations of the unlabelled compound do not interfere pharmacologically with the *in vivo* measurement of the radioligand kinetics (Myers et al., 1992).

The fundamental mechanism of PET is the emission of a positron from an unstable nucleus and the consequent annihilation with a nearby electron. This annihilation produces two almost collinear gamma rays of 511keV each that can be detected in coincidence on either side of the active volume. The localization of the annihilation allows the tracers spatio-temporal distribution to be determined. In addition, the detection of the two gamma photons as opposed to single photons as in conventional nuclear medicine facilitates the determination of absolute tracer concentration (Hoffman and Phelps, 1986). This enables functional parameters to be accurately derived and increases detection sensitivity.

1.3.2 Compartmental modeling

PET provides functional information such as regional blood flow or receptor occupancy during a particular task and anatomical localization. To derive functional information, it is necessary to perform the appropriate tracer kinetic modelling, which allows for the estimation of confound-free biological parameters. These particular models require an arterial blood or

plasma input function while the number of tissue compartments is dictated by the physical, biochemical and pharmacological properties of the system under study. Plasma input models in PET often are treated as gold standard (Sokoloff, 1984; Mintun, 1984). The impulse response function is a sum of exponentials. The nonlinear least squares methods are used to estimate the model parameters. For reversible tissue kinetics, the total volume of distribution, V_D, is given by the integral of the impulse response function. For irreversible tissue kinetics, the irreversible uptake rate constant from plasma, K_I, is given by the final value of the impulse response function (Gunn et al., 2001). The final value of the impulse response function is equal to the limiting slope of a Patlak plot (Patlak et al., 1983).

In order to avoiding blood sampling, the reference tissue models have been developed for neuroreceptor studies (Lammertsma et al., 1996; Gunn et al., 1997; Watabe et al., 2000). Reference tissue models assume that there exists a reference tissue essentially devoid of specific binding sites. The number of identifiable compartments in the reference region and in the region of interest is dependent on the rate of exchange of the tracer between the free, non-specifically bound and specifically bound pools of tracer (Gunn et al., 2001). Parameter estimates may be obtained

by the weighted least squares fitting of these models to measured PET data. The plasma input models in PET are treated as gold standard and reference tissue methods are validated against them.

1.3.3 Receptor imaging

Due to the biochemical selectivity of PET, the neuroreceptor can be investigated at very low concentration, typically in the nanamolar to the picomolar range. Specific radioactive tracers can be designed to bind selectively to molecular targets such as enzymes, transporters and receptors, as well as neuromodulators and second messengers. This has enabled the evaluation of hypotheses regarding neurotransmitter function and regulation that are generated from basic neuroscience studies in animals, and the investigation of the neurochemical substrates of neurological disorders. A variety of radiolabelled ligands have been designed for tracing different signalling systems in the human brain, including the dopaminergic, serotonergic, cholinergic, opiate, and GABAergic system (Grasby et al., 1996; Kessler, 2003). PET therefore provides the unique possibility to identify molecular targets of anesthetics and to probe their action on neurochemical process *in vivo*.

1.3.4 Regional Cerebral Blood Flow and cerebral metabolic rate for glucose

Regional cerebral blood flow (rCBF) and cerebral metabolic rate for glucose (CMRGlu) are two useful indices of regional brain function. In cognitive neuroscience, PET study is often used to map changes in rCBF and CMRGlu caused by well-defined stimuli or tasks. These studies are usually called activation studies. PET studies of anesthesia action in the human brain are often based on comparing brain physiological variables measured under different states of anesthesia. Regional changes in CBF and CMRGlu are assumed to reflect changes in regional neural activity and may provide neuroanatomical evidence for behavioural responses associated with unconsciousness induced by general anesthetics.

The idea that blood flow within a specific region of the brain is closely related to function was first presented by Roy and Sherrington in 1890 (Roy et al., 1890). The theoretical basis for regional rCBF measurements with PET is the animal research by Kety (1951, 1960), which allows assessment of rCBF in laboratory. There is no doubt that activation of brain areas is associated with an increase in rCBF (Friedland et al., 1979) although the exact relationship between those changes and the way they are mediated are not fully understood. In human studies, the tracer of

choice of rCBF measurement is ^{15}O-labeled water ($H_2{}^{15}O$)(Herscovitch, 2001). This molecule can diffuse freely across the blood-brain barrier. Due to its short half-life (2 min) the tracer allows the performance of repeated measurements in a single study session. After injection of a single dose of $H_2{}^{15}O$ PET images are immediately acquired to obtain the brain time activities and to calculate maps of rCBF.

The regional cerebral metabolic rate of glucose utilization (rCMRglu) can be measured with a PET scanner and [^{18}F]fluorodeoxyglucose (^{18}FDG). As a glucose, this tracer is taken up by brain neurones depending on their functional state. It is phosphorylated in the brain tissue by hexokinase to FDG-6-phosphate. Unlike glucose, FDG-6-phosphate becomes intracellularly trapped for at least 45 min without being further metabolized. Uptake of FDG and metabolic trapping of FDG-6-phosphate is nearly complete about 30 min after injection of the tracer. The amount of radioactivity in each region of the brain is related to the glucose uptake and the glucose metabolism in this region. However, this technique has obvious limitations. Due to the long half-life (110 min) and the long uptake period, repeated scans are difficult to perform, many drug studies have been performed using rCBF rather than CMRGlu as an index of local cerebral activity (Herscovitch, 2001).

1.3.5 Role of PET studies in the research of the mechanism of unconsciousness

Alkire et al. (1997, 1999, 2000) have examined the effects of propofol and of two inhalation general anesthetics, isoflurance and halothane, on neuronal activity in humans with the PET-FDG technique. In these studies the anesthetics were incrementally titrated to the point of unresponsiveness and brain glucose metabolism was investigated during steady-state conditions. At the same clinical endpoint, similar results in global brain glucose metabolism were obtained for the three agents. Halothane decreased global glucose metabolism by 40%, isoflurane by 46%, and propofol by 55%. This general decrease in metabolic activity is believed to reflect the reduced synaptic activity across the brain during anesthesia. They also revealed the differences in regional metabolic reduction caused by the volatile agents. They found that both isoflurane and halothane caused a specific relative reduction of regional cerebral glucose metabolism primarily in the thalamus and also in the midbrain reticular formation, basal forebrain, cerebellum, and occipital cortex (Alkire et al., 2000). These findings reflect the importance of the thalamus as a target in inhibition of the flow of information to the cortex.

The results of recent $H_2{}^{15}O$ PET studies in our research group further support the hypothesis that specific neural networks contribute to the unconsciousness induced by anesthetics (Bonhomme et al., 2001; Fiset et al., 1999). Fiset and co-workers (1999) investigated rCBF during graded changes of propofol anesthesia. They found a 20.2% overall decrease in absolute CBF, indicating an overall decrease in cortical neural activity. They also found a strong correlation between the level of consciousness and the reduction in CBF in the thalamus, basal forebrain, and occipital and parietal regions. In addition, a significant covariation between the thalamic and midbrain blood flow changes was observed, suggesting a close relationship between these structures. These findings have been confirmed by another study of our research group (Bonhomme et al., 2001). In this study, a stimulus-induced study design was chosen. Changes in rCBF were measured in order to determine whether different levels of propofol anesthesia would affect subcortical and cortical processing of vibrotactile stimuli in a different way. This study showed a dose-dependent impairment of the processing of vibrotactile stimuli in a different way. Suppression of rCBF response in thalamus was found only when volunteers have lost consciousness. This finding provides further evidence for the importance of thalamus in mediating drug-induced

unconsciousness. Specific changes in rCBF were also reported for midazolam. Veselis et al. (1997B) found that the largest decrease of rCBF was in thalamus during deep midazolam sedation. Other PET studies of benzodiazepines also demonstrated large decrease in regional neural activity in the thalamus after lorazepam (Volkow et al., 1997) and midazolam administration.

Different radioligands have been used to examine different or same receptors binding in PET studies. Accuracy of receptor binding measurement depends on the kinetic property of the radioligands. To quantify muscarinic receptor binding, different PET studies have employed different radiotracers, including [^{11}C]scopolamine (Frey et al., 1992), [^{11}C]tropanyl benzilate (koeppe et al., 1994), [^{11}C]benztropine (Dewy et al., 1990, 1993), and [^{125}I]3-qyunuclidinyl-4-iodobenzilate (Sawada et al., 1990). But these agents share relatively slow dissociation rates from the muscarinic receptor, which may limit the precision of their uses for receptor binding estimates. Additionally, compartmental kinetic analysis is hindered when the rate of ligand binding is rapid relative to the rate of its transport from blood to tissue, because tissue activity levels become delivery limited and receptor estimates become prone to bias from effects of altered blood flow. A novel, radiolabelled, muscarinic receptor

antagonist, [^{11}C]N-methyl-4-piperidyl benzylate (NMPB), was developed by Mulholland et al. (1995), and has more favorable kinetic properties. NMPB has higher dissociation rates than many of the prior radioligands. Tracer kinetic modeling with NMPB has been verify and validated in recent studies published by Zubieta et al. (1998, 2001).

1.4 Study Design

Chapter 2 describes the first study presented in this thesis: PET quantification of muscarinic cholinergic receptors with [N-11C-methyl-benztropine and application to studies of propofol-induced unconsciousness in healthy human volunteers. This study allows us to understand the effect of propofol on central muscarinic receptor availability during general anesthesia. It introduces the kinetic analysis methods for estimation of the receptor availability of the muscarinic receptor using dynamic positron emission tomography (PET) studies with [N-^{11}C-methyl]-benztropine. Chapter 3 presents the second study of the present thesis: a PET investigation of the brain function changes specifically linked to the difference in level of consciousness. In this investigation, we used physostigmine (an anticholinestherase) to restore consciousness induced by propofol. Chapter 4 is the general discussion about a complete

neurophysiological theory of the action of anesthetics to suppress consciousness and a theory of consciousness restored by physostigmine.

Chapter 2 PET Quantification of Muscarinic Cholinergic Receptors with [N-^{11}C-methyl-benztropine and Application to Studies of Propofol-induced Unconsciousness in Healthy Human Volunteers

Xie, G., Gunn R.N., Dagher A., Daloze T., Plourde G., Backman S., Fiset P. (2004). PET Quantification of Muscarinic Cholinergic Receptors with [N-11C-methyl-benztropine and application to studies of Propofol-induced Unconsciousness in Healthy Human Volunteers. Synapse 51: 91-101, 2004.

2.1 Abstract

This work evaluated kinetic analysis methods for estimation of the receptor availability of the muscarinic receptor using dynamic positron emission tomography (PET) studies with [N-^{11}C-methyl]-benztropine. The study also investigated the effect of propofol on central muscarinic receptor availability during general anesthesia. Six volunteers were scanned three times, once for baseline whilst awake, once during unconsciousness, and once after recovery to conscious level. An irreversible two-tissue compartment model was used to estimate the [N-11C-methyl]-benztropine specific binding rate constant k3, a measure of muscarinic receptor availability. Two different estimation methods were used: (1) optimization with positivity constraints on all the parameters; (2) optimization with additional constraints determined from a one-tissue compartment fit to the cerebellum. In regions with low to middle muscarinic receptor density, the k3 values from method (2) had lower standard errors than that for method (1) and gave a higher correlation with the density of muscarinic receptors measured by in vitro studies (r2 of 0.98 for method 2 and r2 of 0.72 for method 1). But the k3 values determined by method 2 had higher errors for regions with high muscarinic receptor density as compared to method 1. For both methods, the mean

k3 values during unconsciousness were generally lower than those during awake for most regions evaluated. Given the higher degree of correlation with in vitro data, the method with additional constraints derived from the cerebellum (method 2) was deemed superior for regions with low to middle muscarinic receptor density. The finding may also suggest propofol-related reductions in muscarinic receptor availability.

2.2 Introduction

The present study was designed to determine the changes in muscarinic receptor occupancy of the brain during general anesthesia with propofol using Positron Emission Tomography. PET has been used to study the distribution and occupancy of muscarinic receptors in the human brain, using [^{11}C]scopolamine, [^{11}C]N-emthy-4-piperidyl benzilate (NMPB), 3-quinuclidinyl-4-iodobenzilate (QNB), and [N-^{11}C-methyl]-benztropine. We have used [N-^{11}C-methyl]-benztropine, a non-selective muscarinic receptor antagonist, and propose a method of analysis that attempts to address some of the challenges in quantifying receptor parameters with an irreversibly bound radiotracer.

The use of PET with ligand displacement techniques for the study of anesthetic mechanism is supported by the fact that some properties of anesthetic drugs, including loss of consciousness and antinociception, have been shown to be related to their specific effects on ligand-gated ion channels, pre- and postsynaptic receptors and second messenger systems (Franks NP et al, 1994; Yamakura T et al., 2001). However, the mechanism underlying loss of consciousness is poorly understood. Many neurotransmitter systems are affected during pharmacological sedation,

including GABA (Mihic SJ et al., 1997; Gyulai FE et al., 2001; Alkire MT et al., 2001), glutamate (Flohr H et al., 1998, Cheng G et al., 2000) and acetylcholine (ACh) (Tassonyi E et al., 2002).

ACh has been a target of investigation in sleep states and anesthetic induced alteration of consciousness. It has been postulated that the level of acetylcholine in the medial pontine reticular formation plays an important role in the generation of REM sleep states. Furthermore, microdialysis studies performed in animals have shown that following the administration of drugs like morphine and halothane, ACh levels in the medial pontine reticular formation were significantly decreased compared to the awake state. Recent rat studies using in vivo microdialysis have also demonstrated that propofol has dose-dependent inhibitory effects on acetylcholine release in the frontal cortex and hippocampus (Kikuchi T et al., 1998; Wang Y et al., 2000). Furthermore, Pain L et al. (2000) showed that a central cholinergic depletion attenuates the sedative effect of propofol in the rat brain. Their results suggest that basal forebrain cholinergic neurons might mediate part of sedative /hypnotic effects of propofol.

ACh is the physiologic agonist for both nicotinic and muscarinic receptors. The nicotinic receptor is a multi-subunit, ligand-gated ion

channel or an ionotropic receptor and the muscarinic receptor is a single-subunit, G-protein-coupled receptor or metabotropic receptor. Despite the fact that neuronal nicotinic receptors are very sensitive to anesthetic agents, it has been suggested that nicotinic receptors in the brain do not have a primary role in unconsciousness, but may be involved in the generation of CNS side effects of general anesthesia (Downie et al, 2000).

On the other hand, it is believed that muscarinic transmission is one of several pathways that play a significant role in the process of sedation (Durieux ME et al., 1996). In the CNS cholinergic transmission is mainly mediated by muscarinic receptors. There are five subtypes that are all expressed in the brain of mammals (m1-m5). The prominent effect on memory and consciousness played by the CNS cholinergic system is evident from the effects of the muscarinic antagonist scopolamine (Durieux ME, 1996). In a series of studies done on human volunteer, our group has shown that physostigmine reverses the propofol-induced unconsciousness in human volunteers. The reversal of the unconsciousness was blocked by pretreatment with scopolamine. Our findings support the hypothesis that the loss of consciousness produced by propofol is mediated at least in part via interruption of central cholinergic muscarinic transmission (Meuret P et al., 2000). The combined

evidence that during anesthesia, ACh levels are decreased in the pontine reticular formation as well as in the projection systems in the cortex, and that scopolamine, possibly via a muscarinic mechanism, mediates conscious levels during anesthesia has led us to study in humans the changes in muscarinic receptor occupancy during anesthesia.

Dewey et al have, in a series of studies, used [N-^{11}C-methyl]-benztropine to map muscarinic receptor density and determine the modulatory effect of various neurotransmitters on muscarinic transmission. They found that the greatest incorporation quotient (IQ) of radioactivity was the corpus striatum and reported smaller values in the frontal, parietal and temporal cortices. The IQ closely corresponded to the distribution of muscarinic receptors as demonstrated by autoradiographic studies of postmortem human brain (Dewey SL et al., 1990). Additionally, using the distribution volume (DV) measured by Logan plot, they demonstrated that drugs acting upon either GABAergic or serotonergic neurons produced profound regional changes in acetylcholine release (Dewey SL et al., 1993). In this study, we developed an approach to estimate the receptor availability using compartmental modeling. Different compartmental models were initially fitted to the data in order to identify an appropriate model.

The aim of this study was to determine an appropriate method to estimate CNS muscarinic receptor availability using PET and [N-^{11}C-methyl]-benztropine. Using the identified method, we tested the hypothesis that the loss of consciousness induced by propofol is mediated at least in part by the reduction of central muscarinic transmission by demonstrating the changes in muscarinic receptor availability during unconsciousness induced by propofol.

2.3 Methods

2.3.1 Subjects

Six healthy volunteers aged 21-35 years (mean 25.8 ± 7.2, 2 men, 4 women) were recruited via local newspaper advertisements and studied after appropriate medical evaluation. The studies were approved by the Research Ethics Committee of the Montreal Neurological Institute and Hospital and informed written consent was obtained. Women were tested for pregnancy no more than 1 week before the experiment and were requested to use an appropriate contraceptive method.

2.3.2 Monitoring and data acquisition

After comfortable installation on the PET scanner bed, anesthesia monitoring devices (EKG, pulse oxymeter and respiratory impedance) were applied. EEG electrodes were placed at FP and FP referred to A1 for measurement of the bispectral index (BIS). BIS is a quantitative EEG variable used clinically for guiding the administration of anesthetic agents. An intravenous catheter was placed in the right forearm for drug infusion. Another catheter was inserted in the left radial artery for procurement of blood samples for determination of propofol plasma levels (Plummer et al., 1987) and radiotracer activity via subsequent counting in a NaI well-counter. Oxygen was administered at a rate of 3L/min through nasal prongs. Subjects are blindfolded, and ambient noise is kept to a minimum.

2.3.3 Drug administration control

Subjects fasted for at least 8h prior to the study. Propofol was given using a computer controlled infusion pump (CCIP) and the infusion program STANPUMP. That program uses pre-determined population pharmacokinetics, the volunteer's pertinent covariates, and a multi-exponential infusion algorithm to quickly reach and maintain a target plasma concentration (Tackley RM et al., 1989). Propofol plasma concentrations of 2.0, 3.0 or 4.0 ug/ml were targeted depending on the

minimal plasma concentration associated with loss of consciousness which was defined as the loss of response to verbal commands (" Move your toes, raise your thumb."). These concentrations were compatible with safe, spontaneous breathing. Once unconsciousness was reached, PET scanning was delayed by 10 minutes to allow for blood-brain equilibration of propofol concentrations (Dutta S et al., 1998).

2.3.4 Scanning procedure

Three separate dynamic PET brain scans (CTI/Siemens HR + PET tomograph, 32-ring, 63-slices) were obtained in each subject: baseline (awake prior to propofol infusion), unconscious (during propofol infusion), and regained consciousness (following cessation of propofol infusion, subject fully awake). Each scan was performed for a period of 60 minutes following an intravenous injection of [N-^{11}C-methl]-benztropine (13 mCi). To measure the plasma input function of [N-^{11}C-methl]-benztropine to the brain, arterial blood samples were obtained every 30sec from 15 sec to 120 sec, and then subsequently at 3, 4, 6, 8, 11, 15, 20, 30, 40, 50, and 60 min after tracer injection. Blood samples were centrifuged to separate plasma, weighted, and their plasma radioactivity was determined for estimation of the input function that is illustrated in Figure 2-1A. Arterial

blood samples for propofol assay were taken just before the injection of benztropine, and twice post-injection (30 min & 60 min). Each subject received an MRI scan on another day to provide adjunct structural data for region of interest definition.

2.3.5 PET data analysis

A summed radioactivity image was generated from each scan and co-registered to the individual's MRI using automated algorithms (Evans et al., 1992). Regions of interest (ROIs) were drawn on each subject's MRI on the anterior cingulate cortex (acc), caudate nucleus (cau), cerebellum (cbl), frontal cortex (frc), globus pallidus (glp), occipital cortex (occ), orbito-frontal cortex (ofc), pons (pon), putamen (put), thalamus (tha), temporal lateral cortex (tlc), and temporal medial cortex. Left and right ROIs were combined for the data analysis. The time-activity curves (TAC) for each ROI were extracted from the dynamic PET data (Figure 2-1B) and used for the regional quantification of the binding of [N-^{11}C-methl]-benztropine.

Figure 2-1: Plasma and tissue time-activity curves

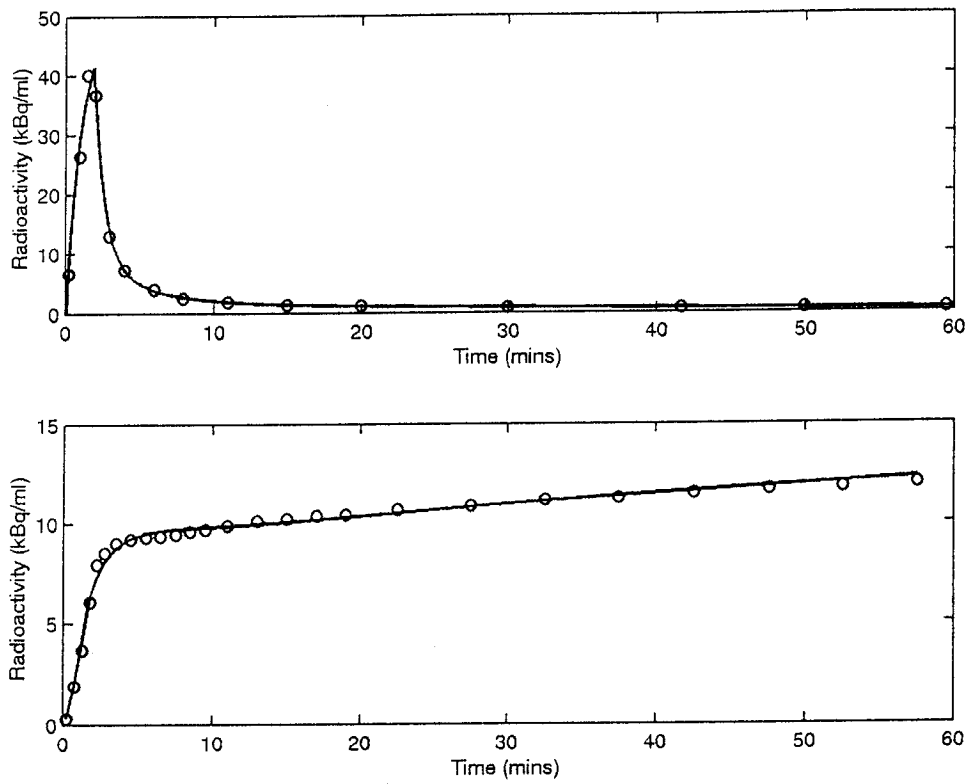

(A) Plasma time-activity curve from one volunteer and (B) tissue time-activity curve from the parietal cortex (o) in the same volunteer and the fit from Method 1 (Positivity constraints).

2.3.6 Arterial input function

The discrete plasma radioactivity measurements were interpolated with a step function (having a value of 1 between the time of injection and peak plasma radioactivity and 0 elsewhere) convolved with a sum of exponentials (the fit was obtained using a non-negative least squares fit of a set of basis functions). As individualized metabolite data was not available a population based metabolite correction was applied according to the published data of Dewey et al. (1990). Dewey et al determined the percent of unchanged [N-^{11}C-methl]-benztropine in human and baboon plasma. They found that the metabolism of [N-^{11}C-methl]-benztropine in human plasma is very slow in sharp contrast to that in baboons. An exponential function was fitted to their human data to allow for an approximate correction of the plasma data. The equation for the parent radiotracer fraction in plasma was $ae^{(-\beta t)}$, where $a=0.98$, $\beta = 0.0056$ min-1, and t is the time after injection. This allowed for an estimate of the parent plasma radioactivity time course based on population metabolite data.

2.3.7 Compartment modeling

To determine an appropriate model for benztropine kinetics, we evaluated three compartment models including a one-tissue compartmental model (2 parameters), and two-tissue compartmental models with (3 parameters - irreversible binding), and (4 parameters - reversible binding) (Figure 2-2; for more detail see Appendix C of Gunn et al., 2001). Model parameters and the residual sum of squares (RSSQ) were estimated for each of the 13 brain regions for the three models by nonlinear least-squares fitting. Weighted least squares fitting were performed with weights determined from the whole brain data and calculated as (frame duration/whole brain TAC). An F test was used to assess the reduction in the sum of squares for more highly parameterized models and thus impart information on the most appropriate model. With the 3 parameter model, 181 out of 234 data sets were fitted significantly better than the 2 parameter model. But with 4 parameter model, only 42 out 234 data sets were fitted significantly better than 3 parameter model. Thus, the irreversible two-tissue compartmental model with 3 parameters was chosen as the most appropriate model for these data. For cerebellum alone, with the 3 parameter model, 13 out of 18 data sets were fitted significantly better than the 2 parameter model. With 4 parameter model, 8 out 18 data sets were fitted significantly better than 3 parameter model.

Figure 2-2: Compartmental models

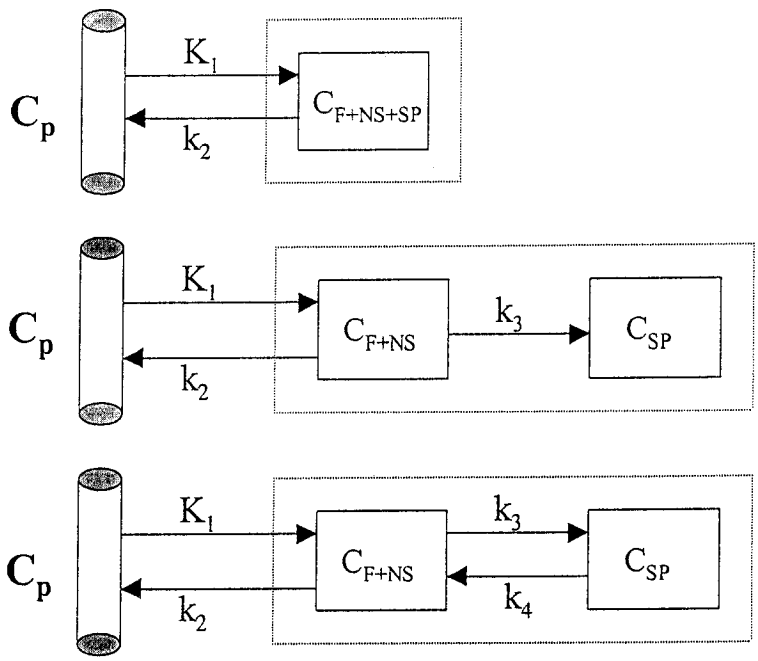

Compartmental model configurations and designated intercompartmental transfer coefficients. Top: One-tissue compartmental (2k) model. Middle: Two-tissue irreversible compartmental (3k) model. The net irreversible uptake rate constant from plasma is given by,

$$K_I = \frac{K_1 * k_3}{k_2 + k_3}.$$

Bottom: Two-tissue reversible compartmental (4k) model. The distribution of receptor-binding ligands includes an intravascular compartment (Cp) and three tissue tracer compartments representing free tracer (C_F), nonspecifically bound tracer (C_{NS}), and specifically bound tracer (C_S). C_{F+NS+S} is the simplification of the model combines all three tissues pools into a single compartment. C_F+N_S is the simplification of the model, which combines two tissue pools into a single compartment.

For the cerebellum the reversible two-tissue compartmental model with 4 parameters was selected.

Accurate estimation of individual parameter values from an irreversible two-tissue compartment model is usually not possible because of the high degree of correlation between the parameters k_2 and k_3. Furthermore, there is also a problem when using a macro parameter such as the net irreversible uptake rate constant from plasma (K_I) as this parameter is not independent of blood flow. In order to improve the accuracy of the individual rate constant estimation process the inclusion of additional constraints was investigated; Method 1 - based on basic biologic properties of the model all parameters were constrained to be non-negative within the non-linear least squares fitting process. Method 2 - The K_1/k_2 ratio in tissue regions was constrained to the volume of distribution (VD) values obtained from a two tissue compartment model fit to the cerebellum data, leaving only two parameters to be estimated by non-linear least squares. Koeppe et al. have explored the possibility of constraining the ratio of the transport parameters (K_1/k_2) as this ratio can be relatively constant across the brain for many PET tracers studied (Koeppe et al., 1999). To evaluate kinetic analysis alternatives for estimation of relative acetylcholinesterase activity using dynamic PET

studies of irreversible tracer [^{11}C] PMP, they constrained the K1/k2 ratio (= 4.0) to the mean estimate across cortical regions of all subjects from the unconstrained fits. They demonstrated that constrained methods yielded lower Coefficient of Variation and were superior in regions with moderate to high AChE activity.

Lin et al. (1986) demonstrated that the density of muscarinic receptor in cerebellum is very low compared with cortex and striatum. Therefore the cerebellum was the most appropriate choice for the region in which to determine the free+non-specific binding volume of distribution. We determined the K_1/k_2 ratio for the cerebellum of each scan of each subject and then fixed this to a constant value for all subsequent irreversible compartmental model fits for that scan of that subject.

2.3.8 Statistical analysis

Changes in the parameter estimates k_3, K_1 and K_I were assessed using a two-way within subject analysis of variance (ANOVA), the first factor being the experimental periods (awake, unconsciousness, recovery), and the second factor being the brain regions (the brain region measured). Tukey's HSD tests were used for the post-hoc comparisons. Due to the variance of K_3 during unconsciousness is lower than those during awake

and recovery condition, which indicates the K_3 value is not normal distributed, we also tested the main effect of experimental condition using the Freedman's test. Then we used Wilcoxon test for post-hoc comparisons. We analyzed the variability of the heart rate (HR), the mean arterial pressure (MAP), and BIS across conditions using a one-factor within-subject ANOVA and Tukey's HSD for post-hoc comparisons. Values are expressed as the mean ± 1 SD unless specified and a $p<0.05$ was considered significant.

2.4 Results

2.4.1 Monitoring

All (six) volunteers enrolled completed the study. The BIS, MAP, and HR were measured at 0' , 10' , 20' , 30' , 40' , 50' , and 60' of each scan. The BIS during unconsciousness was significantly lower than those during awake and recovery ($p< 0.01$). The MAP during unconsciousness was significantly lower than those during awake and recovery ($p < 0.01$). There were no significant differences among three experimental periods concerning HR ($p > 0.05$) (Table 2-1).

2.4.2 PET data analysis

Table 2-1. BIS - Bispectral index, MAP and HR data

	Scan1	Scan2	Scan3
BIS	93.5 ± 3.5	36.8 ± 4.9*	93.9 ± 3.0
MAP (mmHg)	91.9 ± 3.8	69.8 ± 5.9*	91.5 ± 4.0
HR (beats.min^{-1})	69.4 ± 17.7	69.5 ± 5.9	60.0 ± 11.2

Values are mean ± SE.

* P<0.01 compared with Scan1 and Scan3.

2.4.2.1 Method 1 - Parameter positivity constraints

Mean K_1 and K_I were generally higher during unconsciousness and recovery than during awake. A two-way within-subject ANOVA on K_1 and K_I revealed no significant main effect of consciousness states (K_1: $p = 0.60$, K_I: $p = 0.79$), a significant main effect of brain regions ($p < 0.0001$) for K_I, no significant main effect of brain regions ($p = 0.21$) for K_1 (Figure 2-3). Figure 2-4 shows the k_3 values during awake, unconsciousness, and recovery in all regions. Mean k_3 values during unconsciousness were generally lower than those during awake for most regions evaluated. A two-way within-subject ANOVA on k_3 revealed no significant main effect of the experimental periods ($p = 0.087$) and a significant main effect of brain regions ($p < 0.0001$). Using the Friedman's test, we find the significant main effect of the experimental periods in cerebellum ($p=0.03$) and parietal cortex ($p=0.01$). Post-hoc pairwise comparisons using Wilcoxon test revealed k_3 during unconsciousness was significantly lower than that during wake condition in parietal cortex ($p=0.03$) and k_3 during recovery was significantly lower than that during wake condition in cerebellum ($p=0.03$). Figure 2-5 compares the k_3 values measured in our PET study with the known muscarinic receptor distribution measured with [^{3}H]-QNB in human post mortem material (Lin et al., 1986). We found that

Figure 2-3: The K_I and K_1 values estimated with Method 1

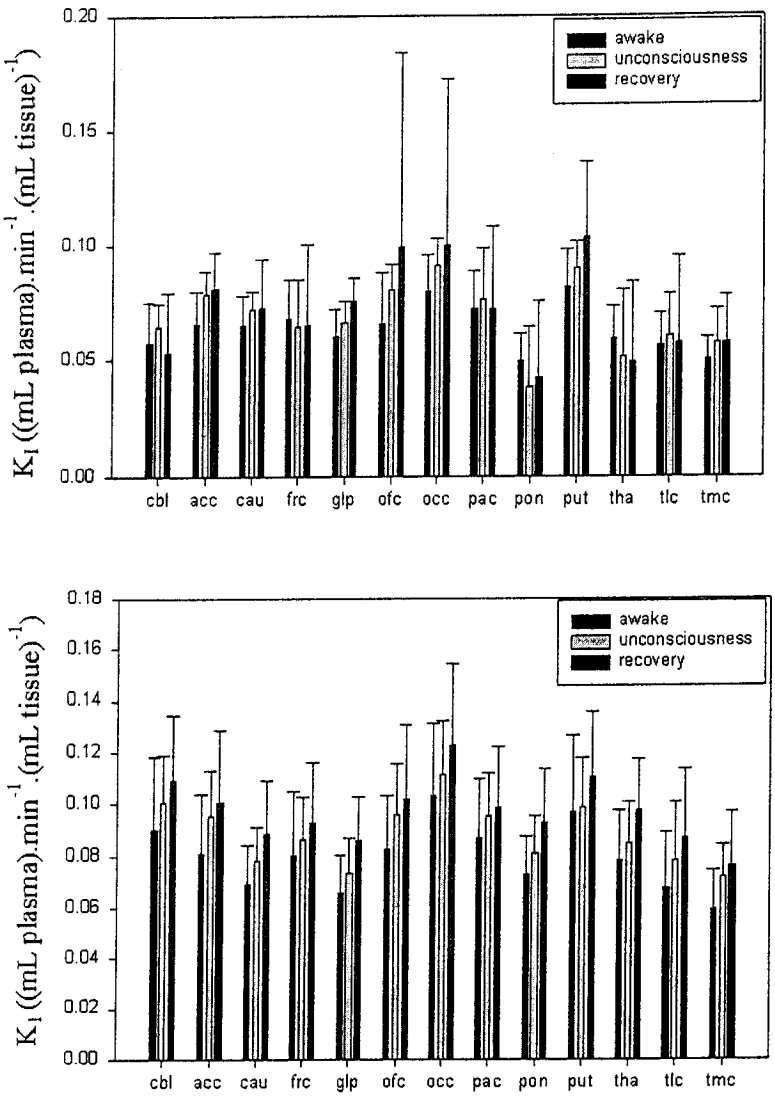

The K_I and K_1 values during awake, unconsciousness, and recovery for different regions of brain with constraints restricting parameters to positive value

Figure 2-4: The k_3 values estimated with Method 1

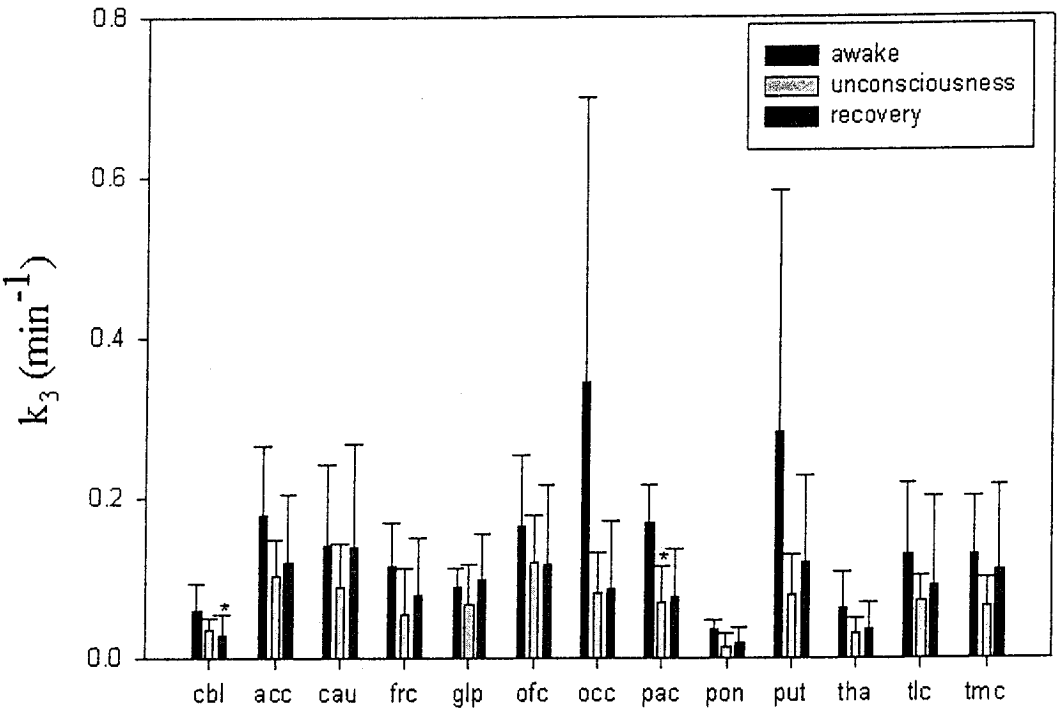

The k_3 values during awake, unconsciousness, and recovery for different regions of brain with constraints restricting parameters to positive value

Figure 2-5: Comparison of k_3 values from Method 1 with the muscarinic receptor density measured in vitro

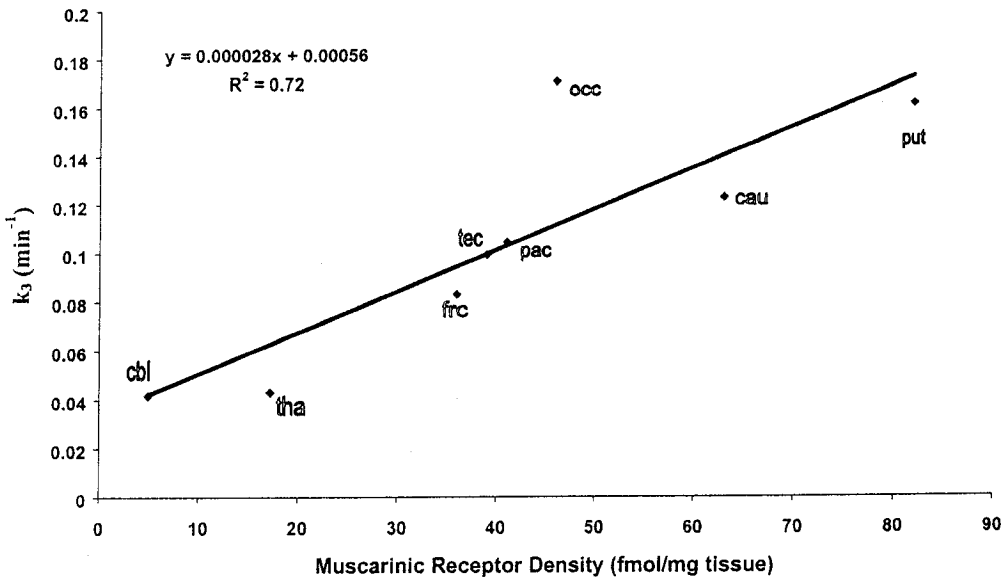

Comparison of k_3 values from Method 1 with the known muscarinic receptor distribution measured with [^{3}H]-QNB in human postmortem material by Lin et al. (R^2 = 0.75 without cau and put)

the k_3 measured in vivo with our PET study is correlated with density of muscarinic receptors measured in vitro study with an r^2 of 0.72.

2.4.2.2 Method 2 - Constraining free+nonspecific VD with values from the cerebellum

Mean K_1 and K_I were also generally higher during unconsciousness and recovery than during awake. A two-way within-subject ANOVA on K_1 and K_I revealed no significant main effect of consciousness states (K_1: $p = 0.089$, K_I: $p = 0.78$), but did reveal a significant main effect of brain regions (K_1: $p < 0.001$, K_I: $p < 0.001$) (Figure 2-6). Figure 2-7 shows the k_3 values during awake, unconsciousness, and recovery in all regions evaluated. Mean k_3 values during unconsciousness were generally lower than those during awake for most regions evaluated, and mean k_3 values during recovery were also generally lower than those during awake, and were generally higher than those during unconsciousness (recovery toward the awake level) for most regions. A two-way within-subject ANOVA on k_3 revealed no significant main effect of the experimental periods ($p = 0.1568$). Using the Friedman's test, we find the significant main effect of the experimental periods in frontal cortex ($p=0.03$), orbital-frontal cortex ($p=0.03$) and temporal medial cortex ($P=0.03$). Post-hoc pairwise

Figure 2-6. The K_I and K_1 values estimated with Method 2

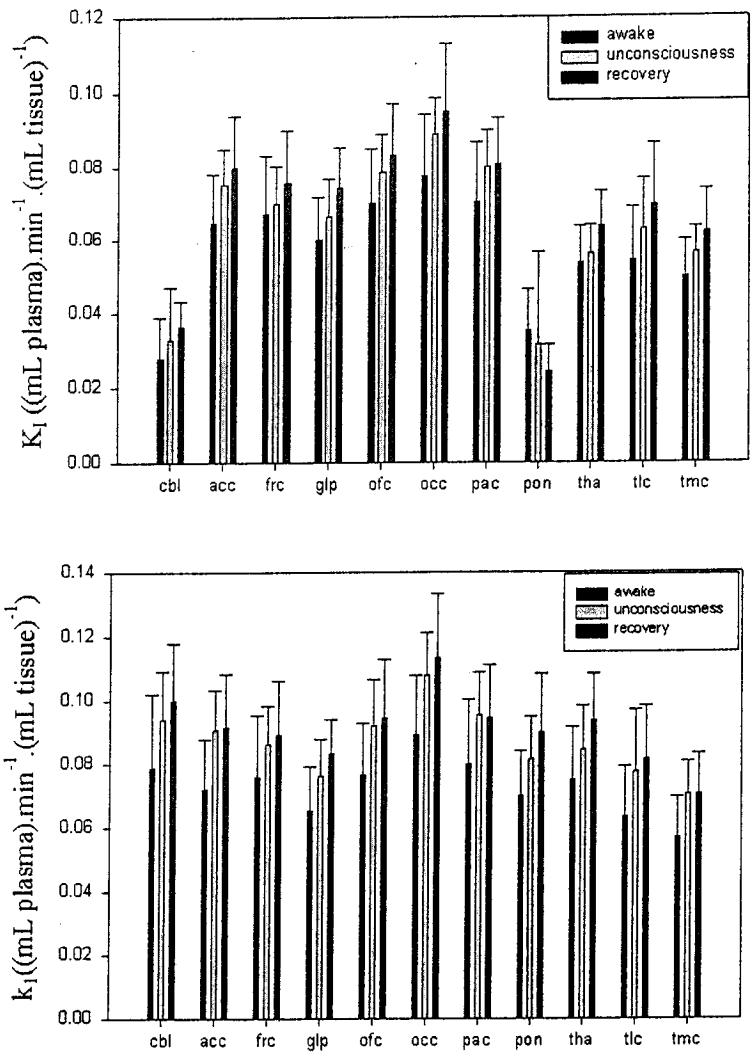

The K_I and K_1 values during awake, unconsciousness, and recovery for different regions of brain with constraints restricting K_1/k_2 to individual value determined by one-tissue modeling

Figure 2-7. The K_3 values estimated with Method 2

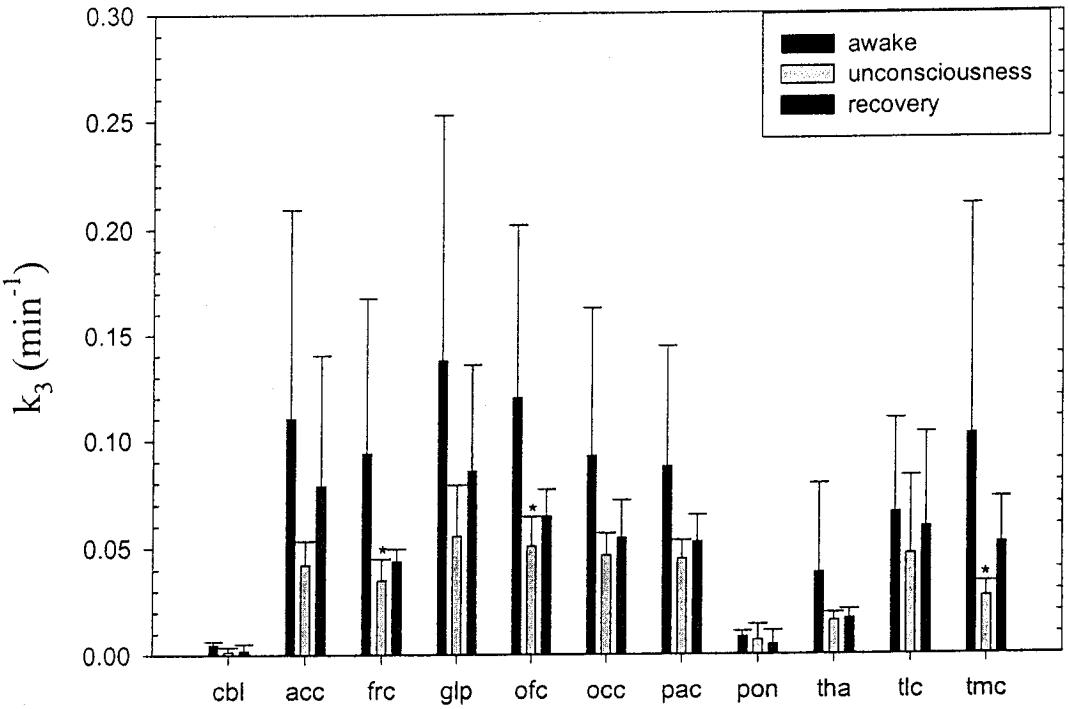

The k_3 values during awake, unconsciousness, and recovery for different regions of brain with constraints restricting K_1/k_2 to individual value determined by one-tissue modeling

comparisons using Wilcoxon test revealed k_3 during unconsciousness was significantly lower than that during wake condition in frontal cortex ($p=0.03$), orbital-frontal cortex ($p=0.03$) and k_3 during unconsciousness was significantly lower than that during recovery condition in temporal medial cortex ($p=0.03$). Figure 2-8 compares the k_3 values measured in our PET study with the known muscarinic receptor distribution measured with [^{3}H]-QNB in human material (Lin et al., 1986). The k_3 estimated in vivo with our PET study is closely correlated with the density of muscarinic receptors measured in vitro study with an r^2 of 0.98.

2.5 Discussion

The main goal of this study was to examine the feasibility of using [N-^{11}C-methyl]-benztropine for the quantification of muscarinic receptor binding during wakefulness, propofol-induced unconsciousness, and recovery in health volunteers. In this study, an irreversible two-tissue compartment model was determined as the most appropriate model for [N-^{11}C-methyl]-benztropine.

Irreversibly bound radioligands are a challenge for quantification methods. Whilst, the net irreversible uptake rate constant from plasma can

Figure 2-8: Comparison of k_3 values from Method 2 with the muscarinic receptor density measured in vitro

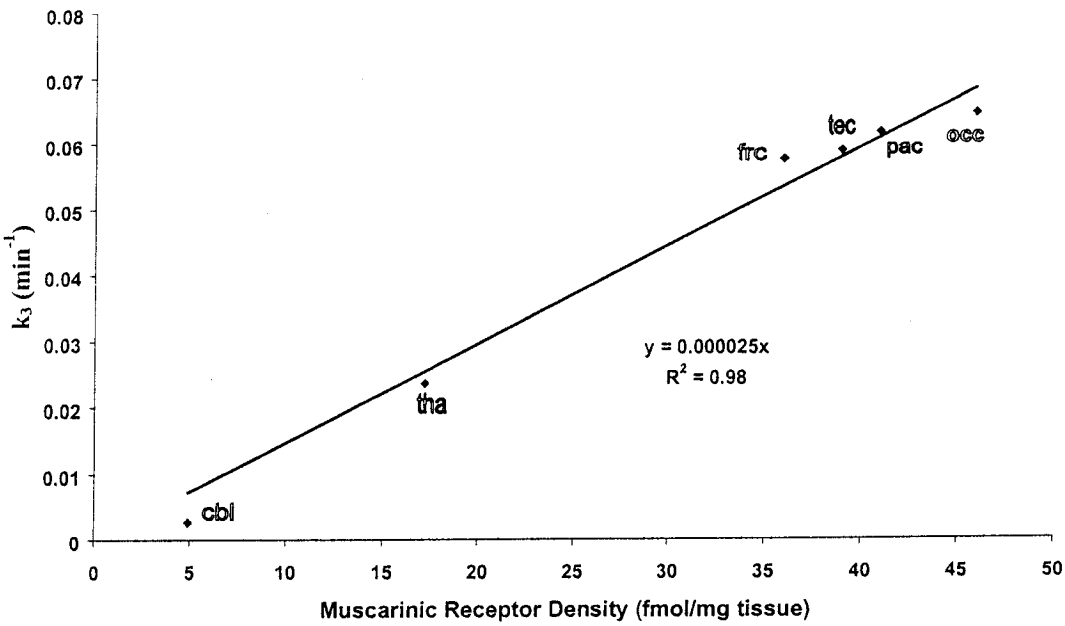

Comparison of k3 values from Method 2 with the known muscarinic receptor distribution measured with [3H]-QNB in human postmortem material by Lin et al. (Compartmental modeling with constraint restricting K1/k2 to that determined by one-tissue modeling of the cerebellum)

be estimated accurately, the parameter itself is confounded by blood flow. Estimation of the individual rate constant k_3, which measures the receptor availability, is compromised by numerical unidentifiability issues related to the parameters high degree of correlation with k_2. The most successful approaches to this problem have involved the addition of constraints to the estimation problem. For example, to estimate the relative acetylcholinesterase (AchE) activity using an irreversible tracer, N-[^{11}C]Methylpiperidin-4-yl propionate ([^{11}C]PMP), Koeppe et al.(1999) compared an unconstrained nonlinear least-squares fit estimating the hydrolysis rate constant k_3 with the methods of constraining the fit by fixing the volume of distribution. They found that the constrained methods are required to yield meaningful estimates and are superior to the unconstrained methods. Lin et al. demonstrated that the density of muscarinic receptor in cerebellum is very low comparing with cortex and striatum (Lin et al., 1986). Thus, in this study, the free and non-specifically bound volume of distribution was approximated from the cerebellum as this region has a low amount of specific binding.

Comparison of methods 1 and 2 revealed that adding constraints derived from the cerebellum provided a better correlation with in vitro measures of the muscarinic receptor density (Method 2 : $r^2 = 0.98$, Figure

2-8 and Method 1 $r^2 = 0.72$, Figure 2-5). Both sets of results are consistent with the specificity of the [N-^{11}C-methyl]-benztropine for the muscarinic sites. The mean coefficients of variation (mCOV) of k_3 values during three PET scans with two different constraints are shown in the Figure 2-9. For the brain regions with low (cbl, pon) and high (cau, put) muscarinic receptor density, the k_3 values estimated by constraining K1/k2 have higher mCOV values comparing with the k_3 estimated with a positivity constraint. For most brain regions with middling muscarinic receptor density, the k_3 values estimated with a constraint on K_1/k_2 have lower mCOV values as compared with the k_3 estimated with positivity constraint.

It has been well documented that a workable irreversible PET radioligand should have not too large a k_3 and a reasonable match between the rate of trapping (k_3) and the rate of BBB transport (k_2) (Koeppe 1996, Frey et al, 1992). If k_3/k_2 is too low, the fraction of tracer trapped is not large enough to give a good signal. If k_3/k_2 is too high the trapping of radiotracer is limited by delivery to the tissue. Whereas K_1 continues to be estimated precisely, the estimates of k_2 and k_3 become extremely variable, yet remain highly correlated. The optimal range for k_3 and k_2 tends to be when the rate constants are of similar magnitudes

Figure 2-9: Mean Coefficients of Variation of k_3 values with two different model constraints

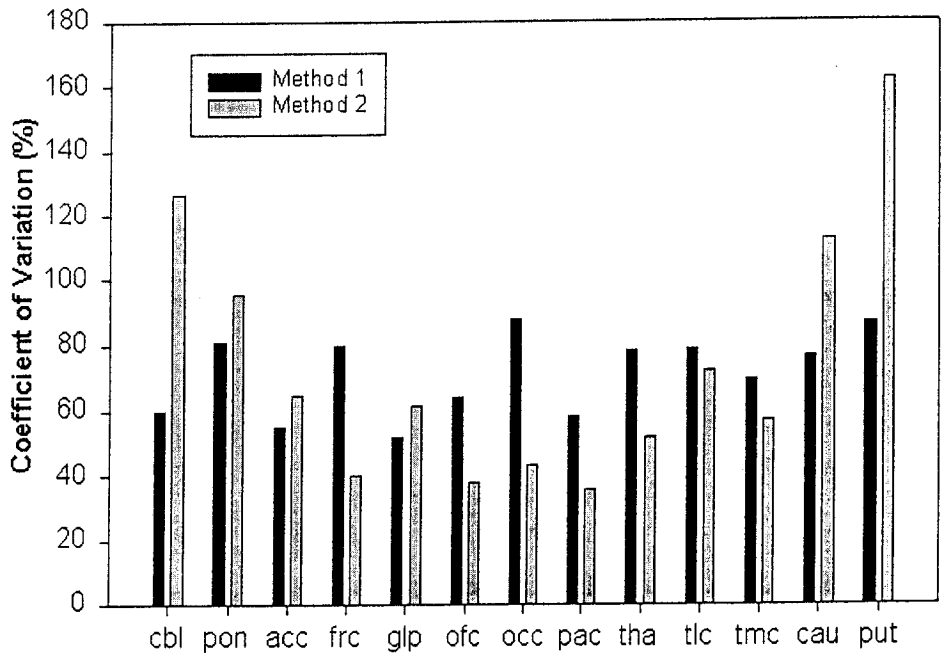

Mean Coefficients of Variation of k_3 values during three PET scans with two different model constraints (Method 1: positive constraints; Method 2: Fixed volume of distribution). Muscarinic receptor availabilities are low in cbl and pon, median in acc, frc, glp, ofc, occ, pac, tha, tlc, tmc, and high in the cau and put.

(Koeppe et al., 1996, 1999). For most regions evaluated in this study (excluding areas of Caudate Nucleus and Putamen), the values of k_3/k_2 during awake tended to be too large for optimal estimation, with mean k_3/k_2 ratios ranging from about 0.3-9.4. The value of k_3/k_2 during unconsciousness and recovery came closer to the optimal range, with mean ranges from 0.1-3.3 and 0.1-4.2. This likely explains the reason for lower COVs of k_3 estimates during unconsciousness and recovery than during awake (Figure 2-10). The estimated k_3/k_2 ratios of subject 1 in Putamen and subject 2 in Caudate Nucleus and Putamen are very high (>500). Therefore, in the areas of high receptor density (Caudate Nucleus and Putamen), accurate estimation of k_3 is not possible (Table 2-2). In these regions, [N-^{11}C-methy]-benztropine suffers the same problem with that of other irreversible tracers, with the irreversible rate of trapping being too rapid rather than too slow.

In a previous human PET study with [N-^{11}C-methl]-benztropine, Dewey et al (1990) determined the incorporation quotient (IQ), which is equivalent to the K_I determined by compartmental modeling in this article. Their mean IQ value (0.099 in frontal cortex) is comparable to our mean K_I values (0.12 for Method 1 and 0.094 for Method 2 in frontal cortex whilst awake).

Figure 2-10: Coefficient of variation of k_3 estimates (Method 2) in the regions with median muscarinic receptor availability

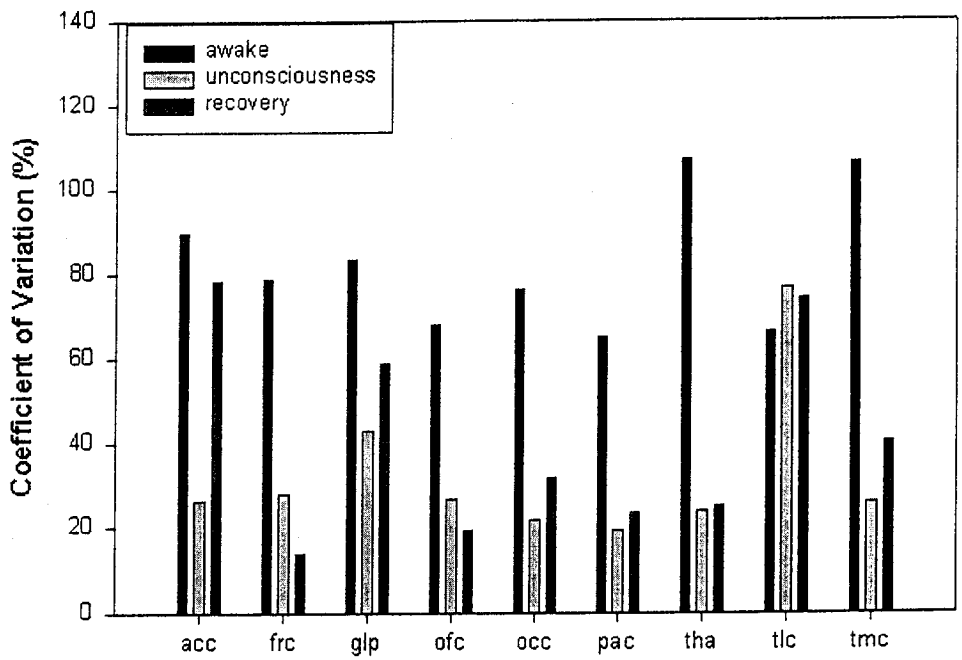

Coefficient of variation of k_3 estimates (Method 2) during awake, unconsciousness, and recovery in the regions with median muscarinic receptor availability model constraints of fixed volume of distribution

Table 2-2. Estimated k_3 (min^{-1})(mean (SD)) in the regions of caudate nucleus (cau) and putamen (put)

Experiment stages	Awake		Unconsciousness		Recovery	
Brain regions	cau	Put	cau	put	cau	put
Method 1						
Positivity constraints on parameters	0.14 (0.10)	0.28 (0.30)	0.09 (0.055)	0.078 (0.05)	0.14 (0.13)	0.12 (0.11)
Method 2						
K_1/k_2 ratio constrained to V_D of the cerebellum	0.22 (0.16)	**2.76 (6.6)**	0.072 (0.055)	0.078 (0.018)	**4.08 (9.6)**	**2.04 (4.74)**

Despite the high variance associated with estimates of k_3, our results demonstrate that k_3 values during unconsciousness were generally lower than those during awake for most regions evaluated. Furthermore, we found that the k_3 measured in vivo with our PET study is closely correlated with the density of muscarinic receptors measured in vitro (r^2 = 0.98), which provides evidence for the specificity of [N-^{11}C-methyl]-benztropine for the muscarinic sites. This result may suggest a propofol-related reduction in muscarinic receptor binding. The related reduction in muscarinic receptor binding theoretically could be caused by the increase of endogenous ACh, although this would contradict the clinical effect of propofol. A significant increase of endogenous ACh in CNS will produce alertness and REM sleep (Durieux ME et al., 1996). Furthermore, in animal studies using vivo microdialysis it has been demonstrated that propofol has dose-dependent inhibitory effects on acetylcholine release in the frontal cortex and hippocampus (Kikuchi et al., 1998; Wang et al., 2000).

Three possible mechanisms for the effects suggested by the present study are discussed. First, muscarinic receptors may be expressed in several conformations, which can be distinguished on the basis of agonist binding affinity (Birdsall et al., 1978). It is possible that propofol decreases

the affinity of muscarinic receptor to ligand and causes a conversion of muscarinic receptors from high affinity states to conformational states characterized by lower affinity. This notion is consistent with the finding from later experiments (Dennison et al., 1987) where [^{3}H] Oxotremorine-M was used as a probe to investigate the effects of halothane on high affinity agonist binding to muscarinic receptors in the brainstem of the rat. Their results suggested that halothane converts both G protein-coupled and uncoupled muscarinic receptors to states of lower agonist affinity. However, benztropine's Kd is 4-7 nmol/L for the muscarinic M1 and M2 site (Snyder et al., 1977). Therefore, it may also bind significantly to receptors in low affinity states. Second, it is possible that propofol directly binds to the muscarinic receptors. Yamamoto et al. (1999) measured the affinity of propofol to muscarinic receptors of myocytes with a competitive binding assay using [^{3}H] QNB. Their results supported the idea that propofol had an affinity for muscarinic receptors. Third, unfortunately it was not possible to guarantee the accurate correction of the plasma data for metabolite contributions as no individual metabolite data was available. Thus, a change in metabolism of the radioligand induced by propofol could account for any changes in the measure of receptor availability.

Meuret P et al (2000) demonstrated that physostigmine reverses propofol-induced unconsciousness and the associated depression of ASSR and BIS in human volunteer. The reversal of the unconsciousness and depression of the ASSR and BIS was blocked by pretreatment with scopolamine. Their findings supported the hypothesis that the loss of consciousness produced by propofol is mediated, at least in part, via interruption of central cholinergic muscarinic transmission. The results of our study may provide a possible explanation for their study although the site of action of propofol in the CNS to produce unconsciousness is still not known.

In conclusion, this study demonstrates that the method with a volume of distribution constraint, derived from the cerebellum, yielded the best estimates of k_3 and is superior to the method with positivity constraints in the regions with low and intermediate muscarinic receptor density. Our results may also indicate a propofol-related reduction in muscarinic receptor binding in CNS. However, the high variability of k_3 related to the irreversible binding property of the tracer prevents us from reporting statistically significant differences. Therefore it may be better to repeat a similar PET study with a more suitable radioligand, such as the reversible tracer NMPB (Zubieta et al., 2001). Furthermore, our study did not provide

any information about the possible change of endogenous Ach. Recently a new tracer, 3-[^{11}C]NMPYB (Skaddan et al., 2002), has been designed for the express purpose of measuring changes in endogenous Ach, which points towards another future research direction.

Chapter 3. How would you Lose and Regain your Consciousness? A PET Study of Unconsciousness Induced by Propofol and Consciousness Restored by Physostigmine.

In the last chapter, our results have suggested a propofol-related reduction in muscarinic receptor binding in CNS, which supports the hypothesis that the loss of consciousness produced by propofol is mediated, at least in part, via interruption of central cholinergic muscarinic transmission. This chapter investigates which brain function changes specifically linked to the difference in level of consciousness by examining thalamic and cortical neural activities during successful and failed attempts to antagonize propofol-induced unconsciousness with physostigmine.

3.1 Abstract

This work aims at identifying the brain function changes specifically linked to changes in levels of consciousness, and separate these from the non-specific drug related physiological alterations. To identify the changes specifically related to consciousness we used physostigmine (an anticholinestherase) to restore consciousness (defined as responsiveness to verbal commands) in 4 subjects anesthetized with a constant concentration of propofol (given with a computer-controlled pump at the lowest concentration producing unconsciousness). The administration of propofol was maintained at the same plasma concentration after physostigmine infusion. PET measures of regional cerebral blood flow (rCBF) were obtained during baseline (BASE), unconsciousness (UNCO), physostigmine (PHYSO) and recovery (RECO). Changes common to the BASE-UNCO and PHYSO-UNCO contrasts were considered functionally linked to the change in level of consciousness independently of any non-specific effect of propofol. These changes occurred in the right thalamus and bilaterally in the precuneus where rCBF decreased significantly during anesthesia and increased significantly after physostigmine. The consciousnes restored by physostigmine related to the significant rCBF increases in bilateral thalami and cuneus. Data from 3 additional subjects

who failed to wake up after physostigmine revealed significant rCBF decreases in the right thalamus and bilaterally in the precuneus during anesthesia but no significant increase after physostigmine. We conclude that the thalamus and precuneus/cuneus jointly play a critical role in controlling the changes in the level of consciousness during general anesthesia.

3.2 Introduction

The loss of consciousness induced by general anesthetics has been considered to involve the same brain structures as those involved in the control of the sleep-awake continuum (Heinke and Schwarzbauer, 2002). Findings of electrophysiological works in animals (Angel, 1993) suggest that the primary basis of anesthesia may be the disruption of sensory information processing through the thalamus. This idea is consistent with the recent findings from human positron emission tomography (PET) studies. Using the 18FDG PET technique, Alkire and co-workers have examined the effects of propofol and two volatile general anesthetics, isoflurance and halothane, on neuronal activity in humans (Alkire et al., 1995, 1997, 1999, 2000). Their results revealed decreased regional metabolism (rCMRgl) in the thalamus, in many cortical areas and in the cerebellum during unconsciousness. Using the H_2O^{15} PET technique, Bonhomme et al. (2001) and Fiset et al. (1999) investigated the regional cerebral blood flow (rCBF) during graded changes of propofol anesthesia with and without vibrotactile stimuli. These results demonstrated that unconsciousness was consistently associated with reduced rCBF in the thalamic and in many cortical areas during the resting condition as well as with suppression of thalamus and cortical activations caused by

somatosensory stimulation (vibration). In addition, Veselis et al. (1997B) have shown that sedative concentrations of midazolam decrease rCBF in the thalamus and in many cortical areas. However, these PET studies did not rule out the possibility that a change in neural activity (such as reduced rCBF or rCMRgl) and a concurrent alteration of the level of consciousness may be independent of each other but affected in a similar, concentration-dependent manner by the anesthetics.

To circumvent this problem, we have developed a strategy using the drug physostigmine, an inhibitor of acetylcholinesterase, which increases synaptic levels of actycholine (Ach). It reverses the effects of anesthesia in animals (Horrigan, 1978; Roy and Stullken, 1981; Zucker, 1991) and humans (Hill et al., 1977; Meuret et al., 2000; Plourde et al., 2003). In this chapter, we examined thalamic and cortical neural activities during successful and failed attempts to antagonize propofol-induced unconsciousness with physostigmine.

3.3 Methods

3.3.1 Subjects

The study was approved by the Research Ethics Committee of the Montreal Neurological Institute and Hospital. Eight healthy subjects participated in the study, all underwent a comprehensive medical evaluation and had no history of neurological, psychiatric, or respiratory problems. Subjects fasted for at least 8 hours prior to induction of anesthesia and were given sodium citrate orally (0.3 M, 30 ml, BDH, Toronto, Ontario, Canada) at their arrival in the positron emission tomography (PET). One subject was excluded from data analyses as the concentration of propofol was not consistently maintained during physostigmine infusions. Therefore seven healthy volunteers (mean age, 30 years; range, 22-40 years) completed the study. There were four subjects who woke up after injecting of physostigmine (responders). The ages of the four subjects were 22, 29, 29, 40, three of them were male and one is female. Three subjects who did not wake up after the injection of physostigmine (non-responder) were ages 28, 28, 32 and were all male.

3.3.2 Instrumentation and safety monitoring

Anesthesia monitoring includes EEG, pulse oximetry, blood pressure

measure and determination of inspired and expired concentration of oxygen and carbon dioxide. The Patient State Index (PSI) was recorded with a 4-channel PSA 4000 monitor (Physiometrix, MA, USA). PSI is a quantitative feature derived from EEG that displays clear differences between hypnotic states (Kearse, 1998), but consistency across anaesthetic agents within the state (Sebel, 1997). EEG data were obtained in all three non-responders but EEG data were not obtained in two of four responders due to a problem with the technique. An intravenous catheter was placed in the right forearm for drug infusion. Another catheter was inserted in the left radial artery for procurement of blood samples for determination of propofol plasma levels (Plummer et al., 1987) and radiotracer activity via subsequent counting in a NaI well-counter. Propofol assay were conducted in Dr. France Varin´s Lab, Univerisity of Montreal. Oxygen was administered at a rate of 3L/min through nasal prongs. Subjects were blindfolded, and ambient noise was kept to a minimum.

3.3.3 Propofol infusion

Propofol was given using a computer controlled infusion pump and the infusion program STANPUMP. This program uses pre-determined

population pharmacokinetics, the volunteer's pertinent covariates, and a multi-exponential infusion algorithm to quickly reach and maintain a target plasma concentration (Tackley et al., 1989). Propofol plasma concentrations of 2.0 ug/ml were targeted at beginning and increased in 0.5 ug/ml increments until unconsciousness was achieved. Unconsciousness was defined as the loss of response to verbal commands (" Move your toes, raise your thumb."). These concentrations were compatible with safe, spontaneous breathing. Once unconsciousness was reached, PET scanning was delayed by 10 minutes to allow for blood-brain equilibration of propofol concentrations (Dutta S et al., 1998). The constant concentration of propofol was maintained by computer-controlled infusion scheme during physostigmine infusion.

3.3.4 Experimental design

Two PET scans were conducted for each condition during wakefulness baseline (BASE), unconsciousness induced by propofol (UNCO), physostigmine infusion (PHYSO), and recovery (RECO) (Figure 3-1). The first two scans were obtained in the waking, unmedicated state. After the subject was given propofol at the lowest concentration sufficient to produce unconsciousness, the second series of two scans were obtained

Figure 3-1: Experimental design

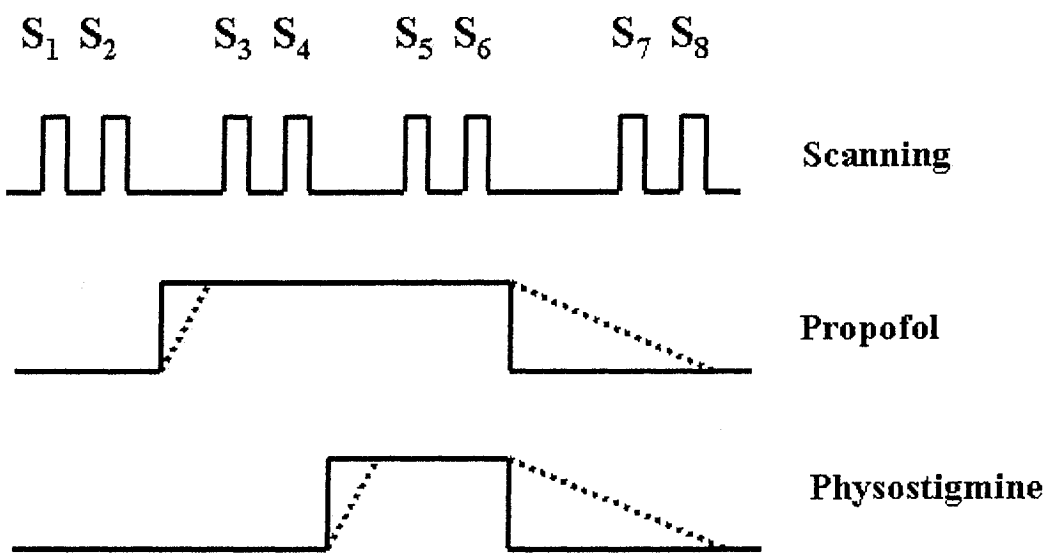

Two PET scans were conducted for each condition during wakefulness baseline (BASE), unconsciousness induced by propofol (UNCO), physostigmine infusion (PHYSO), and recovery (RECO)

With a constant concentration of propofol maintained by a computer-controlled infusion pump, the subjects were given a bolus of physostigmine (28 ug/kg) combined with glycopyrrolate (4.2 ug/kg), followed by continuous infusion of physostigmine (28 ug/kg/hr) combined with glycopyrrolate (4.2 ug/kg/hr) for 30 minutes. Glycopyrrolate is an anti-muscarinic agent given to prevent the peripheral side effects of physostigmine. It dose not cross the blood brain barrier. The third series of two PET scans were obtained after subjects regained consciousness or, if they did not regain consciousness, 10 minutes after the physostigmine bolus. The fourth series of two PET scans were obtained after propofol and physostigmine had been stopped for 20 minutes and subjects were completely awake. Arterial blood samples for propofol assay were taken 4 min before the commencement of each scan during propofol, physostigmine infusion, and recovery.

3.3.5 Data acquisition

PET scans were obtained using a CTI/Siemens HR +, 32-rings, 63-slices tomograph. The $H_2{}^{15}O$ bolus technique was used. Counts were measured during a 3-min scan after a 10-mCi $H_2{}^{15}O$ bolus injection into a

vein of the right ventral forearm. To allow for calculation of the absolute value of CBF, arterial blood samples were acquired throughout the scanning period using the catheter placed into the left radial artery. Arterial blood radioactivity was automatically sampled, corrected for delay and dispersion (Vafaee, 1996), and calibrated with respect to the tomograph. To facilitate localization of the regional change in rCBF, each subject underwent an MRI scan on a separate occasion (high-resolution, T1-weighted, 1.5 T, 160 contiguous sagittal slices, 1 mm thick).

3.3.6 PET data analysis

3.3.6.1 K_1 map

The absolute CBF was calculated for the whole brain for each scan of each subject. We used the two-compartment, three-weighted integral method of Ohta et al. (1996). Cerebral perfusion maps (K_1 maps) were generated for each 3-min dynamic scan using the native PET images across all frames. Mean whole-brain CBF values were then obtained by averaging the K_1 maps. Okazawa and Vafaee (2001) demonstrated that this method could provide rCBF values that are less influenced by vascular radioactivity.

To identify the brain regions where propofol and physostigmine induced changes in blood flow beyond those observed globally, we analyzed the effects of propofol on normalized rCBF. The K_1 images were normalized for differences in global CBF by means of ratio normalization; i.e., the count at each voxel (3-dimensional image element) was divided by the mean counts calculated across all brain voxels (Fox, 1988). The normalized K1 image were co-registered with individual MRIs (Woods, 1993) and transformed into a standardized stereotaxic space by means of an automated feature-matching algorithm (Collins, 1994).

3.3.6.2 T statistic maps

Statistical analysis of rCBF was performed using normalized rCBF of the 4 responders and 3 non-responders. All the calculations were carried out for each of the three-dimensional volume elements (voxels) constituting a volume. The size of a voxel was 1.34x1.72x1.5 mm in x,y,z dimensions, respectively. To assess the differences in rCBF distribution during the different conditions of experiment, we calculated subtraction t-statistic maps between different conditions with 2 scans for each condition. A t-value was calculated for each voxel by dividing the mean CBF difference by its standard deviation pooled across all brain voxels (Worsley, 1992). Four different subtractions were carried out as follows:

BASE-UNCO, PHYSO-UNCO, PHYSO-BASE, and RECO-BASE. A BASE-UNCO subtraction was aimed at revealing effects of unconsciousness induced by propofol. A PHYSO-UNCO subtraction was generated to evaluate the consciousness restored by physostigmine in four responders. A PHYSO-BASE subtraction was aimed at revealing the effect of propofol and physostigmine. A RECO-BASE subtraction was generated to evaluate the effect of residual propofol and physostigmine.

3.3.6.3 Conjunction analysis

The functional conjunction between the BASE-UNCO and PHYSO-UNCO subtractions in four responders is the changes in the level of consciousness. In order to find the brain regions that are specifically linked to the change in the level of consciousness, we performed the conjunction analysis between these two subtraction T maps, which reveals the brain regions that are both deactivated by propofol-induced unconsciousness and activated by physostigmine-restored consciousness.

3.3.6.4 Spherical region-of-interest analysis

In order to demonstrate the relative rCBF changes in the conjunction areas (right thalamus and precuneus) in four responders, we extracted the rCBF value using a spherical region-of-interest (4 mm radius) centered at

the middle of conjunction areas of right thalamus (5,-17,8) and precuneus (1,-67, 32).

3.3.6.5 Region-based regressions

We also carried out the region-based regression to reveal brain regions with blood flow response similar to that present in right and left thalamus in four responders. We regressed rCBF-change in all other voxels with the voxel (8,-18,9) that has the hightest t value in right thalamus in the subtractions of PHYSO-UNCO and the voxel (-7, -16, 6) that has the hightest t value in left thalamus in the subtractions of PHYSO-BASE. We selected different regression seed points from the subtractions of PHYSO-UNCO and PHYSO-BASE because the right thalamic activation in the subtraction of PHYSO-UNCO may be related to the physostigmine-restored consciousness and the left thalamic activation in the subtraction of PHYSO-BASE may be related to drug effect.

3.3.6.6 Spherical region-of-interest analysis

In order to further demonstrate the differences between the responders and non-responders, we extracted the rCBF value using a spherical region-of-interest (4 mm radius) centered at the voxel with the highest T value in right thalamus (8,-18,9) and left thalamus (-3,-16,8).

3.3.7 Statistical analysis

We analyzed the variability of HR, MAP, PCO2, SpO2, global CBF, and relative rCBF extracted with spherical region-of-interest method across four experimental conditions using an one-factor within-subjects ANOVA and Tukey's HSD for post hoc comparisons. For the T statistical map of subtraction, region-based regression, and event regression in responders and non-responders, the presence of significant focal changes was tested by a method based on three-dimensional Gaussian random field theory, which corrects for the multiple comparisons involved in searching across a volume (Worsley et al., 1992). Values equals to or exceeding a criterion of t = 4.5 were considered statistically significant ($p < 0.0001$; two tailed, uncorrected). Correcting for multiple comparisons, a t value of 4.5 yields a false-positive rate of 0.05 in 500 resolution elements (each of which has dimensions 7.7 x 18 x 18 mm), which is approximately the volume of brain gray matter. For BASE – UNCO subtraction of three non-responders, the directed searches of rCBF changes in the thalamus were performed in regions previously shown to be involved in unconsciousness induced by general anesthetics. The significant threshold for these directed searches was $t=2.63$ ($p<0.05$, two-tail), after

corrected for multiple comparisons involving a 6-resel search volume (Worsley et al., 1992).

3.4 Results

3.4.1 Four responders

3.4.1.1 Monitoring

Seven of eight volunteers enrolled completed the study. For four responders, the MAP during unconsciousness was significantly lower than those during other experimental stages ($p < 0.05$); the PaCO2 during unconsciousness was significantly higher than those during other experimental stages ($p < 0.05$); the HR during physostigmine infusion was significantly higher than those during other experimental stages ($p < 0.05$); There were no significant differences in HR and global cerebral blood flow (gCBF) among four experimental periods ($p > 0.05$) (Table 3-1). The measured propofol concentrations were as follows (mean ± SD): unconsciousness, 3.20 ± 0.75 μg/ml; physostigmine, 2.85 ± 0.53 μg/ml; recovery, 1.03 ± 0.22 μg/ml. For two subjects with EEG monitoring, the values of Patient State Index (PSI) were as follows: baseline state, 99, 99; unconsciousness state, 26, 21; physostigmine state, 87, 88; recovery state, 95, 92.

Table 3-1: Vital Signs and global CBF of four responders

	Baseline	Unconsciousness	Physostigmine	Recovery
GlobeCBF (ml/100ml.min)	41.9 ± 4.6	41.2 ± 6.8	38.7 ± 2.9	40.5 ± 6.2
PCO_2 (mmHg)	41.8 ± 2.5	48.5 ± 2.4 #	42.3 ± 3.9	43.3 ± 3.8
PO_2 (mmHg)	207.8 ± 23.0	221.3 ± 40.1	176.3 ± 34.3	176.3 ± 34.3
HR ($beats.min^{-1}$)	60 ± 1.6	60.5 ± 1.7	102 ± 14.3 #	70.5 ± 8.2
MAP (mmHg)	90.5 ± 5.8	69.2 ± 5.4 #	80.3 ± 4.0#	87.0 ± 3.0

Vital signs and global CBF of four subjects who woke up after physostigmine injection (mean ± SE). # $P<0.05$ compared with other scans.

3.4.1.2 Subtraction analysis

For the four subjects who woke after physostigmine infusion, the comparison between the baseline and unconsciousness states demonstrated that the relative rCBF decreased significantly in the unconsciousness state in the bilateral precuneus, the right thalamus, and some convex parietal regions, in comparison with the baseline state (Table 3-2, Figure 3-2). The comparison between the unconsciousness and physostigmine states demonstrated that the relative rCBF increased significantly in the physostigmine state in several regions, the bilateral thalamus, the bilateral cuneus, bilateral precentral gyrus, left medial frontal gyrus and the right fusiform (Table 3-3, Figure 3-3). The comparison between the physostigmine and baseline states demonstrated that the relative rCBF increased significantly in the physostigmine state in the following regions, the bilateral precentral gyrus, the left medial thalamus, right medial frontal gyrus, the left insula, the right cingulate gyrus and left cuneus, in comparison with the baseline state (Table 3-4, Figure 3-4). The comparison between the recovery and baseline states demonstrated that the relative rCBF increased significantly in the recovery state in the

Table 3-2: Areas of significant relative rCBF decreases during propofol-induced unconsciousness in four responders

Anatomical location	BA	Talairach Coordinates			T
		x	y	z	
Positive peaks					
Right precuneus	7	15	-61	48	7.18
Left precuneus	31	-1	-50	30	6.99
Right precuneus	7	1	-68	38	6.82
Right thalamus		5	-16	11	6.22
Right precuneus	7	9	-78	57	5.75
Left inferior parietal lobule	40	-48	-50	54	5.41
Right superior parietal lobule	7	29	-59	63	4.64
Left orbital gyrus	47	-12	34	-23	4.62
Right fusiform gyrus	18	20	-88	-15	4.62
Negative peaks					
Left insula	13	-42	-7	9	-5.61
Left anterior cingulate	32	1	32	21	-5.04
Left medial frontal gyrus	6	-3	-14	48	-4.67

Clusters of voxels showing statistically significant relative rCBF reductions in the BASE minus UNCO subtraction. Only areas with a T score > 4.5 ($P < .05$, corrected with multiple comparison) are considered significant.

Figure 3-2: Regions with significant decrease in relative rCBF during propofol-induced unconsciousness

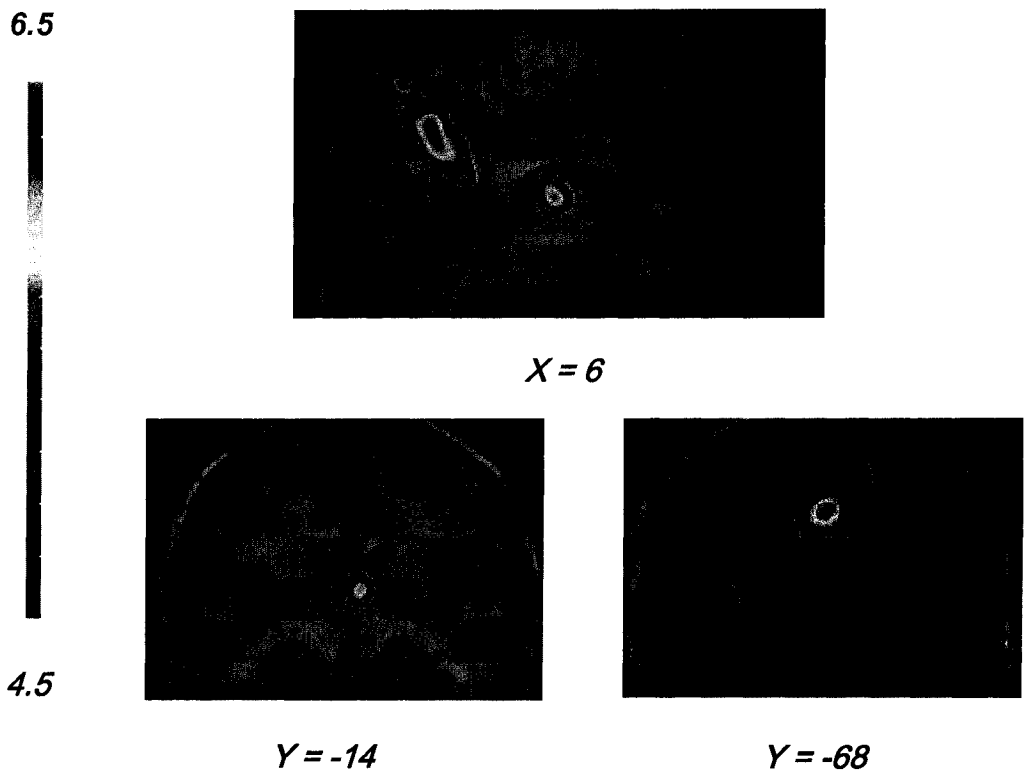

The T statistical map of BASE minus UNCO subtraction revealed that the relative rCBF decreased significantly in the bilateral precuneus, the right thalamus during the unconsciousness state. The range of positive values for the T map is coded by the color scale.

Table 3-3: Areas of significant relative rCBF Increases and decreases during consciousness restored by physostigmine

Anatomical location	BA	Talairach Coordinates			T
		X	y	z	
Positive peaks					
Left thalamus		-3	-16	8	11.5
Right thalamus		8	-18	9	11.18
Right cuneus	18	5	-74	18	9.15
Right cuneus	17	3	-87	9	8.29
Right cuneus	18	24	-87	26	6.6
Left cuneus	19	-12	-83	35	6.55
Left cuneus	19	-21	-88	23	6.3
Left putamen		-24	-1	5	6.02
Left precentral gyrus	4	-40	-13	44	5.5
Right precentral gyrus	6	56	-7	35	5.35
Left medial frontal gyrus	6	-1	-26	63	4.85
Right fusiform gyrus	18	20	-83	-20	4.61
Negative peaks					
Left parahippocampal gyrus	36	-31	-19	-21	-5.01
Right insula	38	35	1	-15	-4.9
Right gyrus rectus	25	9	20	-18	-4.88
Right parahippocampal gyrus	20	35	-16	-21	-4.84
Left medial Frontal Gyrus	8	-12	30	42	-4.74
Right medial Frontal Gyrus	8	28	29	36	-4.68

Clusters of voxels showing statistically significant relative rCBF increases (positive peaks) and decreases (negative peaks) in the PHYSO minus UNCO subtraction. Only areas with a T score > 4.5 ($P < .05$, corrected with multiple comparison) are considered significant.

Figure 3-3: Regions with significant increase in relative rCBF during consciousness restored by physostigmine

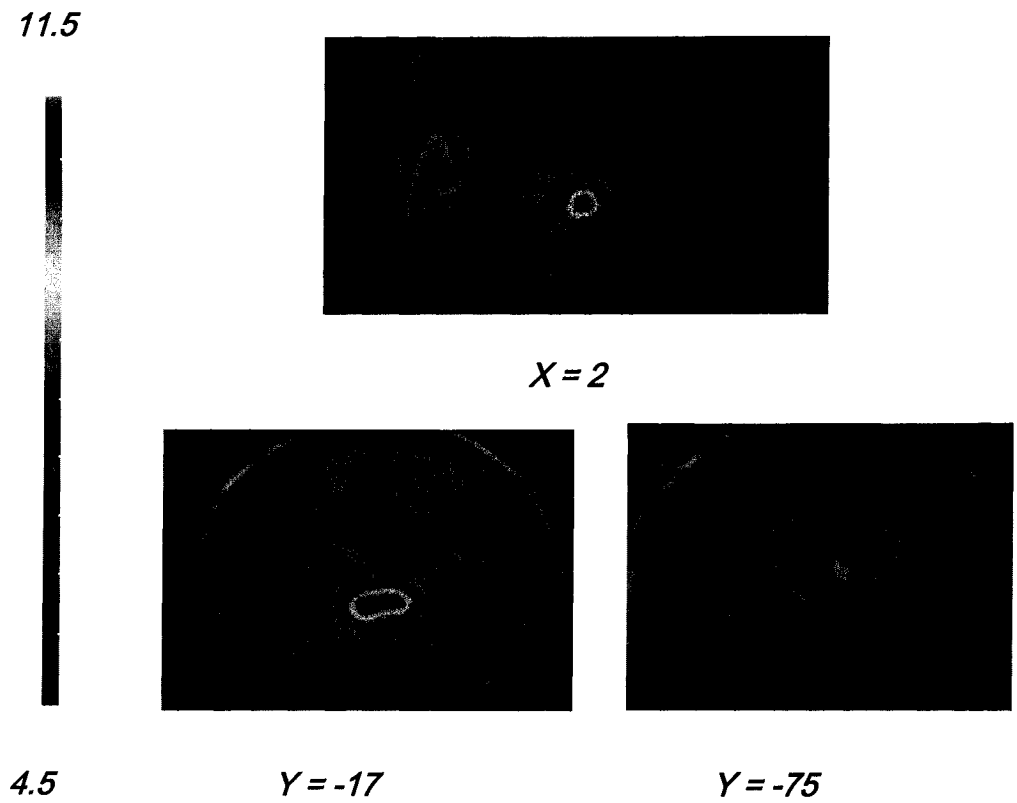

The T statistical map of PHYSO minus UNCO subtraction revealed that the relative rCBF Increased significantly in the bilateral cuneus and the bilateral thalami during the consciousness restored by physostigmine. The range of positive values for the T map is coded by the color scale.

Table 3-4: Areas with significant relative rCBF changes comparing the physostigmine state to baseline state

Anatomical location	BA	Talairach Coordinates			T
		x	y	Z	
Positive peaks					
Left precental gyrus	4	-42	-14	42	7.35
Right precental gyrus	4	47	-11	42	6.31
Left thalamus		-7	-16	6	6.22
Right medial frontal gyrus	6	1	-25	66	6
Left insula	13	-40	-11	11	5.36
Right cingulate gyrus	24	7	3	47	5.02
Right anterior cingulate gyrus	32	4	36	11	4.93
Left cuneus	18	-3	-81	20	4.7
Negative peaks					
Right precuneus	7	15	-61	46	-6.4
Left rectal gyrus	11	-11	32	-21	-6.27
Left cingulate gyrus	31	-1	-49	29	-5.74
Right parahippocampal gyrus		30	-13	-20	-5.57
Left superior frontal gyrus	9	-40	36	30	-5.53
Right cingulate gyrus	31	20	-42	39	-5.34
Right inferior temporal gyrus	20	55	-23	-21	-5.13
Right inferior temporal gyrus	20	52	-47	-9	-4.93
Right middle frontal gyrus	46	43	36	23	-4.83
Fusiform Gyrus	37	-35	-59	-20	-4.71
Superior Frontal Gyrus	6	-16	30	59	-4.59

Clusters of voxels showing statistically significant relative rCBF increases (positive peaks) and decreases (negative peaks) in the PHYSO minus BASE subtraction. Only areas with a T score > 4.5 ($P < .05$, corrected with multiple comparison) are considered significant.

Figure 3-4: Regions with significant changes in relative rCBF when comparing the physostigmine state to baseline state

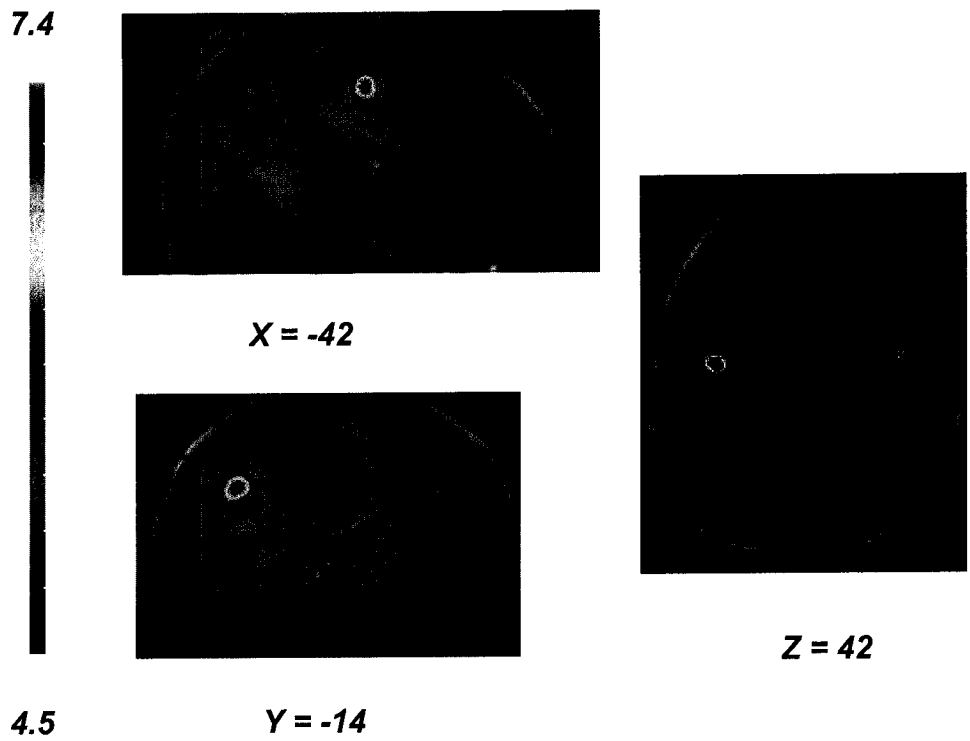

The T statistical map of PHYSO minus BASE subtraction revealed that the relative rCBF increased significantly in the left thalamus and bilateral precental gyrus when comparing the Physostigmine to baseline state. The range of positive values for the T map is coded by the color scale.

following regions, the left medial thalamus, left anterior cingulated gyrus, bilateral medial frontal gyrus, bilateral precentral gyrus, and left insula, in comparison with the baseline state (Table 3-5, Figure 3-5).

3.4.1.3 Conjunction analysis

The functional conjunction between BASE-UNCO and PHYSO-UNCO subtractions reflects the changes in the level of consciousness. In order to find the brain regions that are specifically linked to the change in the level of consciousness, we performed the conjunction analysis between these two subtraction T maps. We found the conjunction areas were right thalamus and bilateral precuneus (Figure 3-6).

3.4.1.4 Spherical region-of-interest analysis

Figure 3-7 shows the relative rCBF values extracted using a spherical region-of-interest (4 mm radius) centered at the middle of conjunction areas of right thalamus (5,-17,8) and precuneus (1,-67, 32) in four experimental periods. We found that the relative rCBF during unconsciousness was significantly lower that of other experimental periods ($P<0.01$), while there is no significant changes in global CBF.

Table 3-5: Areas with significant relative rCBF changes comparing the recovery state to baseline state

Anatomical location	BA	Talairach Coordinates			T
		x	y	z	
Positive peaks					
Left thalamus		-7	-16	8	5.88
Left anterior cingulate	32	-1	32	24	5.77
Right medial frontal gyrus	6	3	-26	66	5.32
Right precentral gyrus	4	46	-13	44	5.22
Left insula	13	-42	-9	11	5.07
Left cingulated gyrus	31	-3	-16	47	4.97
Right medial frontal gyrus	6	5	3	48	4.85
Left precentral gyrus	4	-42	-16	45	4.84
Left medial frontal gyrus	32	-3	6	47	4.74
Negative peaks					
Left rectal gyrus	11	-11	32	-21	-6.23
Right precuneus	7	16	-61	48	-5.93
Right parahippocampal gyrus		29	-13	-20	-5.56
Right fusiform gyrus	37	50	-45	-11	-4.58

Clusters of voxels showing statistically significant relative rCBF increases (positive peaks) and decreases (negative peaks) in the RECO minus BASE subtraction. Only areas with a T score > 4.5 ($P < .05$, corrected with multiple comparison) are considered significant.

Figure 3-5: Regions with significant changes in relative rCBF when comparing the recovery state to baseline state

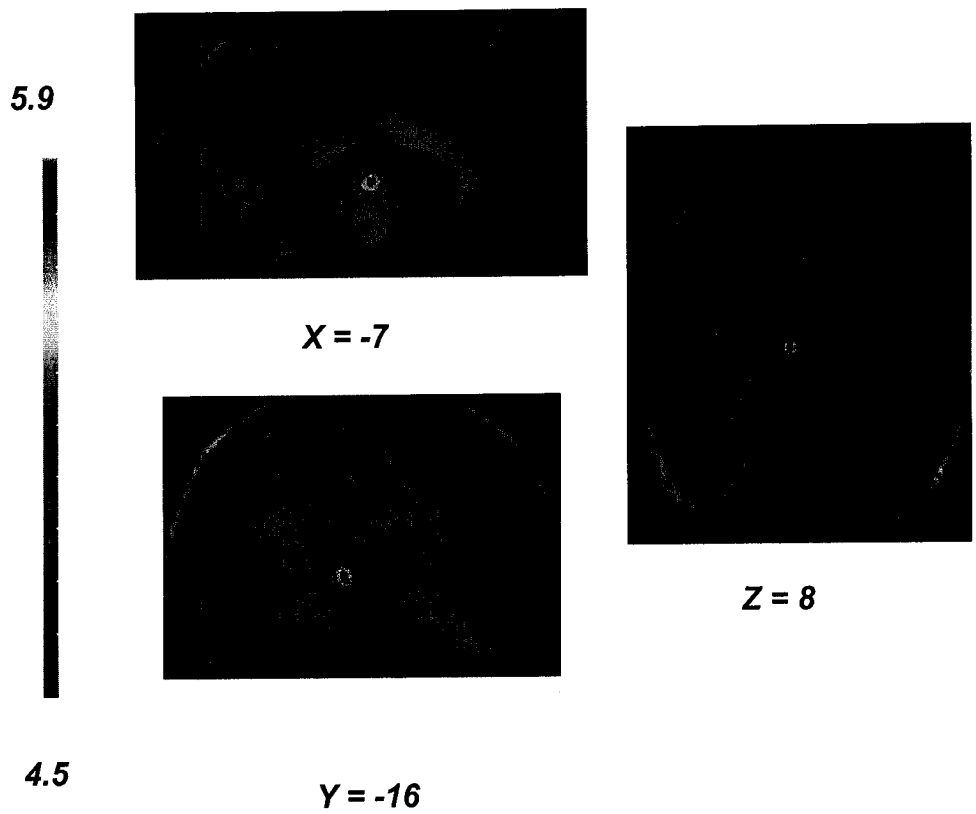

The T statistical map of RECO minus BASE subtraction revealed that the relative rCBF Increased significantly in the left thalamus, cingulated gyrus, and bilateral precental gyrus when comparing the Recovery to Baseline State. The range of positive values for the T map is coded by the color scale.

Figure 3-6: Conjunctive areas between subtraction BASE-UNCO and subtraction PHYSO-UNCO

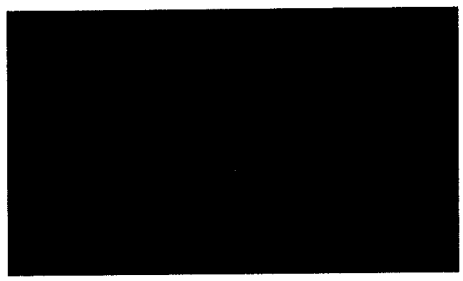

X = 6

Y = -13

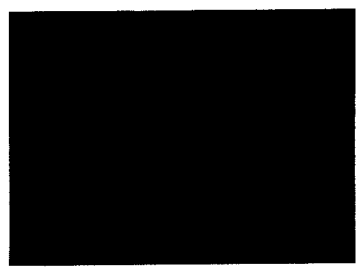

Y = -67

Conjunctive analysis identifying common brain regions both deactivated by propofol-induced unconsciousness and activated by consciousness restored by physostigmine: right medial thalamus and bilateral precuneus. The cutoff T value equals to 4.

Figure 3-7: Relative rCBF in thalamus and precuneus

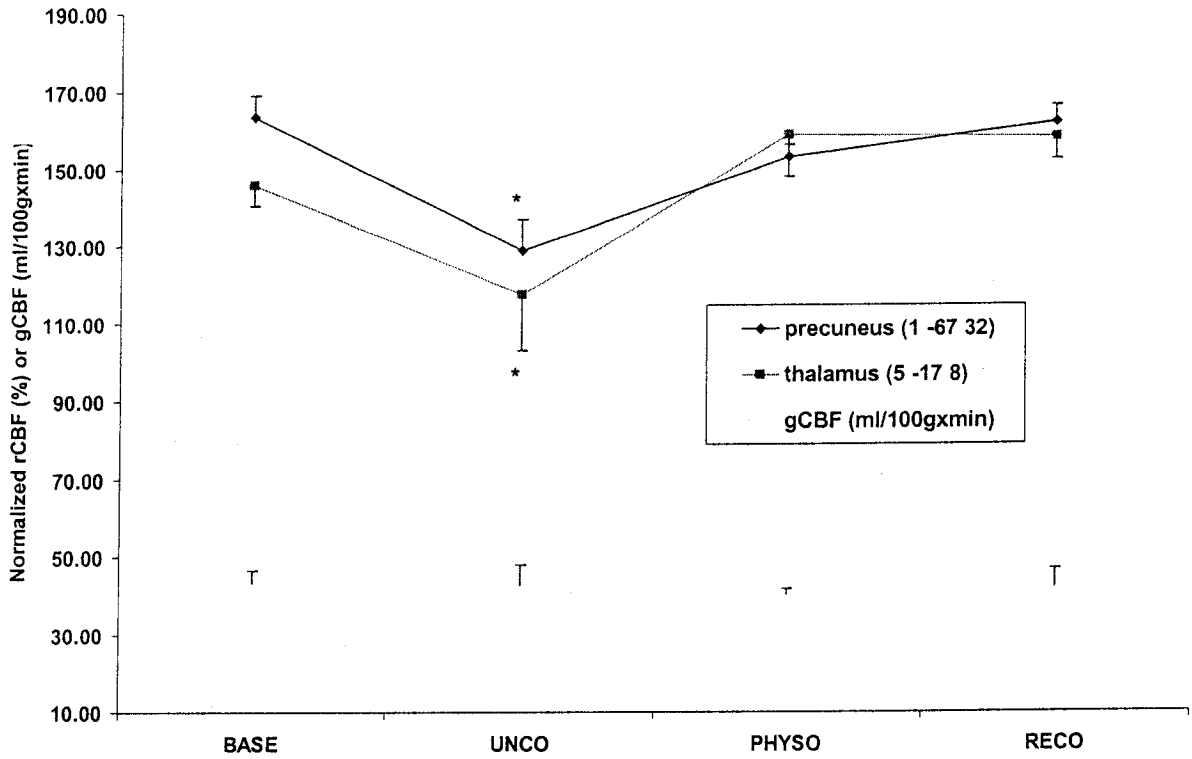

The relative rCBF values extracted using a spherical region-of-interest (4 mm radius) centered at the middle of conjunction areas of right thalamus (5,-17,8) and precuneus (1,-67, 32) in four experimental periods (* $P<0.01$)

3.4.1.5 Region-based regressions

In order to reveal brain regions with blood flow response similar to that present in right thalamus, the rCBF-changes in all other voxels were regressed with the voxel with the highest t value in right thalamus (8, -18, 9). We found that this voxel was positively covariated with nearby voxel in right thalamus, bilateral cuneus and precuneus, and left putamen (Table 3-6, Figure 3-8). The rCBF-changes in all other voxels were also regressed with the voxel with the highest t value in left thalamus (-7, – 16, 6). We found that this voxel was positively covariated with nearby voxel in left thalamus, right thalamus, medial frontal gyrus, bilateral putamen, left cuneus and other cortical areas (Table 3-7, Figure 3-9).

3.4.2 Three non-responders compared with four responders

3.4.2.1 Monitoring

For three subjects who did not wake up after receiving physostigmine, the global CBFs during unconsciousness and physostigmine were significantly higher than those during baseline and recovery stages ($p < 0.05$); the $PaCO_2$ values during unconsciousness and physostigmine were higher than those during baseline and recovery stages but without reaching statistical significance; the HR during physostigmine infusion was

Table 3-6: CBF co-variations with the rCBF changes in the right medial thalamus

Anatomical location	BA	Talairach Coordinates			T
		x	y	z	
Positive co-variations					
Right thalamus		9	-18	11	10.48
Right cuneus	18	9	-73	17	7.25
Right cuneus	18	1	-88	9	7.04
Right cuneus	19	25	-88	24	5.07
Right precuneus	7	16	-61	50	5.03
Left putamen		-24	-2	6	4.87
Left precuneus	31	-4	-52	32	4.84
Left cuneus	19	-15	-85	32	4.79
Negative co-variations					
Left frontal cingulate gyrus	9	-8	37	26	-4.54
Left frontal cingulate gyrus	8	-13	25	38	-4.54

Clusters of voxels showing statistically significant co-variations with rCBF changes in right thalamus (8, -18, 9). Only areas with a T score > 4.5 ($P < 0.05$, corrected with multiple comparison) are considered significant.

Figure 3-8: Region-based regression with the right medial thalamus

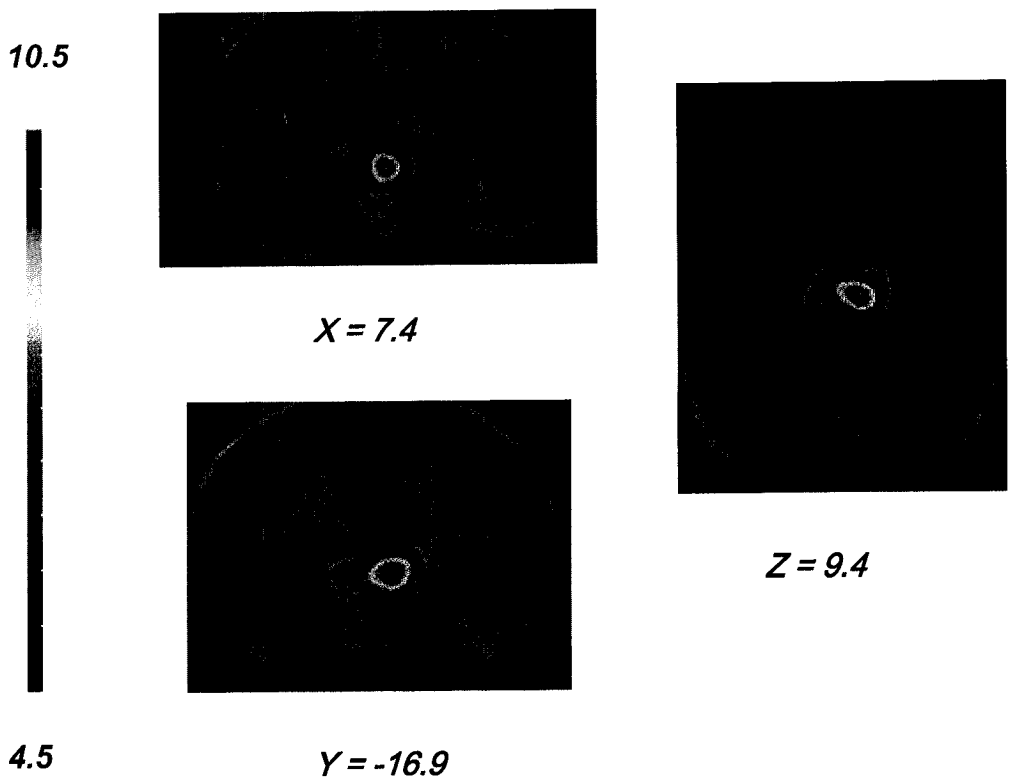

The rCBF changes in the areas of the nearby right thalamic voxels, cuneus, precuneus have a significant positive regression with the rCBF changes in the source region of the right thalamus (8, -18, 9), the right thalamic voxel with the highest T value for all subtractions.

Table 3-7: CBF co-variations with the CBF in the left medial thalamus

Anatomical location	BA	Talairach Coordinates			T
		x	Y	z	
Positive co-variations					
Left thalamus		-5	-18	8	12.55
Right thalamus		13	-18	5	7.06
Right medial frontal gyrus	6	1	-23	66	5.75
Left calcaine gyrus	18	-1	-76	21	5.6
Right putamen		29	6	2	5.59
Left putamen		-16	12	3	5.58
Right parietal-occipital gyrus	19	7	-78	41	5.4
Left central gyrus	4	-40	-16	44	5.28
Left insula	13	-40	-14	9	5.15
Right putamen		32	-7	2	5.12
Right precentral gyrus	4	44	-11	42	4.82
Negative co-variations					
Right parahippocampal gyrus		29	-11	-20	-13.39
Right cingulate gyrus	31	21	-44	39	-10.56
Right cingulate gyrus	24	17	-13	42	-9.4
Right precuneus	7	16	-59	47	-8.83
Right medial frontal gyrus	6	4	-9	57	-8.18
Left precentral gyrus	4	-17	-30	57	-8.12
Left rectus gyrus	11	-11	34	-21	-7.73
Right middle frontal gyrus	8	27	12	35	-6.59
Right middle temporal gyrus	6	9	-25	54	-5.16
Right fusiform gyrus	30	28	-56	2	-4.8

The brain regions listed in this table showed significant positive ($t > 4.5$) and negative ($t < -4.5$) co-variations of CBF with that measured in the left medial thalamus(-7, – 16, 6).

Figure 3-9: Region-based regressions with the left medial thalamus

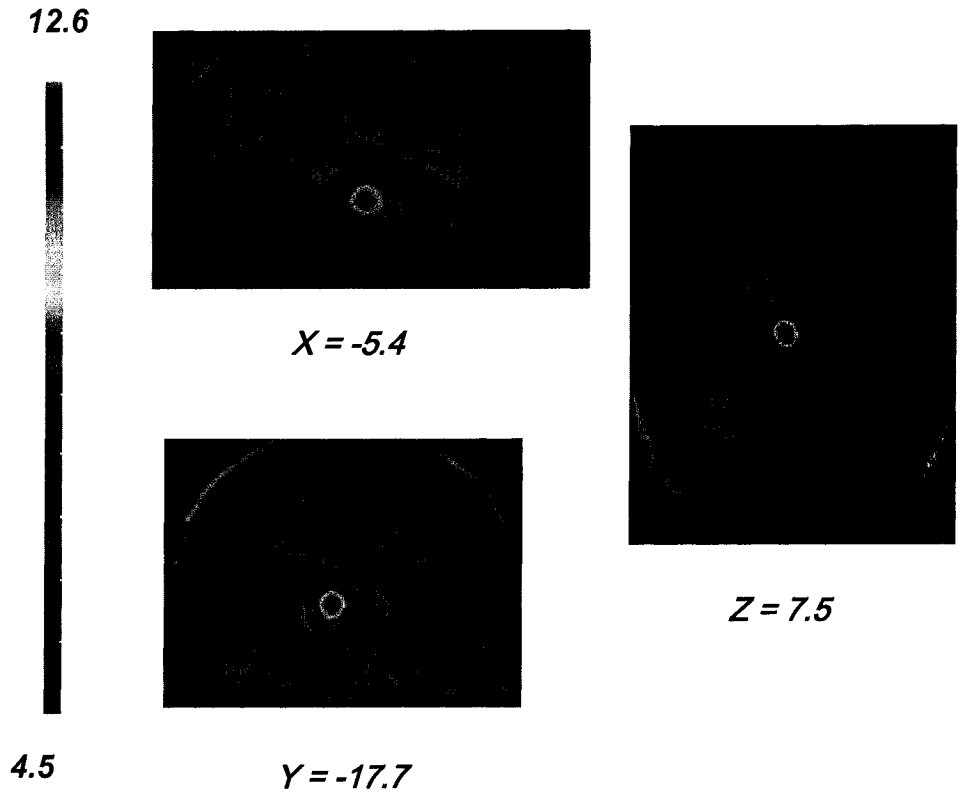

The rCBF changes in the areas of neighbour left medial thalamic voxels, right medial thalamus, and several cortical areas have a significant positive co-variation of CBF with the rCBF in the source region of the left thalamus (-7, – 16, 6), the left thalamic voxel with the highest T value for all subtractions.

significantly higher than those during other experimental stages ($p < 0.05$); the MAP during unconsciousness was significantly lower than those during baseline stages ($p < 0.05$) and the MAP during recovery was significantly higher than those during baseline stages ($p < 0.05$). There were no significant differences in PO_2 among four experimental periods ($p > 0.05$) (Table 3-8). The measured propofol concentrations with HPLC analysis were as follows (mean ± SD): unconsciousness state, 3.60 ± 2.70 μg/ml; physostigmine state, 3.40 ± 0.93 μg/ml; recovery state, 1.20 ± 0.29 μg/ml. Patient State Index (PSI) measured with EEG monitor were as follows (mean ± SD): baseline state, 89.0 ± 9.5; unconsciousness state, 16.0 ± 11.8; physostigmine state, 18.0 ± 10.2; recovery state, 83.0 ± 7.8.

3.4.2.2 Subtraction analysis

For the three subjects who did not wake up after the physostigmine infusion, the comparison between the baseline and unconsciousness states demonstrated that the relative rCBF decreased significantly in the unconsciousness state in several discrete regions, namely, the bilateral precuneus, left cingulated gyrus, right angular gyrus, and right cuneus and thalamus (significant with directed search) in comparison with the baseline

Table 3-8: Vital signs and global CBF of three non-responders

	Baseline	Unconsciousness	Physostigmine	Recovery
Globe CBF (ml/100ml.min)	39.1 ± 3.5	52.9 ± 8.5*	53.2 ± 6.7*	40.5 ± 2.6
PCO_2 (mmHg)	43 ± 6.6	57.7 ± 6.4	56.3 ± 9.0	48.3 ± 2.1
PO_2 (mmHg)	228.3 ± 9.9	210.3 ± 69.2	254.9 ± 28.7	250.0 ± 24.6
HR ($beats.min^{-1}$)	62.3 ± 10.0	79.5 ± 7.5	109.3 ± 2.1 *	75.7 ± 5.5
MAP (mmHg)	79.3 ± 6.4	61.4 ± 9.7 *	67.9 ± 7.9	89.2 ± 3.6*

Vital signs and global CBF of three subjects who did not wake up (non-responders) after physostigmine injection (mean ± SE). * $P<0.05$ compared with baseline

state (Figure 3-10,11,12, Table 3-9); the comparison between the unconsciousness and physostigmine states demonstrated that the relative rCBF increased significantly in the physostigmine state in only following regions, left cuneus, right lingual gyrus, and left thalamus (T=3, borderline significant with directed search) in comparison with the unconsciousness state (Figure 3-10,11,12; Table 3-10).

3.4.2.3 Spherical region-of-interest analysis

Figure 3-13 and 3-14 show the relative rCBF values extracted using a spherical region-of-interest (4 mm radius) centered at right thalamus (8,-18,9) and left thalamus (-3,-16,8) in four experimental periods. We found that the relative rCBF during unconsciousness was significantly lower that of other experimental periods ($P<0.01$) in four responders, while there were no significant changes in relative rCBF in three non-responders.

3.4.2.4 Event regression analysis

The relationship between rCBF and the event of regaining consciousness during physostigmine infusion was evaluated by ANCONA. The event of regain consciousness during physostigmine infusion was defined as "awake" . The variable "awake" equals 1 for four

Table 3-9: Regions with significant decrease in relative rCBF during propofol-induced unconsciousness in three non-responders

Anatomical location	BA	Talairach Coordinates			T
		x	y	z	
Positive peaks					
Right precuneus	7	4	-62	33	7.4
Left precuneus	7	-17	-73	48	5.7
Left precuneus	7	-4	-76	42	5.1
Left precuneus	19	-5	-83	45	5.1
Left posterior cingulated gyrus	31	-4	-40	38	4.8
Right angular gyrus	11	39	-64	45	4.7
Right thalamus		7	-11	11	4.3*
Negative peaks					
Right parahippocampal gyrus		23	-7	-20	-6.3
Left anterior cingulate gyrus	32	-5	17	30	-5.5
Left insula	13	-43	3	-2	-4.8
Left cingulate gyrus	6	-1	-4	50	-4.7

Clusters of voxels showing statistically significant relative rCBF reductions in the BASE minus UNCO subtraction. Only areas with a T score > 4.5 (P < 0.05, corrected with multiple comparison) are considered significant. * Significant with directed research (P <0.05).

Table 3-10: Areas of significant relative rCBF increases and decreases during consciousness restored by physostigmine in three non-responders

Anatomical location	BA	Talairach Coordinates			T
		x	y	z	
Positive peaks					
Left cuneus	23	-4	-73	11	7.3
Right lingual gyrus	17	14	-95	-5	4.8
Negative peaks					
Right inferior frontal gyrus	46	48	18	26	-4.6

Clusters of voxels showing statistically significant relative rCBF increases (positive peaks) and decreases (negative peaks) in the PHYSO minus UNCO subtraction in three non-responders. Only areas with a T score > 4.5 ($P < 0.05$, corrected with multiple comparison) are considered significant.

Figure 3-10: The coronal sections of t maps of subtraction BASE-UNCO and subtraction PHYSO-UNCO in four responders (N = 4) and three non-responders (N = 3)

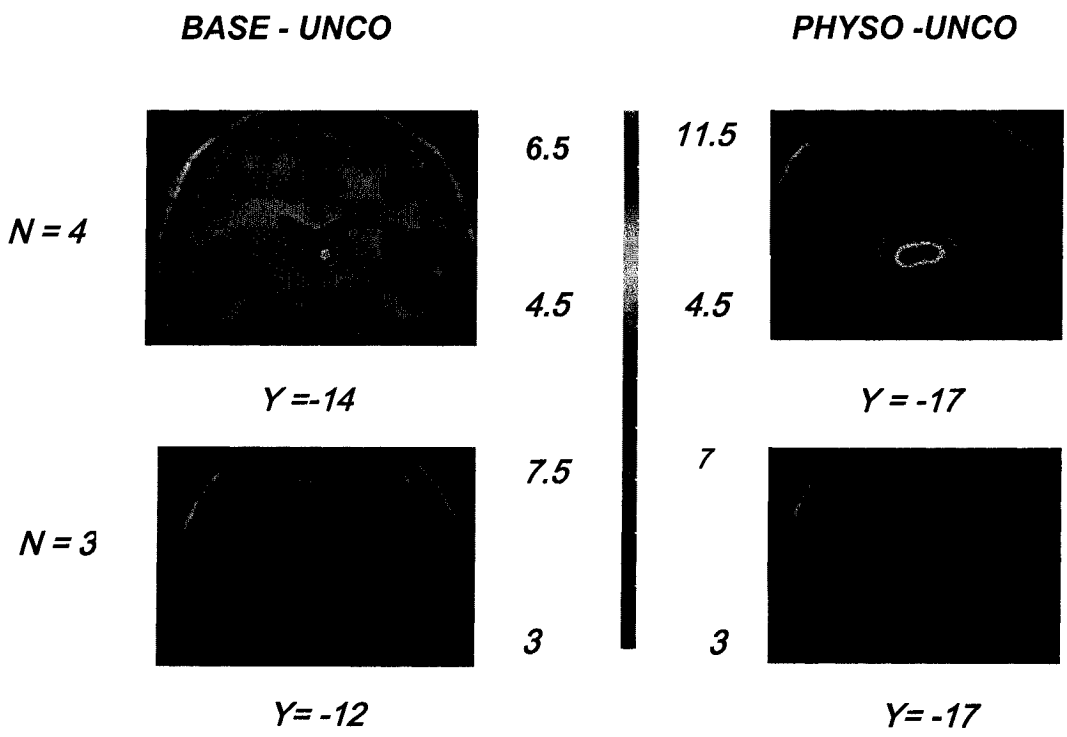

The coronal sections of t maps of subtraction BASE-UNCO revealed that significant rCBF reductions during unconsciousness in right medial thalamus were found in both responders and non-responders. The coronal sections of t maps of subtraction PHYSO-UNCO revealed that significant rCBF increase in bilateral medial thalamus were found in responders but not in non-responders during physostigmine-restored consciousness.

Figure 3-11: The sagittal sections of t maps of subtraction BASE-UNCO and subtraction PHYSO-UNCO in four responders (N = 4) and three non-responders (N = 3)

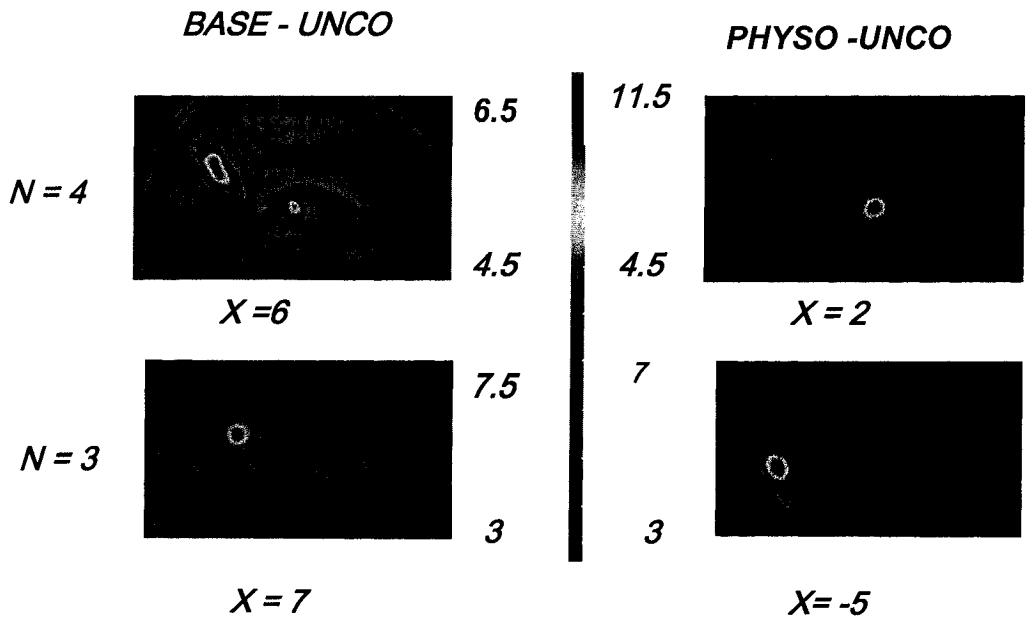

The sagittal sections of t maps of subtraction BASE-UNCO revealed that significant rCBF reductions during unconsciousness in right medial thalamus and precuneus were found in both responders and non-responders. The sagittal sections of t maps of subtraction PHYSO-UNCO revealed that the significant rCBF increase in the medial thalamus and cuneus were found in responders but the significant rCBF increase in the cuneus were found in non-responders during physostigmine-restored consciousness.

Figure 3-12: The horizontal sections of T maps of subtraction BASE-UNCO and subtraction PHYSO-UNCO in four responders (N = 4) and three non-responders (N = 3)

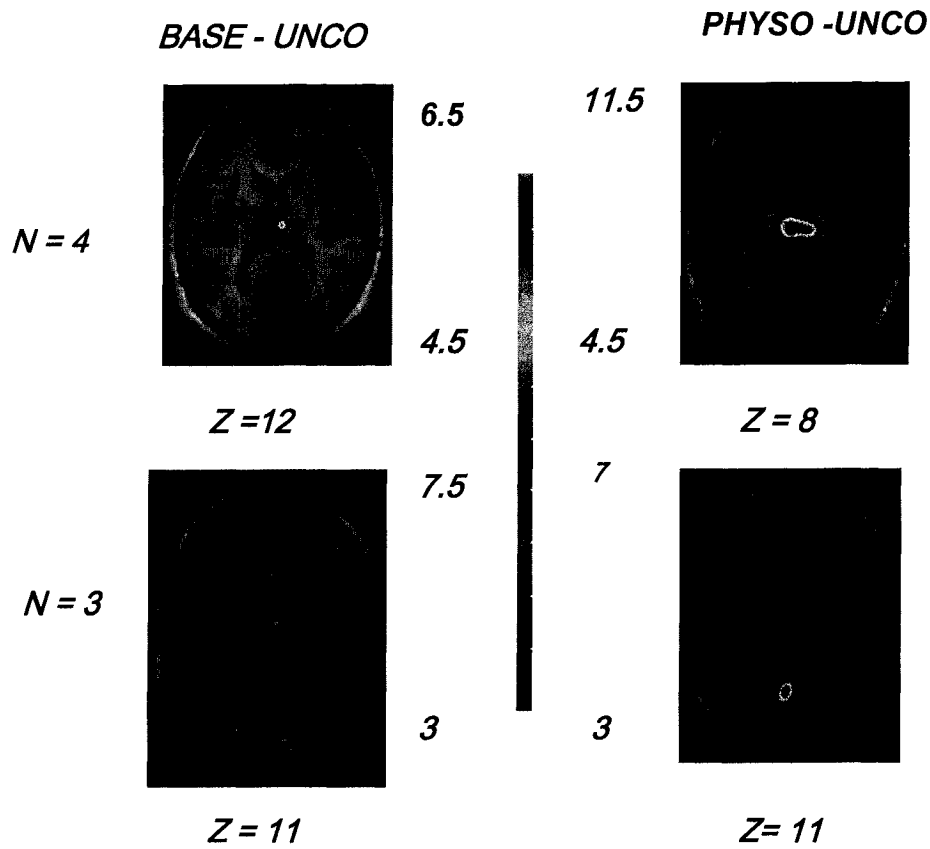

The sagittal sections of t maps of subtraction BASE-UNCO revealed that significant rCBF reductions during unconsciousness in right medial thalamus were found in both responders and non-responders. The sagittal sections of t maps of subtraction PHYSO-UNCO revealed that the significant rCBF increases in the bilateral medial thalamus and cuneus were found in responders but the significant rCBF increase in only the cuneus were found in non-responders during physostigmine-restored consciousness.

Figure 3-13: The relative rCBF in the right thalamus of four responders and three non-responders

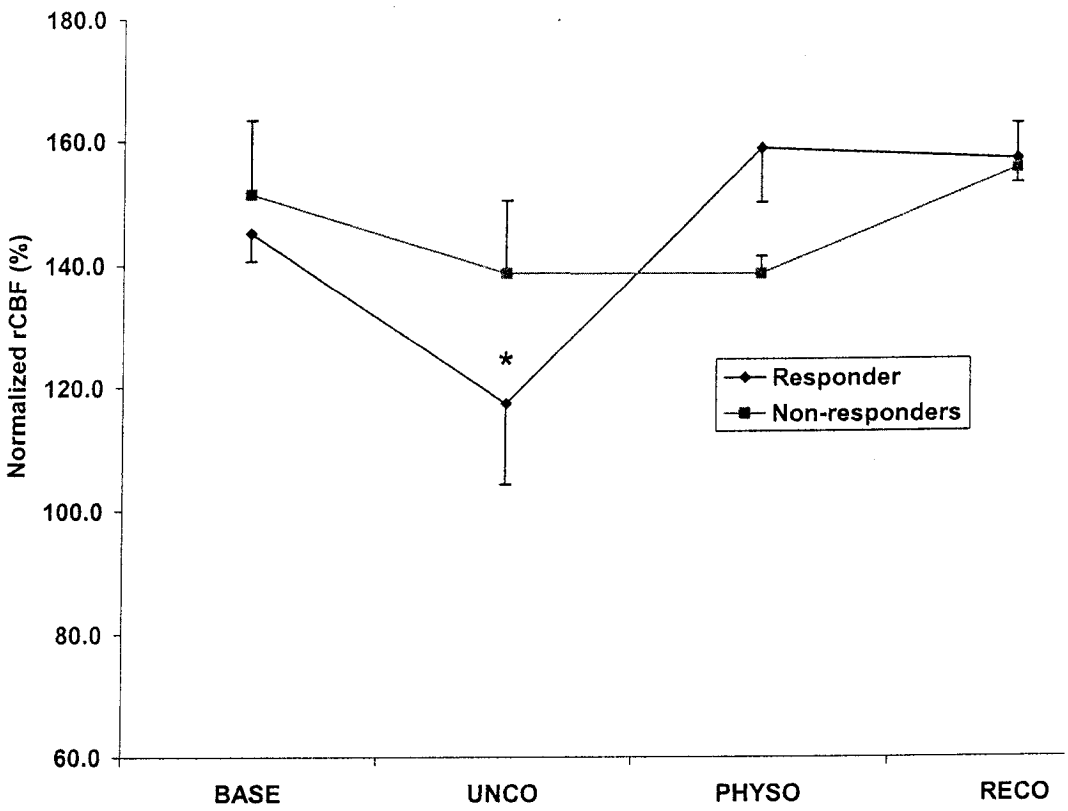

Relative rCBF extracted using spherical ROI with 4 mm radius centred at 8, -18, 9 in right thalamus (* $P < 0.01$ compared with other three conditions)

Figure 3-14: The relative rCBF in the left thalamus of four responders and three non-responders

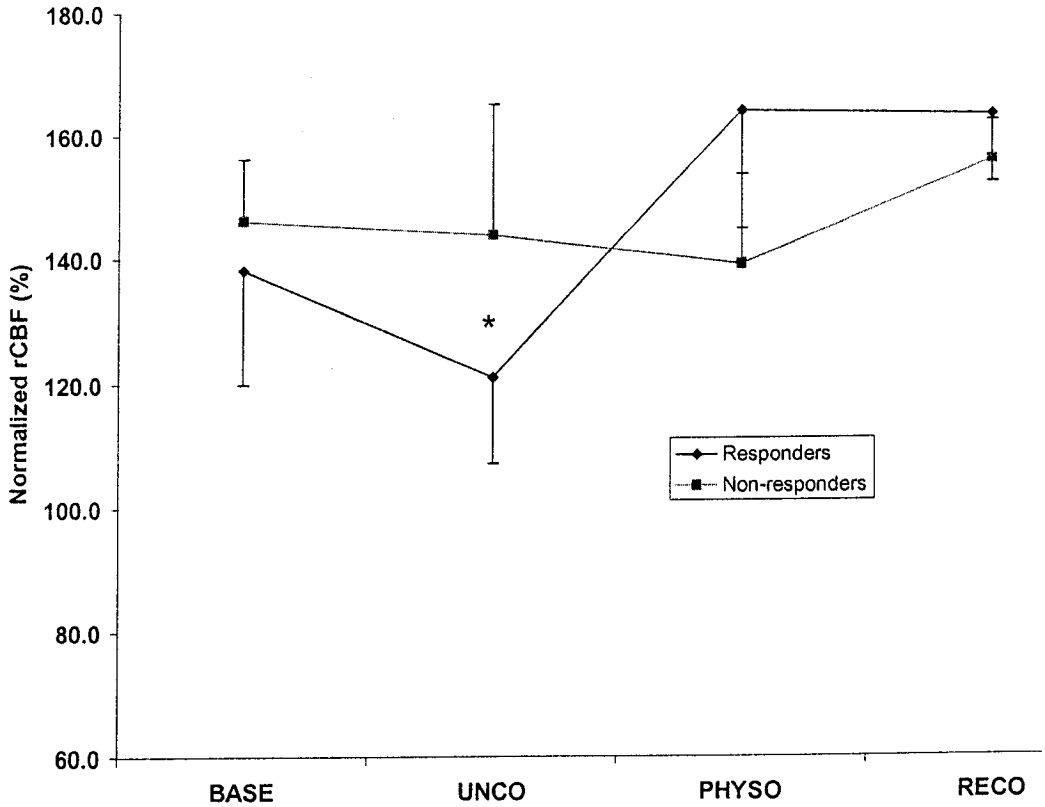

Relative rCBF extracted using spherical ROI with 4 mm radius centred at -3, -16, 8 in left thalamus (* $P < 0.01$ compared with PHYSO and UNCO)

responders and 0 for three responders. On a voxel-by-voxel basis, rCBF values were co-variated with the variable "awake" for each subtraction. Figure 3-15 shows the results of event regression of subtraction between PHYSO and UNCO. There was a significant positive linear relationship between rCBF changes in left thalamus and the event of regain consciousness during physostigmine infusion. Figure 3-16 shows the results of event regression of subtraction between PHYSO and BASE. There was also a significant positive linear relationship between rCBF changes in left thalamus and the event of regain consciousness during physostigmine infusion.

Figure 3-15: Event regression of subtraction PHYSO - UNCO

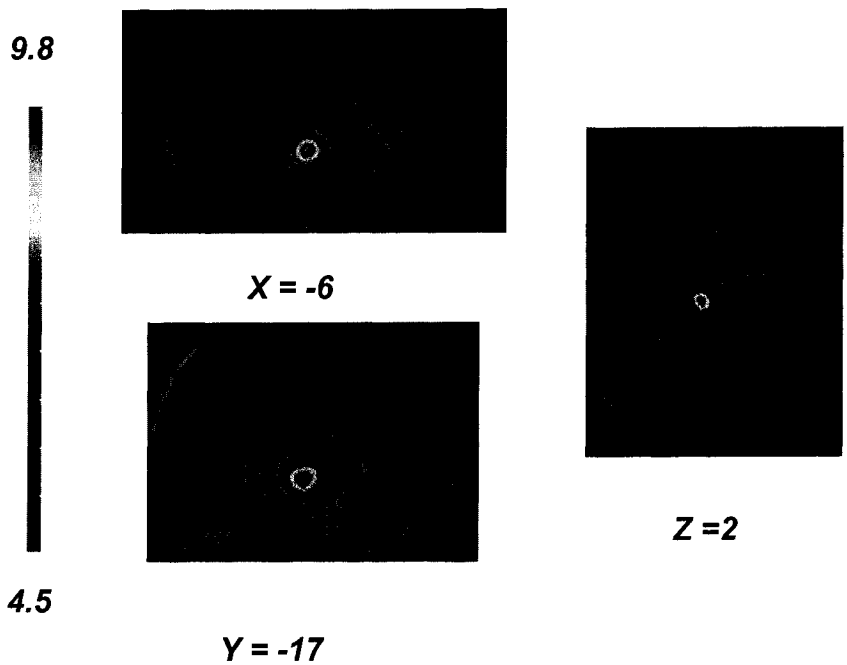

The event regression of subtraction between PHYSO and UNCO revealed a significant positive linear relationship between rCBF changes in left thalamus and the event of regain consciousness during physostigmine infusion.

Figure 3-16: Event regression of subtraction PHYSO - BASE

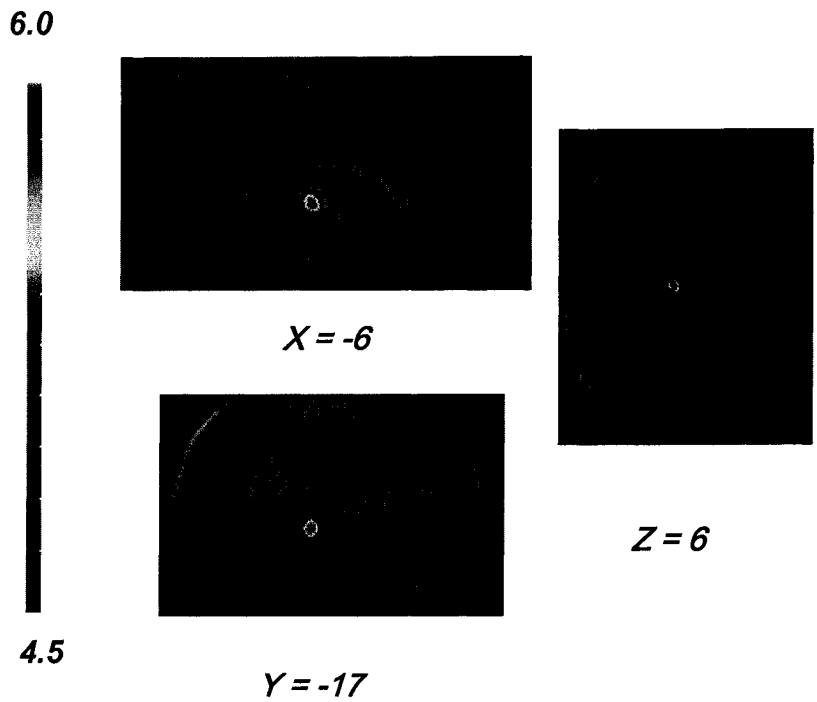

The event regression of subtraction between PHYSO and BASE revealed a significant positive linear relationship between rCBF changes in left thalamus and the event of regain consciousness during physostigmine infusion.

3.5 Discussion

The main goal of this study was to identify the brain function changes specifically linked to the difference in level of consciousness. We used physostigmine to restore consciousness induced by propofol. With the result of both successful and failed attempts to antagonize propofol-induced unconsciousness with physostigmine, we were able not only to determine the brain function changes specifically linked to the difference in level of consciousness but also to determine the brain function changes specifically linked to effect of physostigmine. However, it is important to exclude the effect of other factors such as $PaCO_2$, which may confound our results and to understand the relationship between rCBF changes and brain functional activities.

3.5.1 $PaCO_2$, rCBF changes, and brain activities

It is well known that changes in $PaCO_2$ alter global CBF dramatically (Kitaguchi et al., 1993, Strebel et al., 1994). The change in $PaCO_2$ is an important confounding factor, which is almost inevitable in this type of study unless ventilation is controlled by mechanical ventilation of an unresponsive participant. However, Kasiti et al. (2002) reported that mechanical ventilation of an unresponsive participant may cause a slight

hyperventilation during anesthesia despite the end tidal CO_2 being kept strictly at 4.5%. In spite of the hyperventilation, they also reported a significant decrease in rCBF in the precuneus and thalamus during anesthesia, which is same as the result of most studies with slight hypoventilation without mechanical ventilation. Therefore, the effects of changed PaCO2 on relative rCBF appear to be minor in comparison with those of unconsciousness induced by general anesthetics. Distinct from the effect on global CBF are regional absolute CBF changes related to $PaCO_2$, which can be also sought by normalizing the absolute rCBF by global CBF of each scan to obtain relative rCBF (Fox, 1988). It has recently been reported that the responses of rCBF to $PaCO_2$ changes are not uniform among brain areas. Ito et al. (2000) observed a significant relative rCBF increase in the pons, cerebellum, thalamus, and anterior cingulate gyrus and a significant relative rCBF decrease in temporal and occipital cortices during hypercapnia. In the current study, we found a significant relative rCBF decrease in right thalamus, bilateral precuneus, and other cortical areas, which was different from the effect they observed. The effect of hypercapnia can be easily distinguished from the rCBF changes related to anesthetic-induced unconsciousness. An analysis of rCBF change in relation to PaCO2 revealed a significant positive effect

(same direction as the effect of propofol-induced unconsciousness) from PaCO2 changes itself only in left precentral gyrus, left superior frontal gyrus, and right angular gyrus, which is distant from most regions of the brain that demonstrates the unconsciousness effect for subtraction BASE – UNCO of four responders. Same as the results of previous reports (Ito et al., 2000, Corfield et al., 1995), there was a significant negative effect from PaCO2 changes itself in right parahippocampal gyrus and anterior cingulated gyrus, which is opposite direction as the effect of propofol-induced unconsciousness. There was no significant effect from PaCO2 for other five subtractions of four responders and all subtractions for three non-responders. Therefore, the slight hypercapnia during unconsciousness in the present study does not influence our interpretation of the rCBF changes related to unconsciousness.

The current study examines more directly the effect of drug on the rCBF response. Though neuronal activity was not directly measured, the functional coupling of regional cerebral blood flow and local cerebral glucose metabolism has been established in a wide range of experiments. As more than 85% of cerebral glucose is used by neurons and the remainder may at least partly account for metabolic processes in glial cells, monitoring of regional cerebral blood flow with PET mainly reflects

neuronal and more specifically synaptic activity (Jueptner and Weiller, 1995). The neuronal synaptic activity, which is only indirectly measured by rCBF responses, represents the information transmission in the brain. Although a relationship between changes in brain activity and blood flow has long been a matter of speculation, the neural basis of rCBF changes and the fMRI signal was only recently demonstrated directly in experiments using combined imaging and intracortical recordings (Logothetis et al., 2001; Logothetis and Pfeuffer, 2004).

3.5.2 Mechanism of unconsciousness induced by general anesthetics

3.5.2.1 Brain regions linked specifically to propofol-induced unconsciousness

In our current study, the results of BASE minus UNCO subtractions in four responders support our previous findings of significant decrease in rCBF in the precuneus, the right thalamus, and some parietal regions during unconsciousness (Fiset, 1999). Results of PHYSO minus UNCO subtractions in four responders revealed a new finding that a significant increase in rCBF was found in the regions of the bilateral thalamus, the bilateral cuneus, bilateral precentral gyrus, left medial frontal gyrus and the right fusiform during the physostigmine state. The functional

conjunction between these two subtractions relates to the changes in the level of consciousness (Figure 3-17), which links to the anatomical conjunction between the brain regions deactivated by propofol and the brain regions activated by physostigmine. We found the most significant conjunction areas (T > 4) are right thalamus and bilateral precuneus. A 4-mm spherical volume-of-interest analysis in the conjunction areas reveals that relative rCBF during unconsciousness was significantly lower that of other experimental periods. These functional changes common to the BASE-UNCO and PHYSO-UNCO contrasts were considered functionally linked to the change in level of consciousness independently of any non-specific effects of propofol and physostigmine as these effects have been removed. To our knowledge, there are no previous studies that have distinguished the brain activation caused by the direct effect of drug and the brain activation related to unconsciousness. Although some authors understand the possibility that the regions identified may have nothing to do with the regulation of consciousness, but may simply reflect those areas affected by the agents causing the unconsciousness (Alkire et al., 2000).

Figure 3-17: Functional conjunction between subtraction BASE-UNCO and subtraction PHYSO-UNCO

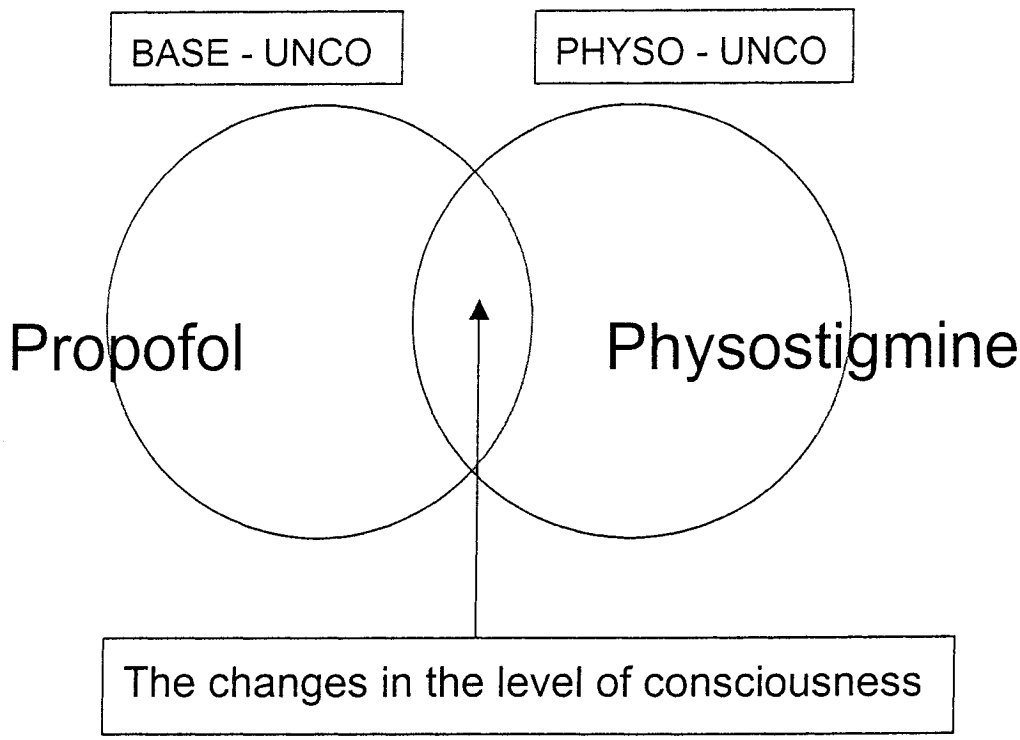

The functional conjunction between BASE-UNCO and PHYSO-UNCO subtractions reflects the changes in the level of consciousness, which is linked to the significant deactivations or activations in the right thalamus and bilateral precuneus.

The region-based regression with right thalamus reveals that rCBF changes in the bilateral precuneus and bilateral cuneus showed a significantly positive covariation with those in right thalamus, which suggested a close functional relationship between thalamus and precuneus/cuneus. On the voxel-by-voxel basis, a number of studies have examined the effects of propofol on the brain rCBF changes in healthy human subjects. Using covariation analysis, Fiset et al. (1999) and Bonhomme et al., (2001) demonstrated that propofol reduced in a dose-dependant manner normalized rCBF in specific brain regions including the right medial thalamus, midline precuneus, and several other cortical areas. Using subtraction analysis, Veselis et al. (2004) revealed that significant decrease in rCBF in right medial thalamus, right precuneus, and other cortical areas. The medial thalamus and midline precuneus are the common brain regions that have significant reduction in rCBF with unconsciousness induced by propofol in all these three studies, which is consistent with our finding in the conjunction analysis.

Based on the resuts of current study together with the findings of previous studies of unconsciousness induced by propofol in healthy subjects, we hypothesize that the joint activities of the medial thalamus, midline precuneus/cuneus, other related cortical areas, contribute to the

unconsciousness induced by propofol. Ogawa et al. (2003) examined the effects of propofol on rCBF in patients with severe depression. Their results, which also revealed the reduction of rCBF in medial thalamus, precuneus, and other cortical areas, are almost entirely consistent with those reported in healthy subjects. These results suggested that the neural structures that are targeted by propofol are basically the same in severely depressed and normal subjects.

3.5.2.2 Brain regions linked to unconsciousness induced by other anesthetics

This hypothesis may be extended to the unconsciousness induced by other anesthetics. Veselis et al. (2004) studied the effect of thiopental on rCBF using PET imaging in 4 healthy volunteers. They found significant decreases of rCBF in bilateral precuneus and cuneus, bilateral cingulated gyrus, left cerebellum and fusiform gyrus but not in thalamus. Although they believed that the small sample size might have caused their failure to detect the significant decrease of rCBF in the thalamus, their results indicated the mechanism of unconsciousness induced by thiopental might be different with other general anesthetics. Kaisti et al. (2002) examined the effects of surgical levels of propofol and sevoflurane anesthesia on

cerebral blood flow in healthy subjects. They revealed significant relative rCBF decreases in the right medial thalamus (8, -26, 6), bilateral precuneus and cuneus, and other cortical areas during 1MAC sevoflurane anesthesia. During propofol anesthesia, they also revealed the significant relative rCBF decreases in the bilateral precuneus but not in the thalamus. Alkire et al. (2000) demonstrated that both isoflurane and halothane caused specific relative reduction of regional cerebral glucose metabolism primarily in right thalamus (10, -12, 18), left cuneus, medial frontal gyrus, inferior temporal gyrus, and cerebellum. Therefore, our hypothesis of mechanism of unconsciousness seems to also be valid for sevofluane, isoflurane, and halothane. In their early PET study of Midazolam, Veselis et al. (1997B) demonstrated that the significant rCBF decrease occurred in the dorsomedial thalamus, the cingulated gyrus, the insula, multiple areas in prefrontal cortex, and parietal and temporal association areas. A significant rCBF decrease was not detected in the precuneus and cuneus during midazolam infusion. It may indicate a different neuronal network for the unconsciousness induced by midazolam or just a technical limitation of early PET studies.

3.5.2.3 Thalamus and precuneus/cuneus as the key elements of neuronal network for consciousness and unconsciousness.

The PET studies cited above have underscored the importance of the thalamus as a putative target of anesthetic action. Different subdivisions of thalamus have their specific functions. The BASE-UNCO subtraction of this study and other two studies (Bonhomme et al., 2001, Veselis et al., 1997B) have revealed that general anesthetics significantly decreased the rCBF of the right medial dorsal nucleus of thalamus, which is closely related to the frontal association cortex. This pathway is reported to maintain vigilance and working memory (Kinomura et al., 1996). Ogawa et al. (2003) reported that propofol significantly decreased the rCBF of the pulvinar nucleus of thalamus, which has been considered to communicate with the posterior part of the parietal lobes and occipital lobes (Burton et al., 1976; Yeterian and Pandya, 1985).

Most of PET studies cited above have also underscored the importance of the precuneus/cuneus as a putative target of anesthetic action. In the region-based regression analysis of right thalamus (Table 3-6, Figure 3-8), significant positive co-variations were observed in the bilateral precuneus, bilateral cuneus, and left putamen. These results suggested a close functional relationship between right thalamus and

bilateral precuneus and cuneus, which strongly support our hypothesis that the medial thalamus, midline precuneus/cuneus, other related cortical areas constitute a neuronal network for consciousness and unconsciousness. In studies of normal conscious state, the precuneus has been identified as a major contributor to two relaxed conscious states: normal resting consciousness and the relaxation meditation in Yogo Nidra (Lou et al., 1999; Kjaer and Lou, 2000). In the reflective self-awareness study, Kjaer et al. (2002) demonstrated differential activity in precuneus and angular gyri during reflection on own personality traits. The precuneus/posterior cingulate regions has repeatly been associated with episodic memory retrieval (Cabeza and Nyberg, 2000). Lou et al. (2004) presented evidence that the function of precuneus is particularly important to explicit self-representation. All these studies highlighted the importance of precuneus for maintaining normal conscious state.

The published PET data described a very reproducible functional neuronal network in sleep, which again underscores the importance of thalamus and precuneus in a neuronal network for consciousness and unconsciousness. There are two types of sleep, slow wave sleep (SWS) and rapic eye movement (REM) sleep (stage 1). In humans, SWS is divided further into light (stage 2) and deep (stages 3,4) SWS. REM sleep

is a state with electrical appearances and cerebral metabolic rate similar to those of wakefullness, accompanied by rapid eye movements and a profound relaxation of limb muscules (Zeman and Reading, 2005). One characteristic common to the sleep stages is reduced reflective self-awareness (Kahan et al., 1997). In REM sleep, significant deactivations were found in precuneus and dorsolateral prefrontal, parietal, and posterior cingulate cortices while significant activations were found in thalamic nuclei, limbic areas (amygdaloid complexes, hippocampal formation, anterior cingulate cortex), and brainstem. In deep SWS, significant deactivations were seen in precuneus, thalami, orbital frontal cortex, basal forebrain, anterior cingulate cortex, and parietal cortex (Marquet et al., 1997). Thus, reduction in activity in the precuneus is common to the two types of sleep, which again emphasizes the importance of precuneus for maintaining normal conscious state. The deactivation during deep SWS and activation during REM sleep in thalamus underline the importance of thalamus in the changes of level of consciousness.

3.5.2.4 The other elements of neuronal network for consciousness and unconsciousness.

Although the thalamus and precuneus/cuneus have repeatedly shown to be deactivated during the unconsciousness induced by general anesthetics, the other cortical areas deactivated have varied from study to study. Conscious experiences have often been ascribed to the executive regions of the frontal lobe, especially prefrontal areas, and the cingulated gyrus. The prefrontal areas were deactivated during the unconsciousness induced by general anesthetics in Veselis et al. (1997, midazolam, BA 10,11,47), Fiset et al. (1999, propofol, BA 11), Alkire et al. (2000, isoflurane and halothane, BA 47), Bonhomme et al. (2001, propofol, BA 10, 46), Kaisti et al. (2002, sevoflurane, BA 9,10,46, propofol, BA 10, 47) Ogawa et al. (2003, propofol, BA 46,47), and Veselis et al. (2004, propofol, BA 9,10,11,47, thiopental, BA 9). In our current study, the orbitofrontal gyrus (BA 47) was deactivated during the unconsciousness induced by propofol. These PET studies cited above have also underscored the importance of the prefrontal cortex as another putative target of anesthetic action. In the auditory vigilance task, large increases in rCBF were observed in the ventrolateral prefrontal cortex (BA 45, 47) as compared with the baseline state (Paus, 1997). This finding is consistent with the

results of lesion study (Wilkins et al., 1987) and supports a role of the prefrontal lobe in the allocation of the capacity-limited attention mechanisms. Dorsolateral prefrontal cortex was activated during working memory (Carpenter and Just, 2000). Kjaer et al. (2001) reported that the prefrontal cortex (BA 10,11) and precuneus (BA 31,7) were activated during awareness of visual verbal stimulation. During the unconsciousness induced by general anesthetics, the attention, awareness, and working memory were lost. Therefore, it is not surprising to see the deactivation in the different areas of prefrontal cortex. During SWS, the prefrontal cortex, especially orbital prefrontal cortex, was depressed more significantly than in other cortical areas (Maquet, 1997), which was supported by Hofle et al. (1997). Braun et al. (1997) and Andersson et al. (1998), who reported that both orbital prefrontal cortex and dorso-lateral prefrontal cortex were deactivated during SWS. The prefrontal cortex was also deactivated during REM sleep (Marquet, 1996; Braun, 1997). Thus, the prefrontal cortex is involved in both normal sleep and unconsciousness induced by general anesthetics.

The anterior cingulated cortex (ACC) sends dense projection to the motor cortex and receives extensive afferents from the midline thalamus, which point to the importance of ACC in arousal state. Veselis et al. (1997)

reported that left anterior cingulated gyrus (BA 9-32) was deactivated during midazolam infusion, but it is a large deactivated cluster in left medial frontal cortex that extended to left ACC. Most of PET studies failed to detect significant rCBF reduction in ACC during the unconsciousness induced by general anesthetics, which may indicate that the inhibitory effects in the limbic system caused the minor rCBF response. In current study, the left ACC (BA 32) was activated during the unconsciousness induced by propofol in the four responders and three non-responders. It may be caused by the slight hypercapnia during unconsciousness. During hypercapnia, significant relative hyperperfusion in the thalamus and left ACC was observed (Ito et al., 2000). Neural activation in the limbic system including ACC during CO2-stimulated breathing has been reported in humans (Corfield et al., 1995). Significant relative hyperperfusion in the thalamus and limbic system during hypercapnia may be related to CO2-stimulated breathing. We noted that the changes of rCBF in the thalamus caused by PaCO2 are in the opposite direction of the changes of rCBF in thalamus found in this study. This finding may explain why some studies (Kaisti et al., 2002; Veselis et al., 2004) failed to detect the thalamic deactivation during the unconsciousness induced by anesthetics. As the ACC was deactivated during SWS, it was expected to find a reduction of

rCBF in the anterior cingulated gyrus during unconsciousness induced by general anesthetics. So far, we are not able to determine if the ACC is involved in the unconsciousness induced by general anesthetics.

3.5.2.5 The hypothesis of Common Medline Core

Kjaer et al. (2002) hypothesized that precuneus, angular gyri, and anterior cingulated gyri constitute a Common Midline Parietofrontal Core of reflective self-awareness and conscious states. Based on the above discussion, we can refine our hypothesis that the joint deactivations of a Common Midline Core, which includes the medial thalamus, midline precuneus/cuneus, prefrontal cortex and other related cortical areas, contribute to the unconsciousness induced by general anesthetics. The role of ACC in the Common Midline Core of unconsciousness would require further investigation.

3.5.3 Mechanism of consciousness restored by physostigmine

3.5.3.1 Responders or non-responders

Among the seven subjects in this study, four regained consciousnes after physostigmine infusion and three remained unconsciousness. In order to understand this phenomenon, we have to look at the relative dose

of propofol and physostigmine. As the experimental design of human studies is constrained by safety issue, the minimum dose of propofol was titrated to produce loss of consciousness in this study. This had practical relevance as subjects were able to maintain spontaneous respiration despite unconsciousness. The dose of physostigmine was also limited for reasons of safety. It is fortuitous that the dose of physostigmine was of sufficient magnitude such that it produced the intended effect, indicating that the dose-effect relationship between the relevant endogenous ligands and receptors were amenable to these pharmacological manipulations (Backman, 2004).

Recently we used ^{11}C-Benzotropine to study muscarinic receptor availability during propofol-induced unconsciousness (Xie, 2004 or Chapter 2). Our results showed that propofol produced a decrease in receptor availability (benztropine binding), which reflecting a decrease in central acetylcholine (ACh) binding, in several brain regions rich in muscarinic receptors. This would support the hypothesis that propofol affects Ach binding in two possible mechanisms. First, it is possible that propofol causes a change in conformational state of the muscarinic receptor from high to low affinity during unconsciousness so that it becomes less available for binding. Alternatively, it is possible that

propofol binds directly with the muscarinic receptor and prevents binging with ACh (or benztropine). Physostigmine inhibits cholinesterase and increases the amount of endogenous ACh, which activates receptors to high affinity state or directly compete with propofol. Therefore, whether physostigmine reverses the unconsciousness induced by propofol depends on the relative dose of propofol and physostigmine. This finding may raise the possibility that depression of central cholinergic transmission is one of the common pathways mediating anesthesia-induced unconsciousness.

3.5.3.2 The brain region and consciousness restored by physostigmine

We hypothesized that consciousness restored by physostigmine involved similar neuronal network but slightly different structures. The consciousnes restored by physostigmine related to not only activation in right thalamus but also the activation in the left thalamus (Figure 3-3; Table 3-3). The bilateral cuneus were activated in the consciousness restored by physostigmine while the bilateral precuneus were deactivated during the propofol-induced unconsciouseness. Comparing the results of PHYSO minus UNCO of four responders and three non-responders (Figure 10,11,12), we can see the activations in bilateral thalami in

responders while no significant thalamic activation in non-responders, which suggests that the significant bilateral strong activations (T > 11) in thalami are specifically linked to the restored consciousness (not the direct drug effect) as the drugs used in responders and non-responders are same. We also noticed that the bilateral cuneus were activated in responders while only left cuneus was activated in non-responders, which implied that physostigmine may activate the left cuneus but right cuneus activation is required to restore consciousness.

For the four responders of this study, subjects were awake and the infusions of physostigmine and propofol were maintained during physostigmine condition. Therefore, a PHYSO minus BASE subtraction was generated to evaluate the effect of propofol and physostigmine, which is linked to the significant increasing of rCBF in the left thalamus, bilateral precental gyrus, right anterior cingulated gyrus, right medial frontal gyrus and other cortical areas. There is still a residual concentration of propofol and physostigmine in the body during the recovery condition. Therefore a RECO minus BASE subtraction was generated to evaluate the effect of residual propofol and physostigmine, which was linked to the significant increasing of rCBF in the left thalamus, bilateral precentral gyrus, left anterior cingulate gyrus, right medial frontal gyrus and other cortical areas.

Now we know that the effect of propofol and physostigmine is linked to the significant rCBF increase in the left thalamus, bilateral precentral gyrus, anterior cingulated gyrus, right medial frontal gyrus and other cortical areas. The next logical step was to differentiate the effect of propofol and effect of physostigmine. If propofol caused the significant rCBF increase in the left thalamus and precentral gyrus, a BASE minus UNCO subtraction could reveal similar changes in rCBF. In fact, a BASE minus UNCO subtraction revealed the significant decrease of rCBF in right thalamus and precuneus and non-significant decrease of rCBF in left thalamus (-17, -19, 14, T = 2.78) but no any rCBF increase, which T value is larger than 2.5, in the left thalamus and precentral gyrus. Therefore, we can hypothesize that the direct effects of physostigmine are linked to the significant rCBF increase in left medial thalamus, bilateral precentral gyrus, anterior cingulated gyrus, and other cortical areas. Region-based regressions revealed that left thalamus was positive covariated with right thalamus, medial frontal gyrus, bilateral putamen, and left cuneus. Furthermore, the event regression revealed that rCBF in left thalamus is significantly positively co-variated the physostigmine-restored consciousness in subtraction PHYSO minus UNCO and PHYSO minus BASE. Based on above evidences, we hypothesize that physostigmine

restores consciousness by first activating the left thalamus and then the right thalamus and other cortical areas. The activations in both sides of thalami are essential for regaining consciousness.

Furey et al. (2000A) assessed the time course of pharmacodynamic and pharmacokinetic effects of physostigmine using PET rCBF technique. They found that physostigmine did not affect resting rCBF in right prefrontal region but physostigmine significantly reduced rCBF in right prefrontal region during task, which is consistent with our finding of the significant reduction of rCBF in right middle frontal gyrus (Table 3-4). Because their goal was to detect the task of working memory related rCBF changes, the subtraction between pre-infusion and after physostigmine infusion was not reported. In another study (Furey et al., 2000B), They demonstrated that the negative correlations, indicating regions in which greater rCBF increases were associated with greater improvement in reaction time, were restricted to medial occipital visual cortex, suggesting that physostigmine may improve task performance by enhancing visual processing. We are not aware of any other previous human studies assessing the direct specific effect of physostigmine on brain rCBF with which our results could be compared.

3.5.4 Conclusion

In conclusion, we have demonstrated that right thalamus and bilateral precuneus are specifically linked to propofol-induced unconsciousness, and ruled out a non-specific effect of propofol on those brain areas. Thus, the results of our study support a hypothesis that the joint activation and deactivation of a Common Midline Core, which includes the medial thalamus, midline precuneus/cuneus, prefrontal cortex and other related cortical areas, contributed to the changes of level of consciousness. We also hypothesized that physostigmine restored consciousness by first activating the left thalamus and cuneus and then the right thalamus and cuneus and other cortical areas. Our data suggested that the activations in both sides of thalamus and cuneus may be essential for regaining consciousness.

Chapter 4 GENERAL DISCUSSION

Immobility, amnesia, and unconsciousness are the three goals that must be achieved in adequate surgical anesthesia. The anesthetics may act on different regions of nervous system to produce these three goals. It has been known that immobilization is very likely mediated by effects on the spinal cord while amnesia is likely mediated by effects on the dorsolateral prefrontal cortex. The results of chapter 2 in thesis may indicate a propofol-related reduction in muscarinic receptor binding in CNS which supports a hypothesis that the loss of consciousness produced by propofol is mediated, at least in part, via interruption of central cholinergic muscarinic transmission. The results of chapter 3 in this thesis support a hypothesis that the joint deactivations of a Common Midline Core, which includes the medial thalamus, midline precuneus/cuneus, prefrontal cortex and other related cortical areas, contribute to the unconsciousness induced by general anesthetics. In order to fully explore the mechanism of unconsciousness induced by general anesthetics, we have to understand the molecular mechanisms of unconsciousness induced by general anesthetics and build a complete neurophysiological theory of the action of anesthetics to suppress consciousness.

4.1 Theoretical explanations of anesthetic action

As experimental evidences contradicted the old lipophilicity hypothesis, which had dominated for more than one century, the work of Franks and Lieb (1984) shifted attention from lipids to proteins as anesthetic targets. They proposed that at the molecular level, anesthetics almost certainly act by binding directly to proteins, which are considered likely to be postsynaptic ligand-gated channels (Franks and Lieb, 1994). Although some anesthetics might act at excitatory synapses, such as ketamine at NMDA receptors and some anesthetics potentiate inhibitory synaptic receptors, such as GABA receptors, both inhibition of excitory synapses and potentiation of inhibitory synapses may be involved in anesthetic effects. Anesthetics may act on a variety of neurotransmission processes, and the effects are widespread throughout the brain. Ion channel proteins integrated with other proteins into a membrane patch, patches are integrated into a nerve cell, nerve cells are integrated into networks, and local networks are integrated into functional units (John and Prichep, 2005). Therefore, it is not sufficient for a theory of anesthesia to be based on demonstration of some primary effects of an anesthetic drug

on neuron receptors or on some particular molecular or cellular sites of action.

Flohr et al. (1998) proposed a theory that the conditions for consciousness state can be defined by a specific computational structure that gives rise to functional states that are identical with states of consciousness. It consists of four hypotheses. (1) The occurrence of states of consciousness depends on the formation of transient higher-order, self-referential mental representations, which is identical with the appearance of consciousness. Loss of consciousness will occur when the brain's representational activity falls below a critical threshold. (2) Higher-order mental representations are instantiated by neural cell assemblies. (3) The formation of such assemblies involves the activation of the NMDA receptor channel complex. The activation state of this receptor determines the rate at which such assemblies are generated. (4) Modification of NMDA-dependent computational processes is the final common pathway of anesthetic action. They proposed that the common mode of anesthetic action is the disruption of NMDA-dependent computational processes. Agents that directly inactivate the NMDA synapse necessarily have anesthetic properties; agents that do not directly affect the NMDA synapse will exert an anesthetic action by inhibiting NMDA-dependent processes.

The concepts from quantum physics have been used to explain the molecular basis of anesthetic action. Woolf and Hameroff (2001) have proposed that rudimentary visual consciousness depends on quantum computation in microtubules in the cytoplasmic interiors of cortical pyramidal dendrites interconnected by gap junctions. These interactions are critically dependent on cholinergic action on pyramidal cell dendrites and on GABAergic interneurons interconnected by electrotonic gap-junction connections. Unfortunately such proposal remain theoretically controversial and without experimental support.

4.2 The neurophysiologic theory of the action of anesthetics to suppress consciousnes

Recordings from the surface of the scalp have long been known to demonstrate rhythmic voltage oscillations derived from the electrical activity of the subjacent neuronal population. With development of modern technology, we can use validated automatic editing algorithms to remove contaminated signals that do not arise from brain electrical activity and we can use computer analysis to describe the power spectrum in each scalp region. For such quantitative electroencephalographic analyses, the quantitative electroencephalogram is conventionally divided into frequency

bands, approximately defined as δ (0.5-4 Hz), θ (4-8 Hz). low α (8-10 Hz), high α (10-12 Hz), β (12-25 Hz), and γ (25-50 Hz).

In the thalamic relay nuclei, some types of neurons diaplay rhythmic oscillations in the frequency range of 6-10 Hz. This oscillatory behavior seems to be an intrinsic property of these neurons. The α activity arises from the interaction between populations of these neurons in the thalamus and in certain areas of the cortex. In the thalamic nuclei, three main types of neurons interact: thalamocortical relay (TCR) nuclei whose axons project to the cortex, reticular nucleus (RE) neurons that interact synaptically with the TCR cells and contribute GABAergic inhitory feedback control, and local intrinsic neurons (Steriade, 1993). By GABAergic action, RE neurons can act to diminish sensory throughput TCR neurons to the cortical receiving areas, slow the mean frequency of the oscillation and shifting the α rhythm toward θ (4-8 Hz). The diminished activation of the cortex by thalamus and the ascending reticular activation system (ARAS) results in the production of a very slow rhythm called δ activity (0.5-4 Hz). The corticocortical interactions generate the β rhythm (12-25 Hz). The feedback from the corticothalamic volley binds the distributed fragments and causes coherent corticothalamocortical loops to

reverberate at the frequency of the γ rhythm (25-50 Hz) (John and Prichep, 2005).

Based on intracerebral recordings, Desmedt and Tomberg (1994) have reported that a brief period of γ activity with zero phase lag appears coherently between prefrontal cortex and parital cortex of human subjects during preformance of perceptual tasks. Their findings are consistent with the suppression of prefrontal cortex and precuneus/cuneus during unconsciousness induced by general anesthetics. After reviewing the recent consciousness-related researches, John and Prichep (2005) propose that the neurophysiological effects that produce amnesia and unconsciousness induced by general anesthetics occur in six steps: (1) depression of the brainstem reduces the influences of the ARAS on the thalamus and cortex; (2) depression of mesolimbic-dorsolateral prefrontal cortex interactions leads to blockade of memory storage; (3) further depression of the ARAS releases its inhibition of the nucleus reticularis of the thalamus, resulting in closure of thalamus gates by hyperpolarizing GABA-mediated inhibitory action of the nucleus reticularis (θ increase), thereby blocking; (4) thalamocorticothalamocortical reverberations and perception (γ decrease); (5) parital-frontal transactions are uncoupleed (γ

coherence decrease), blocking cognition; (6) prefrontal cortex is depressed to reduce awareness (Figure 4-1).

4.3 Functional brain imaging evidence of the neurophysiologic theory

General anesthetics that cause depression of the ARAS in the brainstem can reduce activating and arousal influences on the specific and nonspecific thalamic nuclei and cortex. Fiset et al. (1999) found that there was significant covariation between the thalamic and midbrain blood flow during unconscousnes induced by propofol, which is consistent with the role of the thalamus and the ARAS. Ogawa et al. (2003) reported that significant decreases in rCBF occured in the pontine tegmentum during propofol anesthesia. The significant deactivations were found in midbrain during unconsciousness induced by propofol (Kaisti et al., 2002) , isoflurane and halothane (Alkire et al., 2000). All above evidence of brain imaging demonstrated that the brain stem was suppressed during the anesthetic-induced unconsciousness.

Depression of the ARAS can release complex GABAergic inhibitory effects in the limbic system due to diminution of ARAS inputs that produce cholinergic inhibition of GABA. General ansthetics may diminishes the interactions of the mesolimbic circuits, including the

Figure 4-1: Schematic depiction of six stages hypothesized to explain the unconsciousness induced by general anesthetics.

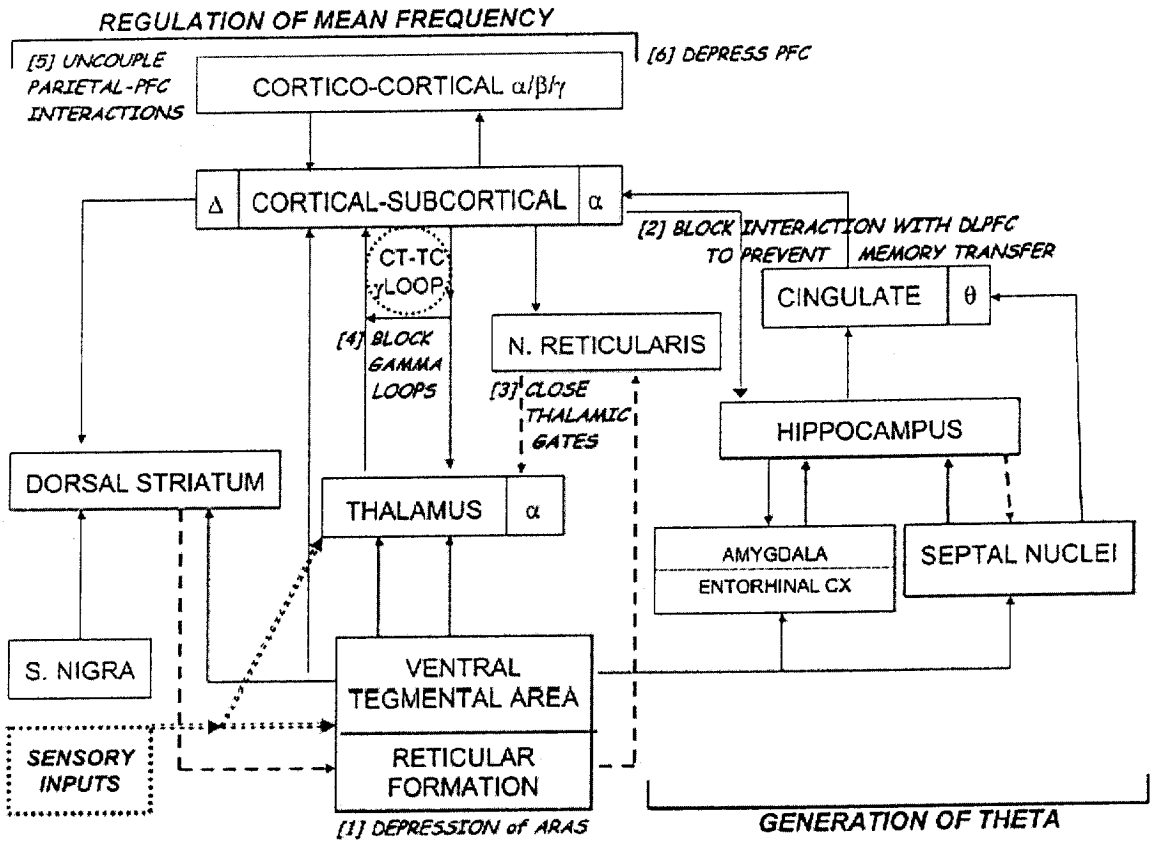

Step 1: depression of the ARAS causing a diminution of availability of ACh, resulting in step 2: decreased reactivity of the limbic system preventing recent memory transfer for storage, followed by step 3: further decrease of ACh disinhibiting the blockade of GABA-mediated inhibition by nucleus reticularis, resulting in closure thalamic gates and leading to step 4: blockade of reverberations in corticothalamocortical loops and interruption of resonance, causing step 5: uncoupling of parietal-prefrontal cortical interaction, resulting in step 6: depression of prefrontal cortex with unconsciousness. (From Zeman 1997)

amygdala, hippocampus-cingulate cortex with the dorsolateral prefrontal cortex, to block the storage of memory and achieve amnesia. Sperling et al. (2002) revealed that the significant decreases were observed in both the extent and magnitude of activation within the hippocampal, fusiform, and inferior prefrontal ROIs with the administration of either lorazepam or scopolamine. Unfortunately most of PET studies failed to detect significant rCBF reduction in limbic system during the unconsciousness induced by general anesthetics. It may indicate that the inhibitory effects in the limbic system caused the minor rCBF response.

The depression of brainstem releases the nucleus reticularis form the inhibiting influence of the ARAS, which can lead to closure of thalamic gates due to the inhibitory action of nucleus reticularis, resulting in diminished cortical input. Decreased thalamocortical input may result either by loss of activation from the ARAS or by dynamic inhibition via nucleus reticularis. Inhibition of either the cortex or thalamic projection nuclei blocks the corticothalamocortical reverberations that are hypothesized to be critcal for consciousness. The thalamical inhibitions were demonstrated during anesthetic-induced unconsciousness in most brain imaging study. The BASE-UNCO subtraction of this study and other two studies (Bonhomme et al., 2001, Veselis et al., 1997B) have revealed

that general anesthetics significantly decreased the rCBF of the right medial dorsal nucleus of thalamus, which is closely related to the frontal association cortex and this pathway is reported to maintain vigilance and working memory (Kinomura et al., 1996). Although the nucleus of thalamus deactiveated in different stuides were different, the deactivation of thalamus were detected during anesthetic-induced unconsciousnes in most imaging studies.

Depression of the parietal cortex interrupt the prefrontal-parietal transactions critical for perception. Inhibition of the prefrontal cortex releases its modulation of nucleus reticularis, resulting in defocusing of attention and reducing activation of the systems medicating speech and movement. This part of theory is strongly supported by results from functional brain imaging studies. In the auditory vigilance task, large increases in rCBF were observed in the ventrolateral prefrontal cortex (BA 45, 47) as compared with the baseline state (Paus, 1997). This finding is consistent with the results of lesion study (Wilkins et al., 1987) and supports a role of the prefrontal lobe in the allocation of the capacity-limited attention mechanisms. Dorsolateral prefrontal cortex was activated during working memory (Carpenter and Just, 2000). The precuneus (medial parietal cortex) has been identified as a major contributor to two

relaxed conscious states: normal resting consciousness and the relaxation meditation in Yogo Nidra (Lou et al., 1999; Kjaer and Lou, 2000). The precuneus/posterior cingulate regions has repeatly been associated with episodic memory retrieval (Cabeza and Nyberg, 2000). These studies highlighted the importance of precuneus for maintaining normal conscious state. In both deep SWS and REM sleep, significant deactivations were seen in precuneus (Marquet et al., 1997). Thus, reduction in activity in the precuneus is common to the two types of sleep, which again emphasizes the importance of precuneus for maintaining normal conscious state.

During the unconsciousness induced by general anesthetics, the attention, awareness, and working memory are all lost. Therefore, it is not surprising to see the deactivation in the different areas of the prefrontal cortex and precuneus. Both the prefrontal areas and precuneus were deactivated during the unconsciousness induced by general anesthetics in most functional brain imaging studies. The region-based regression analysis of right thalamus suggested a close functional relationship between right thalamus and bilateral precuneus and cuneus. The region-based regression analysis of left thalamus suggested a close functional relationship between left thalamus and right medial frontal gyrus. Both results indicate that the interruption of prefrontal-parietal transactions is

related to the deactivation of right thalamus while restoration of prefrontal-parietal transactions related to activation of bilateral thalami. Furthermore, the first study of this thesis demonstrated the significant reduction of muscarinic receptor availability in orbital-frontal cortex and parietal cortex. These results may suggest that the interruption of prefrontal-parietal transactions is caused by the depression of cholinergic system.

4.4 Theory about consciousness restored by physostigmine

We have hypothesized that the joint deactivities of a Common Midline Core, which includes the medial thalamus, midline precuneus/cuneus, prefrontal cortex and other related cortical areas, are contributed to the unconsciousness induced by general anesthetics. This hypothesis is consistent with the neurophysiologic theory of John and Prichep. Thus, we hypothesize that the consciousness restored by physostigmine involved similar neuronal network but slightly different structures. The consciousnes restored by physostigmine related to not only activation in right thalamus but also the activation in the left thalamus. The bilateral cuneus were activated in the consciousness restored by physostigmine while the bilateral precuneus were deactivated during the propofol-induced unconsciouseness. Comparing the results of PHYSO

minus UNCO of four responders and three non-responders, we can see the activations in bilateral thalami in responders while no significant thalamic activation in non-responders, which suggests that the significant bilateral strong activations (T > 11) in thalami are specifically linked to the restored consciousness (not the direct drug effect) as the drugs used in responders and non-responders are same. We also notice that the bilateral cuneus are activated in responders while only left cuneus was activated in non-responders, which imply that physostigmine may activate the left cuneus but right cuneus activation is required to restore consciousness.

From discussion of 3.5.3.2, we know that the direct effects of physostigmine are linked to the significant rCBF increase in left medial thalamus, bilateral precentral gyrus, anterior cingulated gyrus, and other cortical areas. Region-based regressions revealed that left thalamus was positively covariated with right thalamus, medial frontal gyrus, bilateral putamen, and left cuneus. Furthermore, the event regression revealed that rCBF in left thalamus is significantly positive co-variated the physostigmine-restored consciousness in subtraction PHYSO minus UNCO and PHYSO minus BASE. Based on above evidences, we hypothesize that physostigmine restore consciousness by first activating

the left thalamus and then the right thalamus and other cortical areas. The activations in both sides of thalami are essential for regaining consciousness.

Based on above results, 3 stages were hypothesized to explain the consciousness restored by physostigmine. Step 1: activation of left thalamus, left cuneus and reticular formation, resulting in step 2: activation of right thalamus and cuneus, reaching certain threshold of right thalamus and cuneus, and cause cuneusthalamical reverberations, causing step 3: activation of prefrontal cortex to restore the consciousness (Figure 4-2). If the activation of right thalamus and cuneus do not reach the threshold, the cuneusthalamical reverberations will not happen, and the subject will not regain consciousness after infusion of physostigmine.

4.4 General conclusion

The understanding of states of consciousness has been identified as an outstanding intellectual challenge across disciplines ranging from neuroscience through psychology to anesthesiology. The advent of functional imaging combined with sophisticated electroencephalographic techniques is transforming our ability to study the state of consciousness

Figure 4-2: Schematic depiction of 3 stages hypothesis to explain the consciousness restored by physostigmine

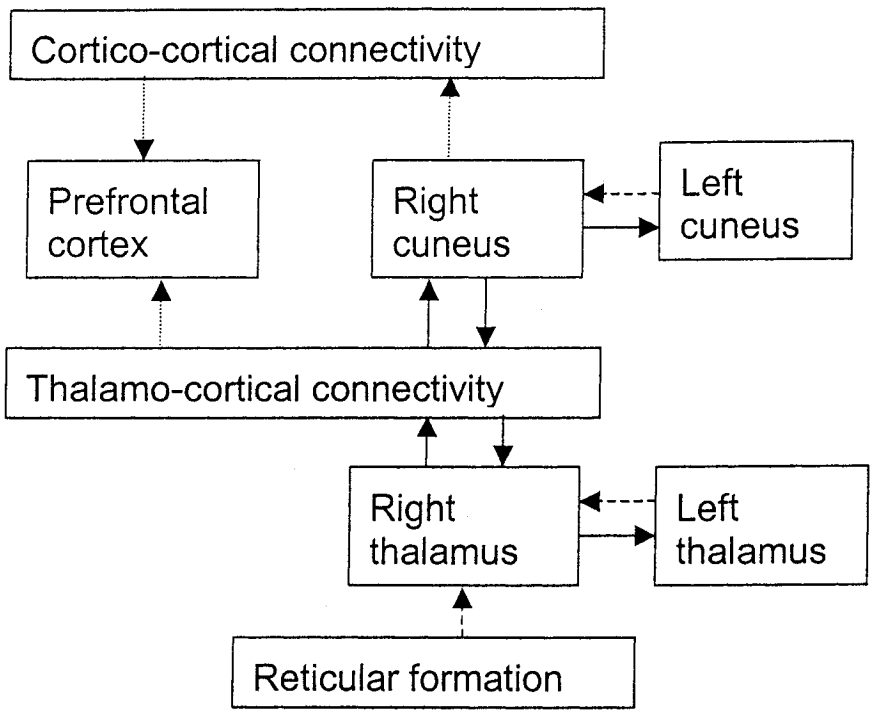

Step 1: activation of left thalamus, left cuneus and reticular formation, resulting in step 2: activation of right thalamus and cuneus, reach threshold of right thalamus and cuneus, cause cuneusthalamical reverberations, causing step 3: activation of prefrontal cortex

directly in humans. With functional brain imaging, the studies in normal conscious state, sleep, and anesthetic-induced unconsciousness demonstrate the critical role of thalamus and precuneus/cuneus in maintaining and losing the state of consciousness. Based on our second study, we hypothesized that the joint deactivations of a Common Midline Core, which includes the medial thalamus, midline precuneus/cuneus, prefrontal cortex and other related cortical areas, contribute to unconsciousness induced by general anesthetics. These joint deactivations disrupt the functional interaction within the thalamocortical and corticocortical neural networks. We also hypothesize that physostigmine restore consciousness by first activating the left thalamus and cuneus and then the right thalamus, cuneus, and other cortical areas. The activations in both sides of thalamus and cuneus may be essential for regaining consciousness.

The first study of this thesis demonstrates that propofol produced a decrease in central acetylcholine bindings in several brain regions rich in muscarinic receptors. This finding suggests that depression of central cholinergic transmission is one of the common pathways mediating anesthesia-induced unconsciousness. The findings of both studies have significant relevance for current theories of consciousness and provide

additional insight into the potential mechanisms of unconsciousness induced by general anesthetics.

LIST OF REFERENCES

Aine CJ, 1995, A conceptual overview and critique of functional neuroimaging techniques in humans: I. MRI/FMRI and PET. Crit Rev Neurobiol 9(2-3): 229-309.

Alkire MT, Haier RJ, Barker SJ, Shah NK, Wu JC, Kao YJ, 1995, Cerebral metabolism during propofol anesthesia in humans studied with positron emission tomography. Anesthesiology 82(2): 393-403.

Alkire MT, Haier RJ, Shah NK, Anderson CT, 1997, Positron emission tomography study of regional cerebral metabolism in humans during isoflurane anesthesia. Anesthesiology 86(3): 549-57.

Alkire MT, Pomfrett CJ, Haier RJ, Gianzero MV, Chan CM, Jacobsen BP, Fallon JH, 1999, Functional brain imaging during anesthesia in humans: effects of halothane on global and regional cerebral glucose metabolism. Anesthesiology 90(3): 701-9.

Alkire MT, Haier RJ, Fallon JH, 2000, Toward a unified theory of narcosis: brain imaging evidence for a thalamocortical switch as the

neurophysiologic basis of anesthetic-induced unconsciousness. Conscious Cogn 9(3): 370-86.

Alkire MT, Haier RJ, 2001, Correlating in vivo anaesthetic effects with ex vivo receptor density data supports a GABAergic mechanism of action for propofol, but not for isoflurane. Br J Anaesth 86: 618-26.

Andersson JL, Onoe H, Hetta J, Lidstrom K, Valind S, Lilja A, Sundin A, Fasth KJ, Westerberg G, Broman JE, Watanabe Y, Langstrom B, 1998, Brain networks affected by synchronized sleep visualized by positron emission tomography. J Cereb Blood Flow Metab 18(7): 701-15.

Angel A, 1993, Central neuronal pathways and the process of anaesthesia. Br J Anaesth 71(1): 148-63.

Backman SB, Fiset P, Plourde G, 2004, Cholinergic mechanisms mediating anesthetic induced altered states of consciousness. Prog Brain Res 145: 197-206.

Birdsall NJ, Burgen AS, Hulme EC, 1978, The binding of agonists to brain muscarinic receptors. Mol Pharmacol 14(5): 723-36.

Bonhomme V, Fiset P, Meuret P, Backman S, Plourde G, Paus T, Bushnell MC, Evans AC, 2001, Propofol anesthesia and cerebral blood flow changes elicited by vibrotactile stimulation: a positron emission tomography study. J Neurophysiol 85(3): 1299-308.

Borges M, Antognini JF, 1994, Does the brain influence somatic responses to noxious stimuli during isoflurane anesthesia? Anesthesiology 81(6): 1511-5.

Braun AR, Balkin TJ, Wesenten NJ, Carson RE, Varga M, Baldwin P, Selbie S, Belenky G, Herscovitch P, 1997, Regional cerebral blood flow throughout the sleep-wake cycle. An H2(15)O PET study. Brain 120: 1173-97.

Burton H, Jones EG, 1976, The posterior thalamic region and its cortical projection in New World and Old World monkeys. J Comp Neurol 168(2): 249-301.

Butterworth JF 4th, Raymond SA, Roscoe RF, 1989, Effects of halothane and enflurane on firing threshold of frog myelinated axons. J Physiol 411: 493-516.

Cabeza R, Nyberg L, 2000, Neural bases of learning and memory: functional neuroimaging evidence. Curr Opin Neurol 13(4): 415-21.

Cariani P, 2000, Anesthesia, neural information processing, and conscious awareness. Conscious Cogn 9(3): 387-95.

Carpenter PA, Just MA, Reichle ED, 2000, Working memory and executive function: evidence from neuroimaging. Curr Opin Neurobiol 10(2): 195-9.

Cheng G, Kendig JJ, 2000, Enflurane directly depresses glutamate AMPA and NMDA currents in mouse spinal cord motor neurons independent of actions on GABA or glycine receptors. Anesthesiology 93: 1075-84.

Cherry SR and Phelps ME, 1996, Imaging brain function with positron emission tomography. In: Brain mapping: the methods. New York: Academic Press, p 165-198.

Chortkoff BS, Gonsowski CT, Bennett HL, Levinson B, Crankshaw DP, Dutton RC, Ionescu P, Block RI, Eger EI 2nd, 1995, Subanesthetic concentrations of desflurane and propofol suppress recall of emotionally charged information. Anesth Analg 81(4): 728-36.

Collins DL, Neelin P, Peters TM, Evans AC, 1994, Automatic 3D intersubject registration of MR volumetric data in standardized Talairach space. J Comput Assist Tomogr 18(2): 192-205.

Corfield DR, Fink GR, Ramsay SC, Murphy K, Harty HR, Watson JD, Adams L, Frackowiak RS, Guz A, 1995, Evidence for limbic system activation during CO2-stimulated breathing in man. J Physiol 488:77-84.

Crick F, 1994, The astonishing hypothesis: The scientific search for the soul. New York: Scribners.

Crick F, Koch C, 2003, A framework for consciousness. Nat Neurosci 6(2): 119-26.

Delgado-Herrera L, Ostroff RD, Rogers SA, 2001, Sevoflurance: approaching the ideal inhalational anesthetic. A pharmacologic, pharmacoeconomic, and clinical review. CNS Drug Rev 2001 7(1): 48-120.

Dennison RL Jr, Anthony BL, Narayanan TK, Aronstam RS, 1987, Effects of halothane on high affinity agonist binding and guanine nucleotide sensitivity of muscarinic acetylcholine receptors from brainstem of rat. Neuropharmacology 26(8): 1201-5.

de Sousa SL, Dickinson R, Lieb WR, Franks NP, 2000, Contrasting synaptic actions of the inhalational general anesthetics isoflurane and xenon. Anesthesiology 92(4): 1055-66.

Delgado-Herrera L, Ostroff RD, Rogers SA, 2001, Sevoflurance: approaching the ideal inhalational anesthetic. a pharmacologic, pharmacoeconomic, and clinical review. CNS Drug Rev 2001 7(1): 48-120.

Desmedt JE, Tomberg C, 1994, Transient phase-locking of 40 Hz electrical oscillations in prefrontal and parietal human cortex reflects the process of conscious somatic perception. Neurosci Lett 168(1-2): 126-9.

Dewey SL, MacGregor RR, Brodie JD, Bendriem B, King PT, Volkow ND, Schlyer DJ, Fowler JS, Wolf AP, Gatley SJ, Hitzemann R, 1990, Mapping muscarinic receptors in human and baboon brain using [N-11C-methyl]-benztropine. Synapse 5(3): 213-23.

Dewey SL, Smith GS, Logan J, Brodie JD, 1993, Modulation of central cholinergic activity by GABA and serotonin: PET studies with 11C-benztropine in primates. Neuropsychopharmacology 8(4): 371-6.

Downie DL, Franks NP, Lieb WR, 2000, Effects of thiopental and its optical isomers on nicotinic acetylcholine receptors. Anesthesiology 93(3): 774-83.

Durieux ME, 1996, Muscarinic signaling in the central nervous system. Recent developments and anesthetic implications. Anesthesiology 84: 173-89.

Dutta S, Matsumoto Y, Muramatsu A, Matsumoto M, Fukuoka M, Ebling WF, 1998, Steady-state propofol brain:plasma and brain:blood partition coefficients and the effect-site equilibration paradox. Br J Anaesth 81: 422-4.

Engel AK, Singer W, 2001, Temporal binding and the neural correlates of sensory awareness. Trends Cogn Sci 5(1): 16-25.

Evans AC, Marrett S, Neelin P, Collins L, Worsley K, Dai W, Milot S, Meyer E, Bub D, 1992, Anatomical mapping of functional activation in stereotactic coordinate space. Neuroimage 1(1): 43-53.

Fiset P, Paus T, Daloze T, Plourde G, Meuret P, Bonhomme V, Hajj-Ali N, Backman SB, Evans AC, 1999, Brain mechanisms of propofol-induced loss of consciousness in humans: a positron emission tomographic study. J Neurosci 19(13): 5506-13.

Flohr H, Glade U, Motzko D, 1998, The role of the NMDA synapse in general anesthesia. Toxicol Lett 100-101:23-9.

Fox PT, Mintun MA, Reiman EM, Raichle ME, 1988, Enhanced detection of focal brain responses using intersubject averaging and change-distribution analysis of subtracted PET images. J Cereb Blood Flow Metab 8(5): 642-53.

Franks NP, Lieb WR, 1984, Do general anaesthetics act by competitive binding to specific receptors? Nature 310: 599-601.

Franks NP, Lieb WR, 1987, Neuron membranes: anaesthetics on the mind. Nature 328: 113-4.

Franks NP, Lieb WR, 1991, Stereospecific effects of inhalational general anesthetic optical isomers on nerve ion channels. Science. 254: 427-30.

Franks NP, Lieb WR, 1994, Molecular and cellular mechanisms of general anaesthesia. Nature 367: 607-14.

Franks NP, Lieb WR, 1998, Which molecular targets are most relevant to general anaesthesia? Toxicol Lett 100-101:1-8.

Franks NP, Dickinson R, de Sousa SL, Hall AC, Lieb WR, 1998, How does xenon produce anaesthesia? Nature. 396(6709): 324.

Frey KA, Koeppe RA, Mulholland GK, Jewett D, Hichwa R, Ehrenkaufer RL, Carey JE, Wieland DM, Kuhl DE, Agranoff BW, 1992, In vivo muscarinic cholinergic receptor imaging in human brain with [11C]scopolamine and positron emission tomography. J Cereb Blood Flow Metab 12(1): 147-54.

Friedland RP, Grant S, 1979, Hematocrit, viscosity and cerebral blood flow. Am Heart J 97(3): 404-5.

Furey ML, Pietrini P, Alexander GE, Mentis MJ, Szczepanik J, Shetty U, Greig NH, Holloway HW, Schapiro MB, Freo U, 2000A, Time course of pharmacodynamic and pharmacokinetic effects of physostigmine assessed by functional brain imaging in humans. Pharmacol Biochem Behav 66(3): 475-81.

Furey ML, Pietrini P, Alexander GE, Schapiro MB, Horwitz B, 2000B, Cholinergic enhancement improves performance on working memory by

modulating the functional activity in distinct brain regions: a positron emission tomography regional cerebral blood flow study in healthy humans. Brain Res Bul l51(3): 213-8.

Grasby P, Malizia A, Bench C, 1996, Psychopharmacology--in vivo neurochemistry and pharmacology. Br Med Bull 52(3): 513-26.

Grossberg S, 1999, The link between brain learning, attention, and consciousness. Conscious Cogn 8(1): 1-44.

Gunn RN, Lammertsma AA, Hume SP, Cunningham VJ, 1997, Parametric imaging of ligand-receptor binding in PET using a simplified reference region model. Neuroimage 6(4): 279-87.

Gunn RN, Gunn SR, Cunningham VJ, 2001, Positron emission tomography compartmental models. J Cereb Blood Flow Metab 21(6): 635-52.

Gyulai FE, Mintun MA, Firestone LL, 2001, Dose-dependent enhancement of in vivo GABA(A)-benzodiazepine receptor binding by isoflurane. Anesthesiology 95: 585-93.

Heinke W, Schwarzbauer C, 2002, In vivo imaging of anaesthetic action in humans: approaches with positron emission tomography (PET) and functional magnetic resonance imaging (fMRI). Br J Anaesth 89(1): 112-22.

Herscovitch P, 2001, Can [^{15}O]water be used to evaluate drugs? J Clin Pharmacol 41:11-20.

Hill GE, Stanley TH, Sentker CR, 1977, Physostigmine reversal of postoperative somnolence. Can Anaesth Soc J 24(6): 707-11.

Hoffman EJ, Phelps ME, 1986, Positron emission tomography: principles and quantitation. In Phelps ME, Mazziota JC, and Schelbert, editors, Positron emission tomography and sutoradiography: principle and applications for the brain and heart, Raven Press, pages 237-86.

Hofle N, Paus T, Reutens D, Fiset P, Gotman J, Evans AC, Jones BE, 1997, Regional cerebral blood flow changes as a function of delta and spindle activity during slow wave sleep in humans. J Neurosci 17(12): 4800-8.

Horrigan RW, 1978, Physostigmine and anesthetic requirement for halothane in dogs. Anesth Analg 57(2): 180-5.

Ito H, Yokoyama I, Iida H, Kinoshita T, Hatazawa J, Shimosegawa E, Okudera T, Kanno I, 2000, Regional differences in cerebral vascular response to PaCO2 changes in humans measured by positron emission tomography. J Cereb Blood Flow Metab 20(8): 1264-70.

John ER, Easton P, Isenhart R, 1997, Consciousness and cognition may be mediated by multiple independent coherent ensembles. Conscious Cogn 6(1): 3-39.

John ER, Prichep LS, 2005, The anesthetic cascade: a theory of how anesthesia suppresses consciousness. Anesthesiology 102(2): 447-71.

Jones BE, 1998, The neural basis of consciousness across the sleep-waking cycle. In: Jasper HH, Descarries L, Castelucci VF, Rossignol S, editors. Consciousness: at the frontiers of neuroscience. Advances in neurology, Vol. 77. Philadelphia: Lippincott-Raven; p. 75-94.

Jueptner M, Weiller C, 1995, Review: does measurement of regional cerebral blood flow reflect synaptic activity? Implications for PET and fMRI. Neuroimage 2(2): 148-56.

Kahan TL, LaBerge S, Levitan L, Zimbardo P, 1997, Similarities and differences between dreaming and waking cognition: an exploratory study. Conscious Cogn 6(1): 132-47.

Kaisti KK, Metsahonkala L, Teras M, Oikonen V, Aalto S, Jaaskelainen S, Hinkka S, Scheinin H, 2002, Effects of surgical levels of propofol and sevoflurane anesthesia on cerebral blood flow in healthy subjects studied with positron emission tomography. Anesthesiology 96(6): 1358-70.

Kearse LA, Rosow C, Zaslavsky A, Connors P, Dershwitz M, Denman W, 1998, Bispectral analysis of the electroencephalogram predicts conscious

processing of information during propofol sedation and hypnosis. Anesthesiology 88: 25-34.

Kendig JJ, Courtney KR, Cohen EN, 1979, Anesthetics: molecular correlates of voltage- and frequency-dependent sodium channel block in nerve. J Pharmacol Exp Ther 210(3): 446-52.

Kendig JJ, 2002, In vitro networks: subcortical mechanisms of anaesthetic action. Br J Anaesth 89(1): 91-101.

Kessler RM, 2003, Imaging methods for evaluating brain function in man. Neurobiol Aging 24 Suppl 1: S21-35.

Kety SS, 1951, The theory and applications of the exchange of inert gas at the lungs and tissues. Pharmacol Rev 3: 1-41.

Kety SS, 1960, Measurements of local cerebral flow by the exchange of an inert, diffusible substance. Methods Med Res 8: 228-36.

Kikuchi T, Wang Y, Sato K, Okumura F, 1998, In vivo effects of propofol on acetylcholine release from the frontal cortex, hippocampus and striatum studied by intracerebral microdialysis in freely moving rats. Br J Anaesth 80(5): 644-8.

Kinomura S, Larsson J, Gulyas B, Roland PE, 1996, Activation by attention of the human reticular formation and thalamic intralaminar nuclei. Science 271(5248): 512-5.

Kitaguchi K, Ohsumi H, Kuro M, Nakajima T, Hayashi Y, 1993, Effects of sevoflurane on cerebral circulation and metabolism in patients with ischemic cerebrovascular disease. Anesthesiology 79(4): 704-9.

Kjaer TW, Lou HC, 2000, Interaction between precuneus and dorsolateral prefrontal cortex may play a unitary role in consciousness. A principle component analysis of rCBF. Consciousness Cognit 9: S59.

Kjaer TW, Nowak M, Kjaer KW, Lou AR, Lou HC, 2001, Precuneus-prefrontal activity during awareness of visual verbal stimuli. Conscious Cogn 10(3): 356-65.

Kjaer TW, Nowak M, Lou HC, 2002, Reflective self-awareness and conscious states: PET evidence for a common midline parietofrontal core. Neuroimage 17(2): 1080-6.

Koeppe RA, Frey KA, Mulholland GK, Kilbourn MR, Buck A, Lee KS, Kuhl DE, 1994, [11C]tropanyl benzilate-binding to muscarinic cholinergic receptors: methodology and kinetic modeling alternatives. J Cereb Blood Flow Metab 14(1): 85-99.

Koeppe RA, Frey KA, Vander Borght TM, Karlamangla A, Jewett DM, Lee LC, Kilbourn MR, Kuhl DE, 1996, Kinetic evaluation of [11C]dihydrotetrabenazine by dynamic PET: measurement of vesicular monoamine transporter. J Cereb Blood Flow Metab 16(6): 1288-99.

Koeppe RA, Frey KA, Snyder SE, Meyer P, Kilbourn MR, Kuhl DE, 1999, Kinetic modeling of N-[11C]methylpiperidin-4-yl propionate: alternatives for analysis of an irreversible positron emission tomography trace for measurement of acetylcholinesterase activity in human brain. J Cereb Blood Flow Metab 19(10): 1150-63.

Krasowski MD, Koltchine VV, Rick CE, Ye Q, Finn SE, Harrison NL, 1998, Propofol and other intravenous anesthetics have sites of action on the gamma-aminobutyric acid type A receptor distinct from that for isoflurane. Mol Pharmacol 53(3): 530-8.

Lammertsma AA, Hume SP, 1996, Simplified reference tissue model for PET receptor studies. Neuroimage 4(3): 153-8.

Lin SC, Olson KC, Okazaki H, Richelson E, 1986, Studies on muscarinic binding sites in human brain identified with [3H]pirenzepine. J Neurochem 46(1): 274-9.

Llinas R, Ribary U, Contreras D, Pedroarena C, 1998, The neuronal basis for consciousness. Philos Trans R Soc Lond B Biol Sci 353(1377): 1841-9.

Logothetis NK, Pauls J, Augath M, Trinath T, Oeltermann A, 2001, Neurophysiological investigation of the basis of the fMRI signal. Nature 412(6843): 150-7.

Logothetis NK, Pfeuffer J, 2004, On the nature of the BOLD fMRI contrast mechanism. Magn Reson Imaging 22(10): 1517-31.

Lou HC, Kjaer TW, Friberg L, Wildschiodtz G, Holm S, Nowak M, 1999, A 15O-H2O PET study of meditation and the resting state of normal consciousness. Hum Brain Mapp 7(2): 98-105.

Lou HC, Luber B, Crupain M, Keenan JP, Nowak M, Kjaer TW, Sackeim HA, Lisanby SH, 2004, Parietal cortex and representation of the mental Self. Proc Natl Acad Sci U S A 101(17): 6827-32.

Ma J, Shen B, Stewart LS, Herrick IA, Leung LS, 2002, The septohippocampal system participates in general anesthesia. J Neurosci 22(2): 1-6.

Maquet P, Peters J, Aerts J, Delfiore G, Degueldre C, Luxen A, Franck G, 1996, Functional neuroanatomy of human rapid-eye-movement sleep and dreaming. Nature 383(6596): 163-6.

Maquet P, Degueldre C, Delfiore G, Aerts J, Peters JM, Luxen A, Franck G, 1997, Functional neuroanatomy of human slow wave sleep. J Neurosci 17(8): 2807-12.

Maquet P, 2000, Functional neuroimaging of normal human sleep by positron emission tomography. J Sleep Res. 9(3): 207-31.

McCarley RW, 2004, Mechanisms and models of REM sleep control. Arch Ital Biol. 142(4): 429-67.

McFarlane C, Warner DS, Dexter F, Ludwig PA, 1994, Minimum alveolar concentration for halothane in the rat is resistant to effects of forebrain ischemia and reperfusion. Anesthesiology 81(5):1206-11.

Meyer H, 1899, Theorie der alkoholnarkose. Arch. Exp. Pathol. Pharmakol 19: 2887-96.

Meuret P, Backman SB, Bonhomme V, Plourde G, Fiset P. 2000. Physostigmine reverses propofol-induced unconsciousness and

attenuation of the auditory steady state response and bispectral index in human volunteers. Anesthesiology 93: 708-17.

Mihic SJ, Ye Q, Wick MJ, Koltchine VV, Krasowski MD, Finn SE, Mascia MP, Valenzuela CF, Hanson KK, Greenblatt EP, Harris RA, Harrison NL, 1997, Sites of alcohol and volatile anaesthetic action on GABA(A) and glycine receptors. Nature 389: 385-9.

Mintun MA, Raichle ME, Kilbourn MR, Wooten GF, Welch MJ, 1984, A quantitative model for the in vivo assessment of drug binding sites with positron emission tomography. Ann Neurol 15(3): 217-27.

Moruzzi G, Magoun HW, 1949, Brain stem reticular formation and activation of the EEG. Electroenceph Clin Neurophysiol 1: 445-73.

Mulholland GK, Kilbourn MR, Sherman P, Carey JE, Frey KA, Koeppe RA, Kuhl DE, 1995, Synthesis, in vivo biodistribution and dosimetry of [11C]N-methylpiperidyl benzilate ([11C]NMPB), a muscarinic acetylcholine receptor antagonist. Nucl Med Biol 22(1): 13-7.

Myers R, Spinks TJ, Luthra SK, Brooks DJ, 1992, Positron emission tomography. In Stewart MG editor, Quantitative methods in neuroanatomy, John Wiley and Sons, pages 117-61.

Ogawa K, Uema T, Motohashi N, Nishikawa M, Takano H, Hiroki M, Imabayashi E, Ohnishi T, Inoue T, Takayama Y, Takeda M, Matsuda H, Andoh T, Yamada Y, 2003, Neural mechanism of propofol anesthesia in severe depression: a positron emission tomographic study. Anesthesiology 98(5): 1101-11.

Ohta S, Meyer E, Fujita H, Reutens DC, Evans A, Gjedde A, 1996, Cerebral [^{15}O] water clearance in humans determined by PET: I. Theory and normal values. J Cereb Blood Flow Metab 16(5): 765-80.

Okazawa H, Vafaee M, 2001, Effect of vascular radioactivity on regional values of cerebral blood flow: evaluation of methods for H(2)(15)O PET to distinguish cerebral perfusion from blood volume. J Nucl Med 42(7): 1032-9.

Pain L, Jeltsch H, Lehmann O, Lazarus C, Laalou FZ, Cassel JC, 2000, Central cholinergic depletion induced by 192 IgG-saporin alleviates the sedative effects of propofol in rats. Br J Anaesth 85(6): 869-73.

Paus T, Zatorre RJ, Hofle N, Caramanos Z, Gotman J, Petrides M and Evans AC, 1997, Time-related changes in neural systems underlying attention and arousal during the preformance of an auditory vigilance task. J Cogn Neurosci 9: 392-408.

Patlak CS, Blasberg RG, Fenstermacher JD, 1983, Graphical evaluation of blood-to-brain transfer constants from multiple-time uptake data. J Cereb Blood Flow Metab 3(1): 1-7.

Plourde G, Chartrand D, Fiset P, Font S, Backman SB, 2003, Antagonism of sevoflurane anaesthesia by physostigmine: effects on the auditory steady-state response and bispectral index. Br J Anaesth 91(4): 583-6.

Plummer GF, 1987, Improved method for the determination of propofol in blood by high-performance liquid chromatography with fluorescence detection. J Chromatogr 421(1): 171-6.

Rampil IJ, Laster MJ, 1992, No correlation between quantitative electroencephalographic measurements and movement response to noxious stimuli during isoflurane anesthesia in rats. Anesthesiology 77(5): 920-5.

Rampil IJ, Mason P, Singh H, 1993, Anesthetic potency (MAC) is independent of forebrain structures in the rat. Anesthesiology 78(4): 707-12.

Rampil IJ, 1994, Anesthetic potency is not altered after hypothermic spinal cord transection in rats. Anesthesiology 80(3): 606-10.

Rampil IJ, King BS, 1996, Volatile anesthetics depress spinal motor neurons. Anesthesiology 85(1): 129-34.

Roy CS, Sherrington CS, 1890, On the regulation of the blood supply of the brain. Journal of Physiology 11: 85-108.

Roy RC, Stullken EH, 1981, Electroencephalographic evidence of arousal in dogs from halothane after doxapram, physostigmine, or naloxone. Anesthesiology 55(4): 392-7.

Sawada Y, Hiraga S, Francis B, Patlak C, Pettigrew K, Ito K, Owens E, Gibson R, Reba R, Eckelman W, 1990, Kinetic analysis of 3-quinuclidinyl 4-[125I]iodobenzilate transport and specific binding to muscarinic acetylcholine receptor in rat brain in vivo: implications for human studies. J Cereb Blood Flow Metab 10(6): 781-807.

Sebel PS, Lang E, Rampil IJ, et al., 1997, A multicenter study of bispectral electroencephalogram analysis monitoring anesthetic effect. Anesth Analg 84: 891-9.

Shafer SL, 1993, Towards optimal intravenous dosing strategies. Seminars in Anesthesia. 12(4): 222-34.

Sinton CM, McCarley RW, 2000, Neuroanatomical and neurophysiological aspects of sleep: basic science and clinical relevance. Semin Clin Neuropsychiatry 5(1): 6-19.

Skaddan MB, Jewett DM, Sherman PS, Kilbourn MR, 2002, (R)-N-[11C]methyl-3-pyrrolidyl benzilate, a high-affinity reversible radioligand for PET studies of the muscarinic acetylcholine receptor. Synapse 45(1): 31-7.

Snyder SH, Yamamura HI, 1977, Antidepressants and the muscarinic acetylcholine receptor. Arch Gen Psychiatry 34(2): 236-9.

Sokoloff L, 1984, Modeling metabolic processes in the brain in vivo. Ann Neurol 15 Suppl: S1-11.

Sonner JM, Antognini JF, Dutton RC, Flood P, Gray AT, Harris RA, Homanics GE, Kendig J, Orser B, Raines DE, Rampil IJ, Trudell J, Vissel B, Eger EI 2nd, 2003, Inhaled anesthetics and immobility: mechanisms, mysteries, and minimum alveolar anesthetic concentration. Anesth Analg 97(3): 718-40.

Sperling R, Greve D, Dale A, Killiany R, Holmes J, Rosas HD, Cocchiarella A, Firth P, Rosen B, Lake S, Lange N, Routledge C, Albert M,

2002, Functional MRI detection of pharmacologically induced memory impairment. Proc Natl Acad Sci U S A 99(1): 455-60.

Steriade M, 1993, Celluar substrates of brain rhythms, Encephalography: Basic Principles, Clinical Applications and Related Fields, 3rd edition, Edited by Neidermeyer E, Lopes Da Silva F. Baltimore, Williams & Wilkins, pp 27-62.

Steriade M, 2004, Slow-wave sleep: serotonin, neuronal plasticity, and seizures. Arch Ital Biol. 142(4): 359-67.

Strebel S, Kaufmann M, Guardiola PM, Schaefer HG, 1994, Cerebral vasomotor responsiveness to carbon dioxide is preserved during propofol and midazolam anesthesia in humans. Anesth Analg 78(5): 884-8.

Tackley RM, Lewis GT, Prys-Roberts C, Boaden RW, Dixon J, Harvey JT, 1989, Computer controlled infusion of propofol. Br J Anaesth 62(1): 46-53.

Tassonyi E, Charpantier E, Muller D, Dumont L, Bertrand D, 2002, The role of nicotinic acetylcholine receptors in the mechanisms of anesthesia. Brain Res Bull 57: 133-50.

Todd MM, Weeks JB, Warner DS, 1993, A focal cryogenic brain lesion does not reduce the minimum alveolar concentration for halothane in rats. Anesthesiology 79(1): 139-43.

Uchida S, Nakayama H, Maehara T, Hirai N, Arakaki H, Nakamura M, Nakabayashi T, Shimizu H, 2000, Suppression of gamma activity in the human medial temporal lobe by sevoflurane anesthesia. Neuroreport 11(1): 39-42.

Vafaee M, Murase K, Gjedde A, Meyer E, 1996, Quantification of Brain Function Using PET. Myers R, Cunningham V, Bailey D, Jones T, Edtors. Academic Press, San Diego, CA pp. 72-75.

Veselis RA, Reinsel RA, Feshchenko VA, Wronski M, 1997A, The comparative amnestic effects of midazolam, propofol, thiopental, and fentanyl at equisedative concentrations. Anesthesiology 87(4): 749-64.

Veselis RA, Reinsel RA, Beattie BJ, Mawlawi OR, Feshchenko VA, DiResta GR, Larson SM, Blasberg RG, 1997B, Midazolam changes cerebral blood flow in discrete brain regions: an H2(15)O positron emission tomography study. Anesthesiology 87(5): 1106-17.

Veselis RA, Reinsel RA, Feshchenko VA, Dnistrian AM, 2002, A neuroanatomical construct for the amnesic effects of propofol. Anesthesiology 97(2): 329-37.

Veselis RA, Feshchenko VA, Reinsel RA, Dnistrian AM, Beattie B, Akhurst TJ, 2004, Thiopental and propofol affect different regions of the brain at similar pharmacologic effects. Anesth Analg 99(2): 399-408.

Volkow ND, Wang GJ, Overall JE, Hitzemann R, Fowler JS, Pappas N, Frecska E, Piscani K, 1997, Regional brain metabolic response to lorazepam in alcoholics during early and late alcohol detoxification. Alcohol Clin Exp Res 21(7): 1278-84.

Wang Y, Kikuchi T, Sakai M, Wu JL, Sato K, Okumura F, 2000, Age-related modifications of effects of ketamine and propofol on rat hippocampal acetylcholine release studied by in vivo brain microdialysis. Acta Anaesthesiol Scand 44(1): 112-7.

Watabe H, Carson RE, Iida H, 2000, The reference tissue model: three compartments for the reference region. Neuroimage 11: S12.

White NS, Alkire MT, 2003, Impaired thalamocortical connectivity in humans during general-anesthetic-induced unconsciousness. Neuroimage 19: 402-11.

Wilkins AJ, Shallice T, McCarthy R, 1987, Frontal lesions and sustained attention. Neuropsychologia 25(2): 359-65.

Woods RP, Mazziotta JC, Cherry SR, 1993, MRI-PET registration with automated algorithm. J Comput Assist Tomogr 17(4): 536-46.

Woolf NJ, Hameroff SR, 2001, A quantum approach to visual consciousness. Trends Cogn Sci 5(11): 472-478.

Worsley KJ, Evans AC, Marrett S, Neelin P, 1992, A three-dimensional statistical analysis for CBF activation studies in human brain. J Cereb Blood Flow Metab 12(6): 900-18.

Xie G, Gunn RN, Dagher A, Daloze T, Plourde G, Backman SB, Diksic M, Fiset P, 2004, PET quantification of muscarinic cholinergic receptors with [N-11C-methyl]-benztropine and application to studies of propofol-induced unconsciousness in healthy human volunteers. Synapse 51(2): 91-101.

Yamakura T, Harris RA, 2000, Effects of gaseous anesthetics nitrous oxide and xenon on ligand-gated ion channels. Comparison with isoflurane and ethanol. Anesthesiology 93(4): 1095-101.

Yamakura T, Bertaccini E, Trudell JR, Harris RA, 2001, Anesthetic and Ion Channels: Molecular Models and Sites of Action 41: 23-51.

Yamamoto S, Kawana S, Miyamoto A, Ohshika H, Namiki A, 1999, Propofol-induced depression of cultured rat ventricular myocytes is related

to the M2-acetylcholine receptor-NO-cGMP signaling pathway. Anesthesiology 91(6): 1712-9.

Yeterian EH, Pandya DN, 1985, Corticothalamic connections of the posterior parietal cortex in the rhesus monkey. J Comp Neurol 237(3): 408-26.

Zeman AZ, Grayling AC, Cowey A, 1997, Contemporary theories of consciousness. J Neurol Neurosurg Psychiatry 62(6): 549-52.

Zeman A, 2001, Consciousness. Brain 124(7): 1263-89.

Zeman A, Reading P, 2005, The science of sleep. Clin Med 5(2): 97-101.

Zentner J, Albrecht T, Heuser D, 1992, Influence of halothane, enflurane, and isoflurane on motor evoked potentials. Neurosurgery 31(2): 298-305.

Zubieta JK, Koeppe RA, Mulholland GK, Kuhl DE, Frey KA, 1998, Quantification of muscarinic cholinergic receptors with [11C]NMPB and positron emission tomography: method development and differentiation of

tracer delivery from receptor binding. J Cereb Blood Flow Metab 18(6): 619-31.

Zubieta JK, Koeppe RA, Frey KA, Kilbourn MR, Mangner TJ, Foster NL, Kuhl DE, 2001, Assessment of muscarinic receptor concentrations in aging and Alzheimer disease with [11C]NMPB and PET. Synapse 39(4): 275-87.

Zucker J, 1991, Central cholinergic depression reduces MAC for isoflurane in rats. Anesth Analg 72(6):790-5.

APPENDEX